

ABSTRACT

Title of Dissertation: UTILIZATION OF FUNCTIONALIZED
CATANIONIC SURFACTANT VESICLES TO
INVESTIGATE PROTEIN-GLYCAN
INTERACTIONS

Amanda C. Mahle, Doctor of Philosophy, 2014

Dissertation Directed By: Professor Daniel C. Stein
Department of Cell Biology and Molecular Genetics

Despite the estimate that more than half of the human proteome is glycosylated, the field of glycomics lags substantially behind proteomics and genomics. The ubiquity of carbohydrates in and on the cell is directly related to the extensive roles they play in the folding and stabilization of protein structure, and in cellular recognition processes. The slow progress in deciphering glycan interactions at a molecular level is in large part due to the absence of a functional system to express, on a large scale, carbohydrates of known structure, in the context of a biologically relevant assay system. The goals of my research are to prepare and characterize glycan-functionalized cationic surfactant vesicles as a platform for glycan synthesis, and to demonstrate that the resulting glycan-functionalized vesicles serve as a scaffold for the interrogation of protein-glycan interactions.

To accomplish this goal, a high-yield method for the purification of *N. gonorrhoeae* lipooligosaccharide (LOS) glycosyltransferase LgtE, an enzyme that catalyzes the addition of galactose onto a terminal glucose found on LOS, was first optimized. Preliminary evidence is presented, suggesting that cationic vesicles solubilize macromolecules found in inclusion bodies, indicating that surfactant vesicles facilitate the purification of insoluble species.

A novel method exploiting differential lectin binding, measured by flow cytometry, was developed to demonstrate LgtE activity on whole cell bacteria and on cationic vesicles functionalized with LOS or a synthetic glycolipid acceptor substrate. The data from these studies confirm the vesicles' robustness in the highly sensitive assay, and demonstrates LgtE mediated oligosaccharide biosynthesis on vesicles, regardless of acceptor origin. Enzyme activity was then characterized on whole cells and LOS functionalized vesicles. Unexpectedly, LgtE is observed to have approximately the same affinity for both terminal glucose and galactose as acceptor substrates for galactosyl transfer. Finally, enzymatic synthesis and retention of the vesicles by hydrophobically modified chitosan coated electrodes is demonstrated by differential antibody binding.

This dissertation presents proof-of-concept that glycan-functionalized cationic vesicles can be used to create a high-specificity and high-throughput glycan array. This array will allow for the investigation of a variety of protein-glycan interactions, and will undoubtedly have applications in many fields of glycomics.

UTILIZATION OF FUNCTIONALIZED CATIONIC SURFACTANT
VESICLES TO INVESTIGATE PROTEIN-GLYCAN INTERACTIONS

By

Amanda C. Mahle

Dissertation submitted to the Faculty of the Graduate School of the
University of Maryland, College Park in partial fulfillment
of the requirements for the degree of
Doctor of Philosophy
2014

Advisory Committee:

Professor Dorothy Beckett, Chair
Professor Daniel C. Stein
Professor Philip DeShong
Professor Catherine Fenselau
Professor Gregory Payne

© Copyright by
Amanda Caroline Mahle
2014

To Dr. Granny and Grandmommy,

Their passionate pursuit of education continues to inspire me to pursue my dreams and to reach for the stars.

Acknowledgements

I must express my sincere gratitude to my advisor, Dr. Daniel Stein. From the first day I rotated in his lab, he has had confidence in my intelligence and scientific skills. Through his guidance and unwavering support I have grown into the person I am today.

I would also like to thank my colleagues in the Stein and Song Labs, especially Lindsey Zimmerman, Dr. Andrzej Piekarowicz, Britney Hardy, Senthil Bhoopalan, Mark Wang, Prar Vasudevan, and Chuka Udeze, for their encouragement, intellectual stimulation, and friendship.

I thank my dissertation committee for encouraging me to expand my intellectual curiosity and scientific aptitude. I am a stronger, more confident person because of them.

I thank all of our collaborators including: Dr. Song and Mr. Ken Class for their assistance with the flow cytometry experiments, and the members of the DeShong lab especially, Dr. Matthew Hurley, Dr. Lenea Stocker, and Dr. Neeraja Dashaputre. I would also like to extend a sincere thank you to Dr. DeShong for generously sharing his time to answer my questions. He has been an indispensable support throughout my training.

Personally, I wish to thank my family. I will be forever grateful of the sacrifices they have made on my behalf. Their continual encouragement and support allowed me to believe that every one of my goals was attainable. Without my Mom, Dad, Lacey, Perry, and Campbell none of this would have been possible. Teddy, you are my best friend and teammate. You have given me the stability, support, and happiness that have allowed me to pursue my dreams, I cannot thank you enough.

The work of this dissertation was partially funded by the NIH T32 training grant on Host- Pathogen Interactions (AI09621).

Table of Contents

Acknowledgements	iii
Table of Contents	v
List of Tables.....	viii
List of Figures	ix
List of Abbreviations	xii
Chapter 1: Introduction.....	1
1.1 Introduction.....	1
1.2 Glycomic Array.....	5
1.3 Surfactant Aggregates.....	6
1.4 Catanionic Surfactant Vesicles	11
1.5 Lipidated Glycans of Bacteria.....	17
1.6 LOS Biosynthesis	22
1.7 Research Objectives	27
Chapter 2: Expression, Purification, and Characterization of LgtE	29
2.1 Introduction.....	29
2.2 Specific Aims and Results	31
2.2.1 Optimization of LgtE Expression in <i>E. coli</i>	31
2.2.2 Purification of LgtE.....	32
2.2.3 Demonstration of <i>In Vitro</i> Glycosyltransferase Activity on Whole Cell Gonococcus.....	33
2.2.4 Novel Purification Technique Using Surfactant Vesicles	35
2.3 Discussion.....	37
2.4 Experimental	37
2.4.1 Bacterial Strains, Plasmids, Oligonucleotides, and Culture Conditions.....	37
2.4.2 Chemicals, Reagents, Enzymes.....	38
2.4.3 Transformation.....	39
2.4.4 Induction and Purification of LgtE.....	39
2.4.5 Protein Purification.....	40
2.4.6 SDS-PAGE Analysis	41
2.4.7 Construction of F62 Ω EcoRI	42

2.4.8	Galactosyltransferase Assay	43
2.4.9	ELISA	43
2.4.10	Surfactant Vesicle Solubilization	44
2.4.11	List of Bacterial Strains and Plasmids Used	45
Chapter 3: Demonstration of Oligosaccharide Biosynthesis by <i>N. gonorrhoeae</i> LgtE on Functionalized Catanionic Surfactant Vesicles		46
3.2	Specific Aims and Results	49
3.2.1	Demonstration of LgtE Glycosyltransferase Activity on Whole Cells and on Functionalized Surfactant Vesicles	49
3.2.2	Differential Lectin Binding Demonstrates the Diversity of Glycoconjugates on Bacterial Cells	51
3.2.3	LgtE Transferase Activity is Maintained on LOS Functionalized Vesicles	55
3.2.4	LgtE is Active on a Synthetic Substrate Incorporated into Surfactant Vesicles	56
3.2.5	Vesicle Integrity is Maintained Following Enzymatic Synthesis	58
3.3	Discussion	59
3.4	Experimental	60
3.4.1	Chemicals, Reagents, Lectins, and Antibodies	60
3.4.2	Preparation of Vesicles	61
3.4.3	LOS Purification for Functionalized Vesicles	62
3.4.4	LOS SDS-PAGE Analysis	63
3.4.5	Flow Cytometry Analysis on Whole Cell Gonococcus	64
3.4.6	Flow Cytometry Analysis on Functionalized Surfactant Vesicles	64
3.4.7	Vesicle Integrity Assay	65
Chapter 4: Utility of Catanionic Surfactant Vesicles as a Novel Glycomic Array Platform		67
4.1	Introduction	67
4.2	Specific Aims and Results	70
4.2.1	LgtE Transferase Activity	71
4.2.2	Interfacial Catalysis	76
4.2.3	Proof of Principle: Functionalized Catanionic Vesicle- Based Glycomic Array	85
4.3	Discussion	88

4.4	Experimental	89
4.4.1	Time Course LOS SDS-PAGE Analysis	89
4.4.2	Enzymatic Assays	89
4.4.3	Vesicle Visualization on HM-Chitosan Coated Electrode	91
Chapter 5:	Conclusions and Prospectus.....	94
Appendices	100
Appendix 1:	Characterization of <i>N. gonorrhoeae</i> Strain F62 Ω EcoRI	100
Appendix 2:	Calculation of Interfacial Catalysis Parameters	101
Appendix 3:	Nonlinear Regression of Kinetic Rates on Whole Cells Using Interfacial Catalysis Model.....	103
Appendix 4:	Nonlinear Regression of Kinetic Rates on Vesicles Using Interfacial Catalysis Model	104
Appendix 5:	Residual plot of nonlinear regression fit to the standard Michaelis- Menten equation	105
Appendix 6:	Contribution to published works.....	106
Bibliography	108

List of Tables

1.1. Mean packing parameters of amphiphilic molecules and the predicted aggregate structures	8
3.1. Quantification of gel analysis on LOS functionalized vesicles following incubation with LgtE	51
4.1. Kinetic parameters of LgtE catalyzed LOS modification	85

List of Figures

1.1. Glycosidic bond synthesis.....	2
1.2. A. Surfactants partition at water: air or polar: non-polar interfaces.....	6
1.3. The association of monomer into equilibrium aggregate structures.....	9
1.4. A. Structure of the cationic surfactant CTAT and the anionic surfactant SDBS.....	12
1.5. Phase diagram of the CTAT/SDBS system in water.....	14
1.6. A. Illustration of the ion pair complex that forms between the cationic head group CTA+, and the anionic head group DBS-.....	15
1.7. Incorporation of amphiphilic glycoconjugates into the outer leaflet of cationic vesicles.....	17
1.8. General structure of LPS.....	18
1.9. Diagram of <i>N. gonorrhoeae</i> LOS.....	20
1.10. Δ lgtA truncated LOS structure.....	25
1.11. Proposed reaction mechanism of the inverting β -1,4-galactosyltransferase LgtE.....	28
2.1. 15% Tris-HCl SDS-PAGE of 8M urea solubilized LgtE.....	32
2.2. 15% Tris-HCl SDS-PAGE of purified LgtE.....	33
2.3. Schematic of the indirect ELISA experimental setup.....	34
2.4. Quantification of LgtE catalyzed modification of whole cell LOS by indirect ELISA.....	35
2.5. Vesicle extraction of membrane associated molecules.....	36

3.1. Glycan density and spatial arrangement have a significant influence carbohydrate binding protein affinity	48
3.2. SDS-PAGE of whole cell LOS and LOS functionalized vesicles following LgtE modification	50
3.3. Gel analysis of LOS functionalized cationic surfactant vesicles following reaction with LgtE	51
3.4. Schematic of differential lectin binding as assessed by flow cytometry	52
3.5. LgtE mediates the transfer of a galactosyl group, <i>in vitro</i> , to whole cell F62 Ω EcoRI	54
3.6. LgtE mediates the transfer of a galactosyl moiety to Δ lgtE LOS functionalized vesicles.....	55
3.7. Structure of <i>n</i> -Dodecyl- β -glucopyranoside, or C ₁₂ -glucose.....	56
3.8. LgtE mediates the transfer of a galactosyl moiety to C ₁₂ -Glucose functionalized vesicles.....	57
3.9. Vesicles are intact following enzymatic synthesis.	58
4.1. Methodology of glycan immobilization.....	69
4.2. Steady-state conditions for <i>in vitro</i> activity assay	72
4.3. Activity of LgtE on whole cell <i>N. gonorrhoeae</i> F62 Ω EcoRI	75
4.4. Activity of LgtE on Δ lgtE LOS functionalized cationic surfactant vesicles	75
4.5. Model of LgtE interfacial catalysis.....	76
4.6. Hopping and scooting model describing enzyme dynamics in a membrane. The enzyme is depicted in blue	78
4.7. Proposed model of LgtE catalysis	81

4.8. Schematic of the preparation of carbohydrate microarrays using HM-chitosan and SDBS-rich functionalized vesicles	86
4.9. Visualization of LgtE mediated, catalytic modification on functionalized vesicles by fluorescently labelled antibodies	87
5.1. Galectin-3 overexpression mediates tumor metastasis and proliferation.....	96
5.2. Lectin microarray profiling of cancer tissue	97
5.3. The work of this dissertation provides proof-of-concept that cationic surfactant vesicles along with recombinant glycosyltransferases can be utilized to develop diagnostic tool for immunoprofiling	98
A1. A. Confirmation that the Ω interposon of pLgtDE Ω EcoRI is located in the expected region.	100
A2. Coomassie Blue stain of 15% Tris-HCl SDS-PAGE analysis of LgtE expression conditions	101
A3. Equation 4.5 from text as a user-defined equation in GraphPad Prism.....	102
A4. Tabulated results of fitting the whole cell reaction initial rates versus [LOS] to equation 4.5.....	103
A5. Tabulated results of fitting the vesicle reaction initial rates versus [LOS] to equation 4.5	104
A6. Residual plot of the nonlinear regression fit of LgtE activity	105
Figure 4. Flow cytometry analysis of Opa expression	106
Figure 11. Flow cytometry using anti-gonococcal IgG FSNs	107

List of Abbreviations

°C	Degrees Celsius
μg	Microgram
μl	Microliter
μm	Micrometer
μM	Micromolar
AF	Alexa Fluor®
AgNO ₃	Silver Nitrate
ASGP-R	Asialoglycoprotein Receptor
BSA	Bovine Serum Albumin
C-terminus	Carboxyl-terminus
C ₁₂ -glucose	<i>n</i> -Dodecyl- β- glucopyranoside
CAZy	Carbohydrate-Active Enzymes
CMC	Critical Micelle Concentration
CMP-NANA	Cytidine-monophosphate <i>N</i> -acetylneuraminic acid
ConA	Concavalin A
CTAB	Cetyltrimethylammonium Bromide
CTAT	Cetyltrimethylammonium Tosylate
DLS	Dynamic Light Scattering
DNA	Deoxyribonucleic acid
DXD	Asp-any residue-Asp
<i>e</i>	Elementary charge (1.602x10 ⁻¹⁹ C)
<i>E. coli</i>	<i>Escherichia coli</i>
EDTA	Ethylenediaminetetraacetic acid
ELISA	Enzyme-Linked Immunosorbent Assay
FACS	Fluorescence-Activated Cell Sorting
FDA	U.S. Food and Drug Administration
g	Gram
Gal	Galactose

Gal-3	Galectin-3
GalNAc	N-Acetylgalactosamine
GBP	Glycan Binding Protein
GCK/ GCP	Gonococcal media base
Glc	Glucose
GlcNAc	N-acetylglucosamine
GT-A	Glycosyltransferase-A
H+L	Heavy and Light chain
H ₂ O	Water
HEPES	4-(2-Hydroxyethyl)-1-piperazineethanesulfonic acid
HM-chitosan	Hydrophobically-Modified chitosan
IgG	Immunoglobulin G
IPTG	Isopropyl β-D-1-thiogalactopyranoside
<i>k</i>	Boltzmann constant (1.38×10^{-23} J. K ⁻¹)
kb	Kilobases
kcal	Kilocalorie
<i>k_{cat}</i>	Catalytic turnover rate
K _D	Dissociation constant
kDa	Kilodalton
KDO	3-Deoxy-D-manno-oct-2-ulosonic acid
L	Liter
L,D-Hep	L-glycero-D-mannoheptose
LB	Luria Bertani
<i>lgt</i>	Lipooligosaccharide glycosyl transferase
LOS	Lipooligosaccharide
LPS	Lipopolysaccharide
m	Meter
M	Molar
mA	Milliamphere
MAb	Monoclonal Antibody

ml	Milliliter
Mn ²⁺	Manganese
MnCl ₂	Manganese Chloride
mol	Mole
mV	Millivolts
N-terminal	Amino-terminal
<i>N. gonorrhoeae</i>	<i>Neisseria gonorrhoeae</i>
<i>N. meningitidis</i>	<i>Neisseria meningitidis</i>
NaCl	Sodium Chloride
NaH ₂ PO ₄	Sodium Phosphate Monobasic
NaOH	Sodium Hydroxide
Ni ²⁺ -NTA	Nickel- Nitrilotriacetic Acid
OD	Optical Density
PBS	Phosphate Buffered Saline
PEtN	Phosphorylethanolamine
PFA	Paraformaldehyde
PID	Pelvic Inflammatory Disease
PMSF	Phenylmethylsulfonyl Fluoride
PNA	Peanut Agglutinin
Poly-G	Poly-guanine
RPM	Revolutions Per Minute
SAMDI-MS	Self-assembled monolayers with matrix-assisted laser desorption-ionization mass spectrometry
SDBS	Sodium Dodecylbenzene Sulfonate
SDS	Sodium Dodecylsulfate
SDS-PAGE	Sodium Dodecyl Sulfate Polyacrylamide Gel Electrophoresis
SEC	Size Exclusion Chromatography
S _N 2	Substitution Nucleophilic Bi-molecular
Surfactant	Surface Active Agent

<i>T</i>	Temperature
TLR4	Toll-Like Receptor 4
Tris-HCl	Tris-Hydrochloride
UDP	Uridine Diphosphate
wt %	Weight percent
Ω	Omega interposon

Chapter 1: Introduction

1.1 Introduction

The term glycobiology was first coined in 1988 by the biochemist Raymond Dwek to recognize the linkage between carbohydrate chemistry and biochemistry.³ Carbohydrates are the most abundant, naturally occurring biopolymers found in nature. All cells are covered in carbohydrate structures expressed as glycoconjugates, covalently coupled to lipids or proteins.⁴ A glycan can also exist as a free entity in, or be secreted by, cells.⁴ However, it was not until the 1970s and 1980s that an appreciation for the role of complex glycans in governing a variety of biological processes was demonstrated.⁵

Carbohydrates have critical roles in protein folding,⁶ cell adhesion,⁷ host-pathogen interactions,⁸ cancer metastasis,⁹ activation and attenuation of innate and adaptive immunity,^{10, 11} and in cell signaling.^{3, 7} The diverse biological activity of carbohydrates is mediated through recognition by cognate proteins, termed glycan-binding proteins (GBPs), triggering downstream effects.⁷ Little is known, however, about the structure-function relationships of carbohydrates, and how structure influences the ligand recognition by GBPs. Lack of mechanistic understanding of protein-carbohydrate interactions is a direct result of the inherent structural complexity of carbohydrates.⁵

Carbohydrates are chains of polyhydroxyl aldehydes or ketones that can be hydrolyzed into monosaccharides.⁴ Glycosyl groups, cyclic monosaccharides lacking the hydroxyl group of the hemiacetal or hemiketal carbon, are linked together by a glycosidic bond, either α or β , depending on the orientation with respect to the anomeric carbon of

the reducing sugar. Linkage results in oligo- and polysaccharide structures, forming extended hydrated chains (Figure 1.1).

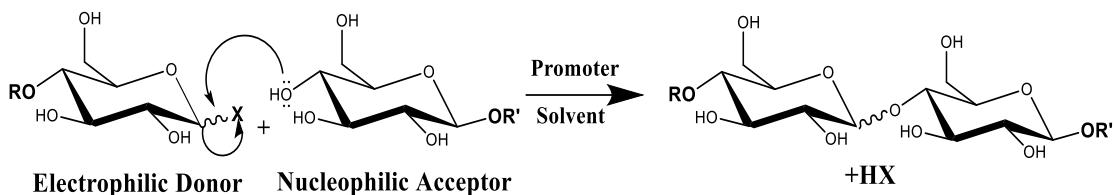


Figure 1.1. Glycosidic bond synthesis. The leaving group (X) on the anomeric carbon of the donor is displaced due to a nucleophilic attack by the alkoxy group on the acceptor moiety. R and R' in this figure are non-participating groups. Figure adapted from reference 13.

Polysaccharides are more structurally diverse than amino and nucleic acids. A consequence of the many regio- and stereochemistries possible with the furanose and pyranose rings is a branched polysaccharide structure.¹² Illustrating this structural complexity, three nucleotides or amino acids can generate just six different trimers, whereas three different hexoses can generate anywhere from 1,056 to 27,648 distinct trisaccharides.⁴ Further increasing the diversity of carbohydrate structure, a hydroxyl of a glycoside can be substituted with a variety of functional groups. For example, a hydroxyl can be replaced with a hydrogen atom to form a deoxy sugar, or with an acetyl group or an amino group forming an acetyl sugar or an amino sugar, respectively, among others.¹³

A major challenge facing the field of glycomics is a lack of methodology for *in vitro* carbohydrate synthesis. *In vitro* isolation of glycans from glycoconjugates is complicated by microheterogeneity.⁴ The glycosylation site on a protein expressed in a cell can have a variety of carbohydrates attached to it. Therefore, isolation of homogenous glycan moieties is rarely accomplished.¹⁴ Organic synthesis of polysaccharides is complicated by protective group chemistry of the free hydroxyls, a necessary measure to distinguish one hydroxyl from another, and by the liability of the

glycosidic bonds (Figure 1.1),¹⁵ requiring multiple synthetic steps and generating mixed anomers of low yield.⁵

Carbohydrates are not encoded in an organism's genome, but are synthesized through sequential enzymatic reactions catalyzed by glycosyltransferases that recognize a specific glycan structure.³ Glycosyltransferases (EC 2.4.x.y) are present in both eukaryotes and prokaryotes and catalyze the transfer of an activated sugar moiety onto a growing carbohydrate chain generally with high regio- and stereospecificity, generating significant yields of the defined glycosidic linkages.¹⁴ The Carbohydrate-Active Enzyme (CAZy) Database (www.cazy.org), maintained by Université de Provence/ Université de la Méditerranée, Marseille, France, has cataloged over 200 families of glycosyltransferases, along with other carbohydrate-active enzymes.¹⁴

Glycosyltransferases catalyze the formation of glycosidic linkages between a donor and an acceptor molecule. The acceptor can be another saccharide, a lipid, or a protein.¹⁴ All glycosyltransferases can be grouped according to their preferential donor substrate as belonging to the Leloir or non-Leloir pathway. Additionally, they are subclassed as either retaining or inverting based on if the glycosidic bond has α or β stereochemistry with respect to anomeric configuration of the product to the donor substrate.⁶

Enzymes of the Leloir pathway utilize sugar nucleotides as a donor substrate. Non-Leloir glycosyltransferases utilize phosphorylated monosaccharides (i.e. dolichol phosphomannose), as the donor substrate. Leloir pathway glycosyltransferases predominate over their non-Leloir counterparts, due to the inherent chemical properties that make sugar nucleotides ideal donor substrates.¹⁴ Sugar nucleotides are synthesized in

a multistep metabolically irreversible process in which a kinase activates a specific monosaccharide. The phosphorylated monosaccharide is further activated by a nucleotide transferase/phosphorylase through a condensation reaction, typically with uridine-triphosphate.⁶ The formation of the glycosidic bond between the donor and a specific hydroxyl in the acceptor, with a free energy of approximately +16 kcal/mol, is driven by the hydrolysis of the donor precursor and is facilitated by the strong leaving group nature of the nucleotide diphosphate.¹⁴

Increased recognition of the diverse roles carbohydrates play in biology suggests that glycosyltransferases could be exploited for the *in vitro* synthesis of complex carbohydrates.^{14, 16} Glycosyltransferase reactions are typically carried out in aqueous solutions at a physiological pH.⁵ They have high regio- and stereoselectivity, eliminating the need of protecting and deprotecting groups. Emphasizing the potential exploitation of glycosyltransferases, Toone *et al.* has stated that no other class of organic compounds is more amenable to enzymatic synthesis than carbohydrates.⁵ Mammalian glycosyltransferases are typically transmembrane proteins with low solubility, complicating protein purification. Alternatively, bacterial glycosyltransferases are noncovalently associated with cellular membranes making them attractive candidates for *in vitro* synthesis.

To advance the molecular understanding of the biological roles of carbohydrates, a method for the facile expression and purification of recombinant glycosyltransferases must be developed. A related but equally important requirement is the development of appropriate assay tools to investigate protein-carbohydrate interactions.

1.2 *Glycomic Array*

Glycan binding proteins mediate a variety of biological responses. Protein-carbohydrate interactions are dependent on the spatial orientation and density of ligand presentation.¹⁷ Generally, glycan binding proteins have weak monovalent interactions with their cognate ligand, the monomeric dissociation constant (K_D) being in the millimolar range.¹⁸ High affinity ligand recognition is accomplished through multivalent interactions of multiple glycan binding domains.^{17, 18} Ligand presentation is important in establishing these multivalent complexes. However, investigating these interactions is limited by the availability of homogenous carbohydrate structures.

Arrays have been previously developed employing a variety of platforms to which glycans are covalently or noncovalently immobilized.¹⁹ These platforms include silica plates,²⁰ glass slides,²¹ nitrocellulose,²² and the immobilization of neoglycoconjugates.²³ While each has provided researchers a means to investigate protein-carbohydrate interactions, reproducibility of protein binding profiles remains elusive. Variations in ligand density and orientation, in the physical properties of the platform such as surface charge, and length and flexibility when a linker is used to facilitate glycan surface attachment, can all significantly influence protein binding.^{17, 23, 24} There is a pressing need in the field of glycomics for the development of an array platform in which carbohydrates are easily immobilized and presented for protein binding, and in which ligand density can readily be varied such that the influence of special orientation on protein recognition can be investigated.

1.3 Surfactant Aggregates

The term surfactant describes amphiphilic molecules that are **surface active agents** that partition at water: air or polar: non-polar interfaces (Figure 1.2A). Common surfactants are commercially available in detergents, soaps, and emulsifiers. Like phospholipids of cell membranes, surfactants are composed of a long single or double non-polar alkyl tail and a polar head group. The chemical properties of the head group serve as a means of classification. Non-ionic surfactants, such as octyl phenol ethoxylate (Triton X-100), are composed of an uncharged but highly polar head group. Ionic surfactants can be further grouped as cationic, such as cetyltrimethylammonium bromide (CTAB), if the polar head group has an overall positive charge, or anionic if it has an overall negative charge. A common anionic surfactant is sodium dodecylsulfate (SDS). Zwitterionic surfactants carry both a negative and positive charge. Two of the most abundant phospholipids in the mammalian cell bilayer, phosphatidylcholine and phosphatidylethanolamine, are zwitterionic.

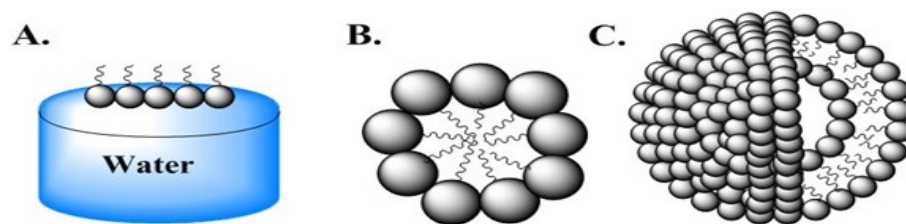


Figure 1.2. A. Surfactants partition at water: air or polar: non-polar interfaces B. Cartoon depiction of a micelle formed from a single-tailed surfactant C. Cartoon depiction of a unilamellar bilayer vesicle.

Amphiphilic molecules in solution will spontaneously self-assemble into colloidal aggregates. Micelles and bilayer vesicles are equilibrium structures that form upon rearrangement of amphiphilic molecules, so as to reduce the exposure of the hydrophobic tail to the aqueous environment. Amphiphile rearrangement is thermodynamically driven

by the hydrophobic effect, such that spontaneous self-assembly into aggregates minimizes the free energy of the system. Micelles are the simplest form of a self-assembled structure, with the polar head groups exposed to the exterior environment and the non-polar tails sequestered in the center. Vesicles form when a planar bilayer assumes curvature. They can be unilamellar, consisting of a single bilayer, or can contain more than two monolayers, in which case a multilamellar structure forms. The type of aggregate that forms is dependent on the size, shape, and charge of the amphiphilic molecule. These characteristics are collectively termed an amphiphile's molecular geometry.

Israelachvili first described the relationship between an amphiphile's geometry to the predicted aggregation structure in 1976.²⁵ The geometry of a surfactant molecule can be described by the dimensionless packing parameter, P , described in equation 1.1 as:

$$P = \frac{v}{a_o l}$$

(Equation 1.1)

where v is the volume of the hydrocarbon tail, a_o is the effective area of the hydrophilic head group, and l is the critical length of the hydrocarbon chain. The packing parameter value can be thought of as a measure of membrane curvature, surfactant molecules with smaller packing parameters are predicted to have a more highly curved aggregate structure.²⁶

Amphiphiles with a large head group area and a small hydrocarbon tail volume have a packing parameter value of less than 1/3 and are entropically driven to form spherical micelles. Amphiphiles with a smaller a_o or larger v have a packing parameter

value in the range of $1/3$ to $1/2$ and form cylindrical micelles. Cylindrical amphiphiles have a packing parameter that equals approximately 1. These molecules cannot pack into a small micellar structure, rather the molecules aggregate into planar bilayers. For amphiphiles to form a bilayer, the a_o and chain length being the same, the v must be approximately twice that of a micellar-amphiphile. Bilayers, however, are not thermodynamically stable due to the presence of energetically unfavorable edges. To eliminate the edges, fusion of the bilayer ends occurs and vesicles are formed (Table 1.1).

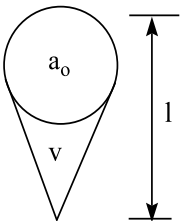
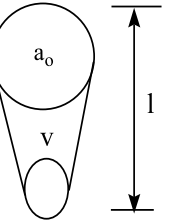
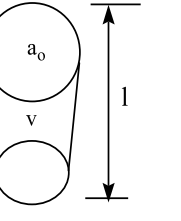
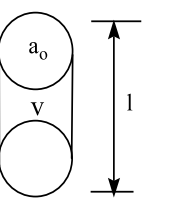
Packing Parameter $P=v/(a_o * l)$	Amphiphile Geometry	Structure of Aggregate Predicted
$<1/3$		Spherical Micelle
$1/3-1/2$		Cylindrical Micelle
$1/2-1$		Curved Bilayers-Vesicles
1		Planar Bilayers

Table 1.1. Mean packing parameters of amphiphilic molecules and the predicted aggregate structures. Adapted from reference 26.

In a single surfactant system the packing parameter value allows for the prediction of aggregate structure with a high degree of certainty. In mixed surfactant systems with more than one amphiphile present in solution, the packing parameter for the individual surfactants cannot provide an accurate prediction. An understanding of the thermodynamics of self-assembly, and a description of how the aggregates form, provides an explanation for this discrepancy.

Spontaneous formation and stability of equilibrium structures is determined by the thermodynamics of self-assembly, intra-aggregate forces, as well as inter-aggregate forces. It is important to note that the equilibrium structures, such as micelles, formed upon amphiphile aggregation are not static entities. They are in constant thermal motion within an aggregate and are in equilibrium between the aggregate and dispersed monomers (Figure 1.3).²⁵

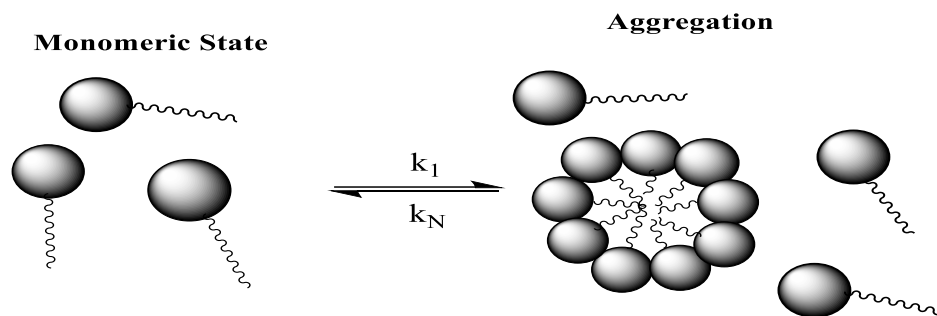


Figure 1.3. The association of monomer into equilibrium aggregate structures. The association and dissociation constants of aggregate formation are denoted as k_1 and k_N respectively. Adapted from reference 26.

The type of colloidal aggregate formed in solution is based on the anisotropic binding forces acting between different parts of the amphiphilic molecules. The hydrophobic tails give rise to attractive interfacial tension forces. In contrast, the amphiphilic molecules experience repulsive forces due to steric and electrostatic

contributions of the hydrophilic head group. The opposing forces dictate that micelle formation will only occur above a certain monomer concentration. The concentration of a particular amphiphile at which the monomers no longer behave as isolated entities is denoted the critical micelle concentration (CMC). Below the CMC only monomers are present in solution. Above the CMC, amphiphiles spontaneously form self-assembled structures and further addition of amphiphiles results in the formation of more aggregates, leaving the monomer concentration constant. The mean aggregation number, N , of molecules in a micelle can be determined from the equation:

$$N = \frac{[S] - cmc}{[M]}$$

(Equation 1.2)

where S is the total surfactant concentration and M is the concentration of micelles in the system.

Accounting for both the attractive and repulsive forces involved in micelle self-assembly, the interaction free energy of molecules, μ_N^0 , in an aggregate of aggregation number, N , can be determined from the equation:

$$\mu_N^0 = \mu_\infty^0 + \frac{\alpha kT}{NP}$$

(Equation 1.3)

where μ_∞^0 is the chemical potential of a molecule in an aggregate of infinite aggregation number. P is the packing parameter previously described in equation 1.1, k is the Boltzmann constant, and T is the temperature in Kelvin. α is a positive constant that depends on the strength of the intermolecular interactions in the aggregate. α can be determined from the equation:

$$\alpha = \frac{4\pi r^2 \gamma}{kT}$$

(Equation 1.4)

where r is the effective radius of the amphiphilic molecule, and γ is the interfacial free energy per unit area of a molecule. The term, αkT , in equation 1.3 describes the monomer-monomer interaction energy in an aggregate relative to isolated free monomers in solution. Equation 1.3 dictates that μ_N^0 decreases asymptotically towards μ_∞^0 as N increases. This mathematical relationship implies that in a system there is a finite minimum value of N where the free energy of interaction is minimized. The inverse relationship between the free energy of interaction and the aggregation number is necessary for spontaneous self-assembly, as the negative free energy difference thermodynamically drives aggregation (Figure 1.3).

1.4 Catanionic Surfactant Vesicles

Bangham *et al.* first described vesicles in 1964 with the observation that double tailed phospholipids in an aqueous solution self-assemble into multilamellar vesicle aggregates, later termed liposomes.²⁷ This research led to the understanding that phospholipids are the permeability barrier of all eukaryotic cells.²⁸ Unilamellar phospholipid derived liposomes have since been extensively researched and described as both a cell membrane model and as a method for drug delivery.²⁹ Phospholipid molecules however have a packing parameter of 1. The geometry of phospholipids favors the formation of planar bilayer colloidal aggregates. Unilamellar liposome formation is not thermodynamically favored. To induce the formation of monodispersed vesicles, an input of mechanical energy is required, such as sonication or extrusion through a filter.³⁰

Liposomes are therefore metastable, bilayer integrity is maintained for an average of two days.³⁰

In 1989, Kaler *et al.* demonstrated the spontaneous formation of unilamellar vesicles in an aqueous mixture of two single-tailed surfactants with oppositely charged head groups.³¹ The cationic surfactant in the system is cetyltrimethylammonium tosylate (CTAT), with a cetrimonium cation head group and a tosylate counter ion (Figure 1.4A). Sodium dodecylbenzene sulfonate (SDBS), with an anionic sulfonate head group and sodium counter ion (Figure 1.4B), is the anionic surfactant in the system. The cationic/anionic, or catanionic, surfactant vesicles are more stable than phospholipid-derived liposomes. Studies conducted by Kaler *et al.* and by other groups observed that catanionic vesicles maintained bilayer integrity for over a year at room temperature.^{31, 32} Moreover, the degree of bilayer curvature, as well as the magnitude of surface charge, or

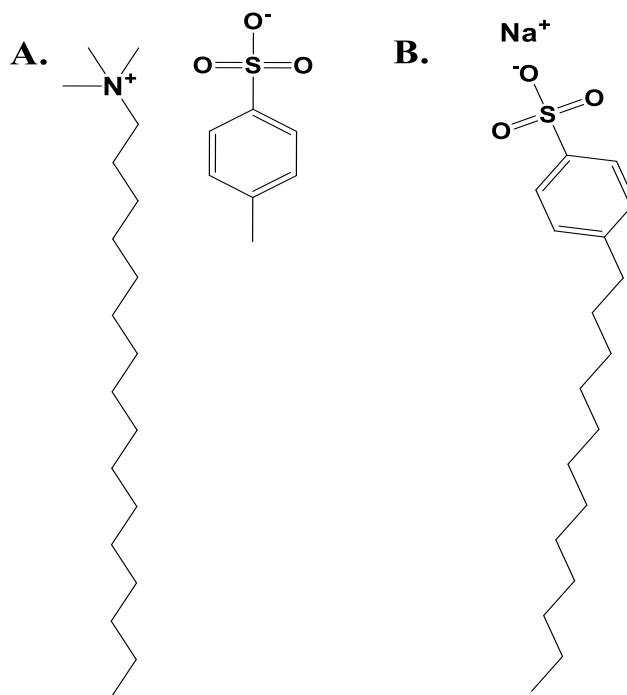


Figure 1.4. **A.** Structure of the cationic surfactant CTAT. **B.** Structure of the anionic surfactant SDBS.

zeta potential, could be readily varied by changing the proportions of the individual surfactants and/or the addition of nonionic surfactants.³¹

The observation by Kaler *et al.* that aqueous mixtures of CTAT and SDBS spontaneously form unilamellar catanionic vesicles was unexpected. In contrast to aggregates composed of double tailed amphiphiles with a packing parameter of 1, single tailed surfactants are not expected to form bilayer structures. CTAT and SDBS both have packing parameters of approximately 1/3, predicting micellar aggregates. Experimental observations by Kaler and co-workers confirmed that SDBS formed spherical micelles in an aqueous solution whereas CTAT formed cylindrical micelles. When mixed together at the appropriate concentrations unilamellar vesicles formed.³¹

The mechanism underlying spontaneous catanionic vesicle formation has been previously reported.³³ Koehler *et al.* examined the physical properties of the CTAT/SDBS mixed surfactant system and constructed a phase diagram based on the behavior of the surfactants at various concentrations (Figure 1.5).³³ Significantly, catanionic vesicles will only form in solution if either the cationic or the anionic surfactant is in molar excess of the other. Specifically, a weight ratio of ~70/30 is critical for the formation of catanionic vesicles, outside this region two-phase structures or precipitation occurs.

It is clear from the work of Kaler *et al.*, Koehler *et al.*, and other groups that the SDBS/CTAT mixed surfactant system behaves differently than the individual surfactants alone in solution.^{31,33} Spontaneous self-assembly of SDBS and CTAT into vesicle aggregates, can be explained by electrostatic interactions between the two ionic head groups. Aggregate formation and stability is dependent on a balance of the attractive and

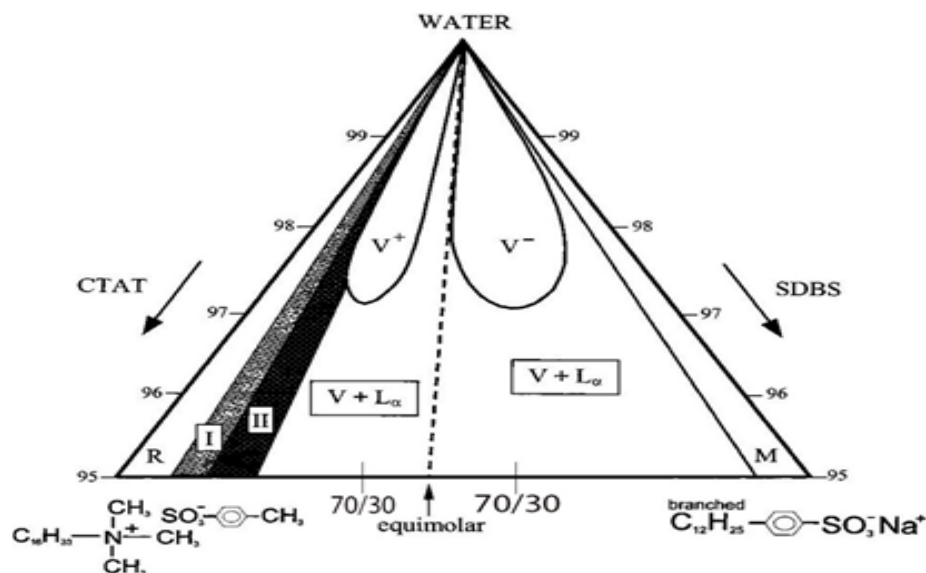


Figure 1.5. Phase diagram of the CTAT/SDBS system in water. Rod-like micelles are formed in the CTAT-rich corner (R). Region I and II are micelle/vesicle two-phase regions. At higher SDBS concentrations spontaneous vesicles (V) and lamellar structures (L_{α}) form. In the SDBS-rich corner micelles (M) are observed. The CTAT and SDBS-rich vesicles lobes are denoted at V^{+} and V^{-} respectively. The numbers on the outside of the pyramid designate percent aqueous solution, i.e. percent surfactant by weight. Adapted from reference 34.

repulsive forces involved in monomer-monomer interaction.²⁵ In the mixed surfactant system, the cationic head group, CTA^{+} , and the anionic, DBS^{-} , head group can physically associate to form ion pair complexes. Ion pairs mimic the geometry of double-tailed zwitterionic phospholipids, as illustrated in figure 1.6A. These pseudo-double-tailed surfactants have an increased hydrocarbon tail volume and a decreased average head group area, such that the packing parameter increases from $\sim 1/3$ for the individual surfactants to approximately $1/2 - 1$,³⁴ and predicts a curved bilayer aggregate.

Ion pair complexes explain the formation of bilayers, and vesicles were previously described as curved bilayers that fuse in order to eliminate energetically unfavorable ends.²⁵ A model describing the spontaneous curvature of bilayer vesicles composed of two ionic surfactants that individually form micelles was proposed by

Safran *et al.*³⁵ In the model, equilibrium vesicles of an ideal radius are stabilized by curvature energy that arises from mixing two surfactants. Mixing allows the formation of monolayers with different concentrations of the surfactants (Figure 1.6B). Differing monolayer composition, together with the formation of ion pairs, results in monolayers with equal but opposite curvature.³⁵

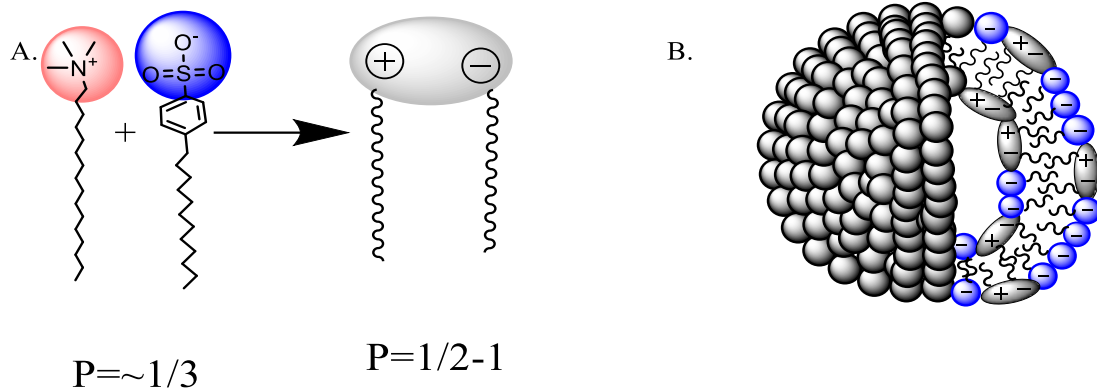


Figure 1.6. **A.** Illustration of the ion pair complex that forms between the cationic head group CTA+, and the anionic head group DBS-. **B.** Cross-section of SDBS-rich vesicle bilayer. The inner monolayer contains a higher mole fraction of ion pair complexes than the outer monolayer.

To describe the free energy that stabilizes unilamellar vesicle formation, Safran *et al.* begin with a vesicle containing two oppositely charged surfactants, surfactant 1 and surfactant 2. The vesicle's inner monolayer has a composition, c_i , which is different from the outer monolayer, c_o . The curvature elastic energy of the vesicle per unit area, f_c , can be determined from the equation:

$$f_c = 2K[(c + c_o)^2 + (c + c_i)^2] \quad (\text{Equation 1.5})$$

where c is the bilayer curvature and K is the bending elastic modulus. The asymmetrical distribution of surfactants to each monolayer influences the surfactant packing density in each monolayer.³⁵ If the hydrophobic tails of both surfactants are the same length, the

curvature of each monolayer is dependent on the bond distances between the polar head groups of the monolayer. As illustrated in figure 1.6A, the formation of ion pairs decreases the effective head group area of the surfactant molecules, decreasing the bond distance between two molecules. The curvature elastic energy is minimized at a finite curvature of $c_i = -c_o$, which can only occur if there are attractive interactions that stabilize the vesicle and impart a positive ($c_i > 0$) curvature to the inner monolayer. The outer monolayer must have an equal, but negative ($c_o < 0$), curvature, achieved in catanionic vesicular systems by partitioning the excess surfactant to the outer monolayer.^{31, 35} Therefore, the SDBS-rich vesicles employed in this work spontaneously form unilamellar vesicles with an excess negative charge on the outer monolayer (Figure 1.6B).

The excess charge of catanionic surfactant vesicles imparts important physical properties. It is a repulsive inter-aggregate force, giving vesicles superior colloidal stability as compared to liposomes. Studies conducted in the DeShong laboratory as well by other groups have demonstrated that catanionic surfactant vesicles are stable for years at room temperature.^{32, 36} Additionally, the surface of catanionic vesicles can be decorated with glycans conjugated to hydrophobic moieties.^{32, 37} In this case, the hydrophobic tail of the glycoconjugate spontaneously inserts into the vesicle outer leaflet and anchors the glycan to the outer surface of the vesicle (Figure 1.7). Recent also studies indicate that catanionic surfactant vesicles can be immobilized on a variety of surfaces, and that the incorporated moieties are recognized by ligand specific proteins.^{37, 38}

The thermodynamic principles outlined in this discussion as well as the other briefly mentioned studies led to the hypothesis that catanionic surfactant vesicles could be employed as a novel platform for investigating protein-glycan interactions. The

superior stability, facile preparation, and the low cost of the individual surfactants make the SDBS/CTAT system an ideal option for *in vitro* studies. This work investigates the utility of SDBS-rich catanionic vesicles as a platform for the *in vitro* biosynthesis of oligosaccharides. SDBS-rich vesicles have a surface charge of -35-70 mV, a value comparable to the zeta potential of a Gram-negative bacteria cell.³⁷ Therefore, a glycosyltransferase that *in vivo* modifies glycans presented on the inner bacterial cell membrane could, in principle, catalyze the transfer of a donor sugar to an acceptor molecule presented on the surface of a surfactant vesicle. The next section will describe the introduction of a bacterial oligosaccharide into the leaflet of catanionic vesicles, and the utilization of the resulting glycan-functionalized vesicles as a substrate for a glycosyltransferase. This system serves as a model for *in vitro* carbohydrate investigations and synthesis.

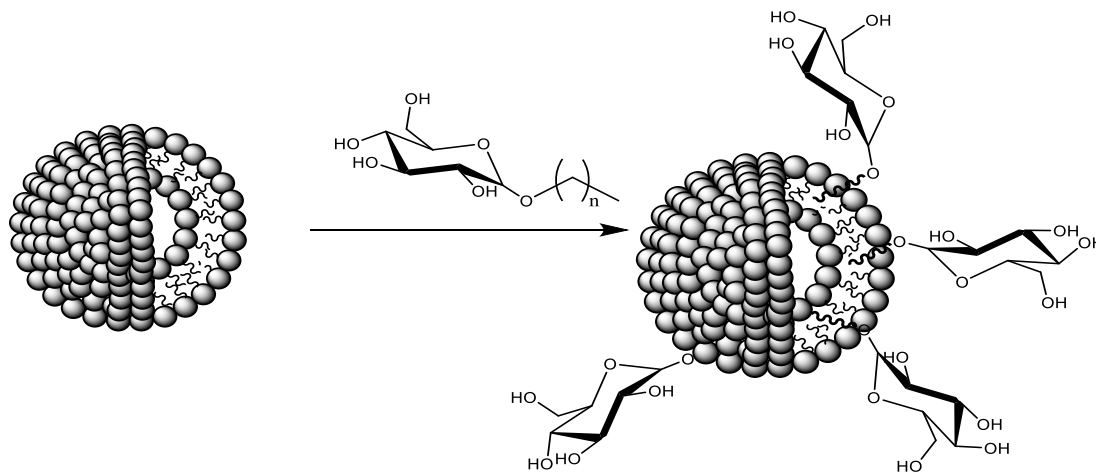


Figure 1.7. Incorporation of amphiphilic glycoconjugates into the outer leaflet of catanionic vesicles.

1.5 Lipidated Glycans of Bacteria

Lipopolysaccharide (LPS) is a major component of the outer membrane of Gram-negative bacteria and is essential for viability.³ It is composed of three sequential regions:

the lipid A domain, a nonrepeating core oligosaccharide region, and the O-antigen polysaccharide (Figure 1.8). Lipid A is a hydrophobic moiety that is essential for outer membrane integrity and for cell viability. It is a potent immune modulator, recognized by

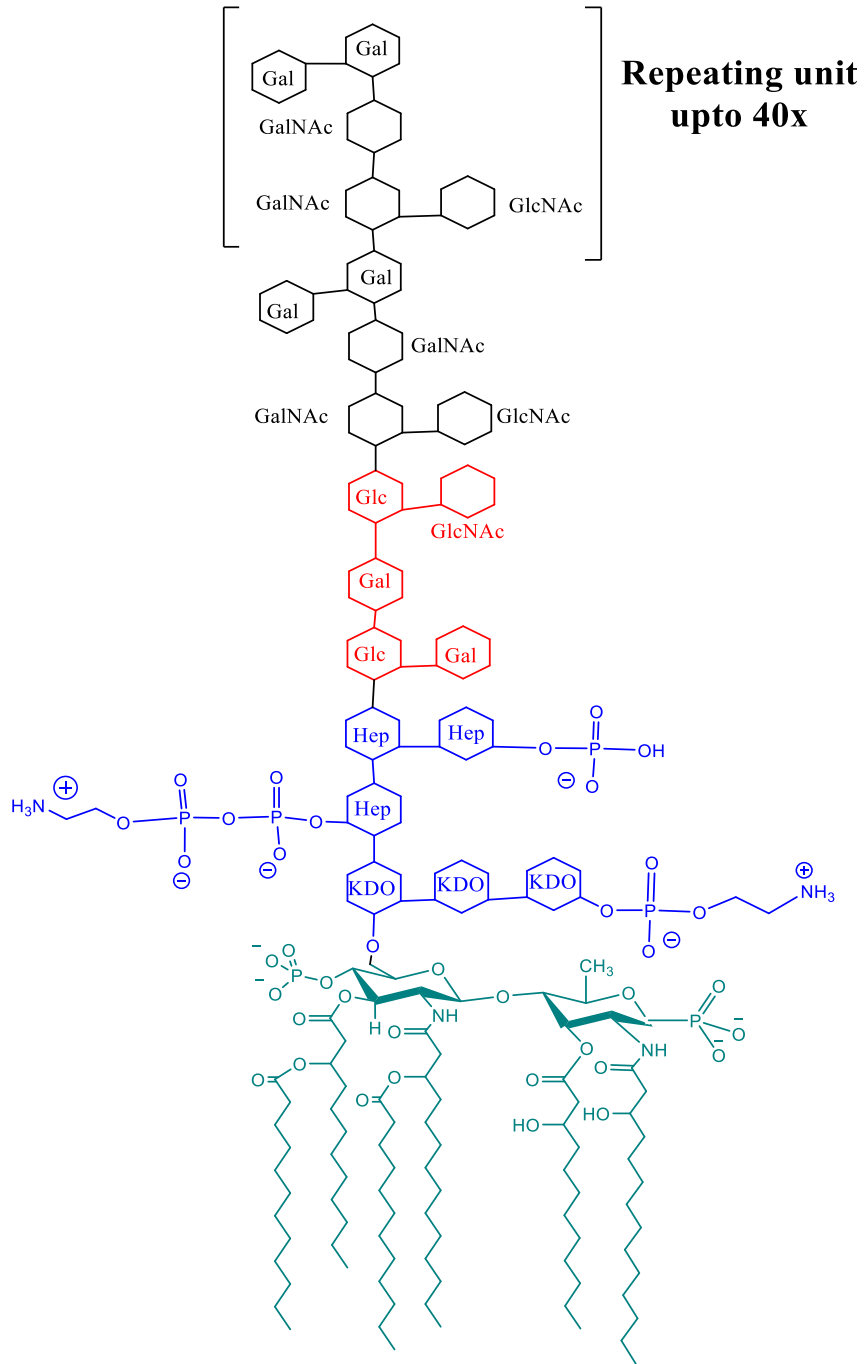


Figure 1.8. General structure of LPS. Sequentially: lipid A (green), inner core (blue), outer core (red), O-antigen (black).

the toll-like receptor 4 (TLR4) triggering inflammation.³⁹ Attached to the lipid A moiety is the core oligosaccharide region, composed of the inner and outer core. The inner core consists of monosaccharides unique to prokaryotes including the acidic 3-deoxy-D-manno-oct-2-ulosonic acid (KDO) and L-glycero-D-mannoheptose (L,D-Hep).³⁹ Additionally, the inner core glycans can be decorated with phosphates or phosphorylethanolamine (PEtN), which modulate the charge and conformation of the structure.^{3, 39, 40} The outer core displays more structural diversity than the inner core, but this variation appears to be limited within a particular genus and species of bacteria.³⁹

In many non-mucosal Gram-negative bacteria, including *Enterobacteriaceae*, *Pseudomonadaceae*, *Pasteurellaceae*, and *Vibrionaceae*, the outer core in the nascent lipid A-core LPS molecule serves as the acceptor for a long repeating polysaccharide known as the O-antigen.³⁹ The O-antigen is structurally diverse, with more than 60 monosaccharides identified as components.³⁹ Further amplifying the diversity are variations in glycosidic linkages and non-carbohydrate substitutions. The heterogeneity of expressed LPS molecules modulate a bacterium's infectivity and fitness through a number of mechanisms. A particular LPS structure can impart resistance to cationic antimicrobial peptides,⁴¹ facilitate the evasion of complement-mediated cell lysis,⁴² and influences bacterial binding to host cell receptors.³⁹

Lipooligosaccharide (LOS) is a structural variant of LPS that terminates at the outer core region (Figure 1.9). LOS is found on mucosal pathogens such as *Bordetella pertussis*, *Haemophilus influenzae*, *Neisseria gonorrhoeae*, and *N. meningitidis*.⁴³ In contrast to LPS, LOS can be branched with one to three oligosaccharide chains extending from the inner core heptose molecules. LOS, like LPS, is immunogenic, and in the case

of *N. gonorrhoeae* is responsible for uterine scarring, predisposing females to the development of ectopic pregnancies and infertility.⁴⁴

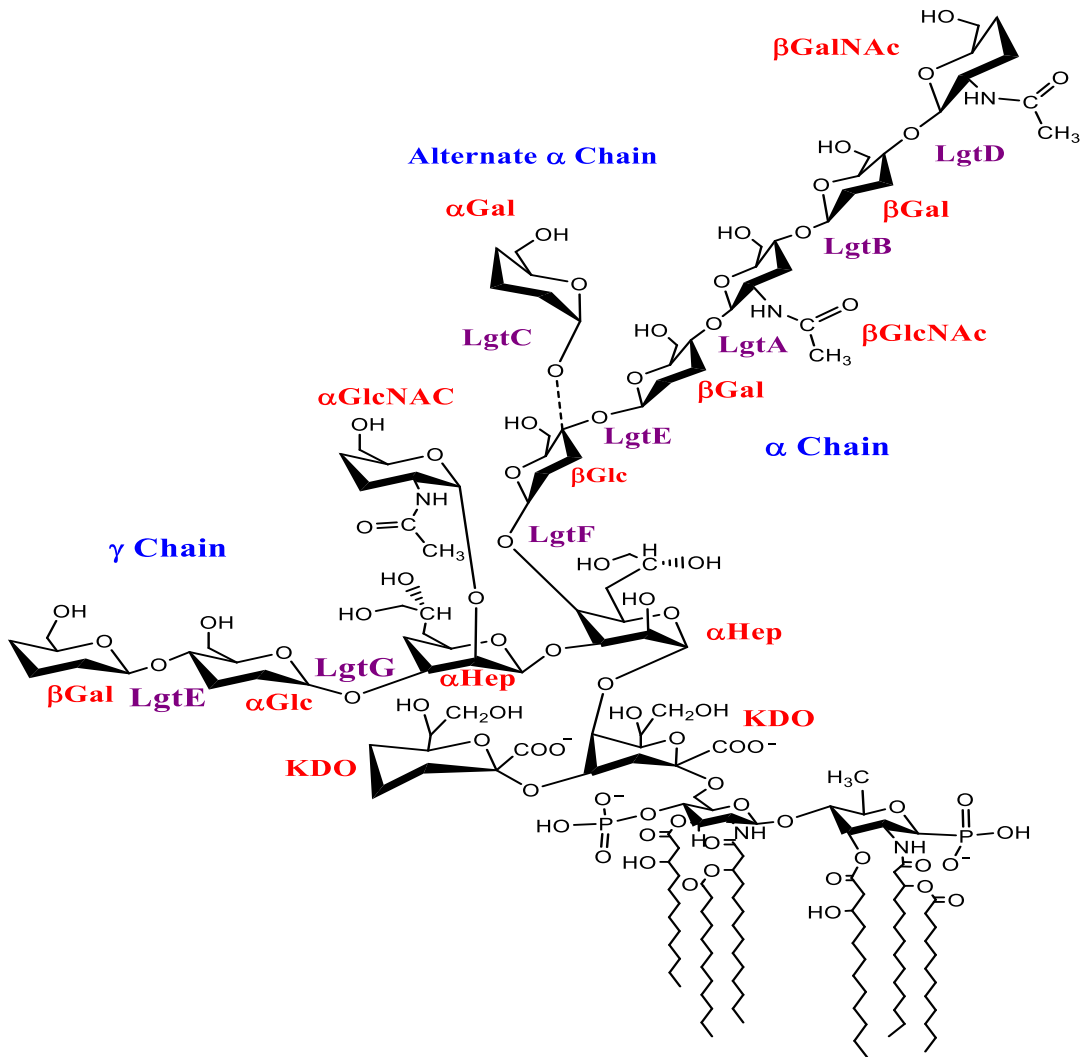


Figure 1.9. Diagram of *N. gonorrhoeae* LOS. The incorporated monosaccharides are indicated in red. The glycosyltransferases responsible for glycosidic bond formation are indicated in purple. The branched chains of LOS are indicated in blue.

The outer core of LOS exhibits a high degree of inter- and intra-strain variability due to the selective pressures of host environment and immune response.³⁹ *N. gonorrhoeae* LOS displays considerable antigenic variation, and distinct structural variants are often simultaneously expressed on the same bacterium.^{45, 46} Exemplifying the extreme heterogeneity of LOS, a strain of *N. gonorrhoeae* isolated from a patient with

pelvic inflammatory disease (PID) was determined to simultaneously express six different LOS epitopes on a single cell.⁴⁷ Monoclonal antibody binding studies indicate that *N. gonorrhoeae* LOS antigenic variation occurs at a frequency of 10^{-2} - 10^{-3} , indicating a genetic regulatory mechanism.⁴⁵ LOS structural modulation can influence *Neisseria* interactions with host tissues and can direct the course of infection.⁴⁶

The outer core structure of *N. gonorrhoeae* LOS often mimics human glycosphingolipids. For example, the LOS epitope lacto-*N*-neotetraose (Gal β 1-4GlcNAc β 1-3Gal β 1-4Glc) found on *N. gonorrhoeae* mimics human paragloboside, a glycosphingolipid expressed on human red blood cells.⁴³ The addition of *N*-acetylgalactosamine to lacto-*N*-neotetraose (GalNAc β 1-3 Gal β 1-4GlcNAc β 1-3Gal β 1-4Glc) is often observed in wild-type *Neisseria* LOS and mimics human gangliosides.⁴⁵ The ability of *Neisseria* to mimic human glycans is not only a mechanism by which the organism can evade the host immune response, but is also a means to exploit exogenous molecules from the host that associate with the mimicked glycan.⁴⁶ Apicella *et al.* determined that the lacto-*N*-neotetraose LOS epitope bound asialoglycoprotein receptors (ASGP-R) expressed on primary human urethral epithelial cells, promoting endocytosis and facilitating infection of host tissues.⁴⁸

LOS can also influence a host's response to infection. LOS is the target for bactericidal activity of human sera in individuals suffering from gonorrhea.⁴⁹ Bactericidal activity is an innate immune response induced by complement-mediated cell lysis.⁵⁰ *N. gonorrhoeae* can resist complement mediated killing by sialylation of its LOS *in vivo*.^{45, 50} The gonococcus expresses an α -2-3-sialyltransferase on its outer membrane and uses exogenous cytidine-monophosphate *N*-acetylneuraminic acid (CMP-NANA) from the

host as a donor substrate.⁸ While sialic acid deposition affords serum resistance, it also reduces the bacterium's ability to invade epithelial tissues.^{45, 46} LOS antigenic variation, therefore, increases *N. gonorrhoeae* fitness *in vivo* by allowing the gonococcus to switch from an invasive to a serum-resistant phenotype depending on environmental stimuli.

Distinct glycoforms appear to be favored at different stages of infection.^{12, 44} The exact causes of this selective pressure and their influence on host: pathogen interactions remain undefined. The ambiguity is in large part due to the fact that *in vitro* investigations of LOS and the conjugate glycan binding proteins remains a challenge because of the insolubility of the lipid A moiety.¹⁴ LOS binding proteins are often determined in the context of a synthetic LOS structure,^{15, 51} in a whole cell background,² or on O-deacylated LOS.¹⁴ To fully elucidate the influence of LOS structure in *Neisseria* pathogenesis, a platform devoid of other bacterial outer membrane components, but that mimics the bacteria cell in charge, outer membrane composition, and presents the glycan in a biologically relevant manner, is necessary. SDBS-rich cationic surfactant vesicles meet these requirements and could be used as a *N. gonorrhoeae* cell mimic. We hypothesized that cationic vesicles decorated with LOS would present the glycan in such a way that the glycan would serve as a substrate for bacterial glycosyltransferases.

1.6 LOS Biosynthesis

The glycan component of *Neisseria* LOS is synthesized by the protein products of seven lipooligosaccharide glycosyl transferase (*lgt*) genes. Five genes, *lgtABCDE*, are clustered in a single locus in the *Neisseria* chromosome. The *lgt* locus has been characterized genetically by the Stein Lab as well as other groups.^{44, 45, 52, 53} Gotschlich determined that the *lgtA*, *lgtC*, and *lgtD* genes in *N. gonorrhoeae* contained runs of

guanine within the coding sequence of these genes, termed poly-G tracts.⁴⁵ These poly-G tracts are a mechanism of phase variation, allowing for strand slippage during DNA replication, ultimately resulting in in-frame or out-of-frame transcripts. Further studies demonstrated a *N. gonorrhoeae* strain that had *lgtA* frame shifted to the “off” position, continued to synthesize a basal level of LgtA positive LOS structures.^{44, 52} The observation was explained by translational strand slippage of the ribosome on the out of frame mRNA, resulting in an in-frame protein product. Braun *et al.* demonstrated that there are multiple promoters within the *lgtABCDE* locus eliciting complex transcriptional control, with limiting concentrations of LgtA, LgtB, LgtC, LgtD, and LgtE being made. This results in the production of multiple LOS structures.⁴⁴ These observations indicate that the glycosyltransferases involved in LOS biosynthesis are extremely efficient. The translational products act sequentially to synthesize the full-length α -chain, as well as the alternate α -chain (Figure 1.9). The *lgtA* gene encodes for a β -1,3-*N*-acetylglucosaminyltransferase, whereas *lgtD* encodes a β -1,4-*N*-acetylglucosaminyltransferase. LgtA and LgtD both utilize UDP-*N*-acetylglucosamine as a donor substrate. *lgtB* and *lgtE* encode β -1,4-galactosyltransferases, both utilizing the common donor substrate UDP-D-galactose. The middle open reading frame in the cluster, *lgtC*, encodes a α -1,4-galactosyltransferase.

Another property of the *lgt* operon is the high degree of homology between the *lgtA* and *lgtD* genes and between the *lgtB* and *lgtE* genes.⁴⁵ The amino acid sequence of the gene pairs is nearly identical in the amino-terminus, but diverges towards the carboxyl-terminus.⁴⁵ The observed sequence homology and divergence is explained by the activities of these gene products. These gene pairs encode for glycosyltransferases

that utilize the same donor substrate, UDP-GlcNAc and UDP-Gal, respectively. The *lgtABDE* sequence analysis suggests that the N-terminus of these Leloir glycosyltransferases is responsible for donor substrate binding, whereas the C-terminus imparts acceptor substrate binding specificity.

Following the identification of the LOS biosynthetic genes, numerous groups have characterized the protein products. Coding sequences for LgtA, LgtB, LgtC, and LgtE have been cloned and expressed in *E. coli*, and subsequently purified.^{2, 15, 44, 54} The kinetic parameters of LgtA, LgtB, and LgtC for various synthetic acceptors have also been determined. For LgtC the $K_{M(\text{app})}$ for the acceptor substrate *p*-nitrophenol- β -D-lactoside was determined to be 1.4 ± 0.1 mM.¹⁵ LgtA had a similar $K_{M(\text{app})}$, 4.3 mM, for the same substrate.⁵⁴ LgtB was determined to have a $K_{M(\text{app})}$ for *p*-nitrophenol *N*-acetyl- β -D-glucosaminide of 0.6 ± 0.1 mM.¹⁵ The implication of these $K_{M(\text{app})}$ values in the millimolar range is that the enzymes appear to have low affinity for the acceptor substrate. The conclusion from the biochemical data, however, contradicts the *in vivo* observations that minimal concentrations of these enzymes are needed to synthesize the corresponding LOS.

Further discrepancies arise in studies examining the *in vitro* activity of LgtE. An early study did not observe LgtE activity on *p*-nitrophenol *N*-acetyl- β -D-glucosaminide, and concluded that the enzyme had stringent acceptor specificity, requiring the terminal glucose to be linked to a heptose molecule as in LOS.¹⁴ Work conducted by Piekarowicz *et al.*, however, indicated that LgtE had flexible acceptor substrate specificity, mediating the transfer of galactose to both glucose terminal and galactose terminal whole cell LOS

structures.² It is clear from these inconsistent observations that the acceptor substrate presentation influences LgtE activity.

The work of this dissertation focuses on the exploiting the unique biochemical properties of LgtE. Previous studies indicate that the enzyme is extremely efficient *in vivo*,⁴⁴ however, the *in vitro* activity appears to be exquisitely sensitive to substrate presentation.¹⁴ LgtE, therefore, is uniquely qualified as a model enzyme to examine the utility of cationic surfactant vesicles as a platform for oligosaccharide biosynthesis.

LgtE is an inverting galactosyltransferase that mediates the transfer of a galactose moiety on to a terminal glucose LOS acceptor molecule (Figure 1.10). The *in vitro* synthesis of oligosaccharides onto a terminal glucose has wide-spread applicability as many prokaryotic glycoconjugates have a terminal glucose containing disaccharide.⁵⁵

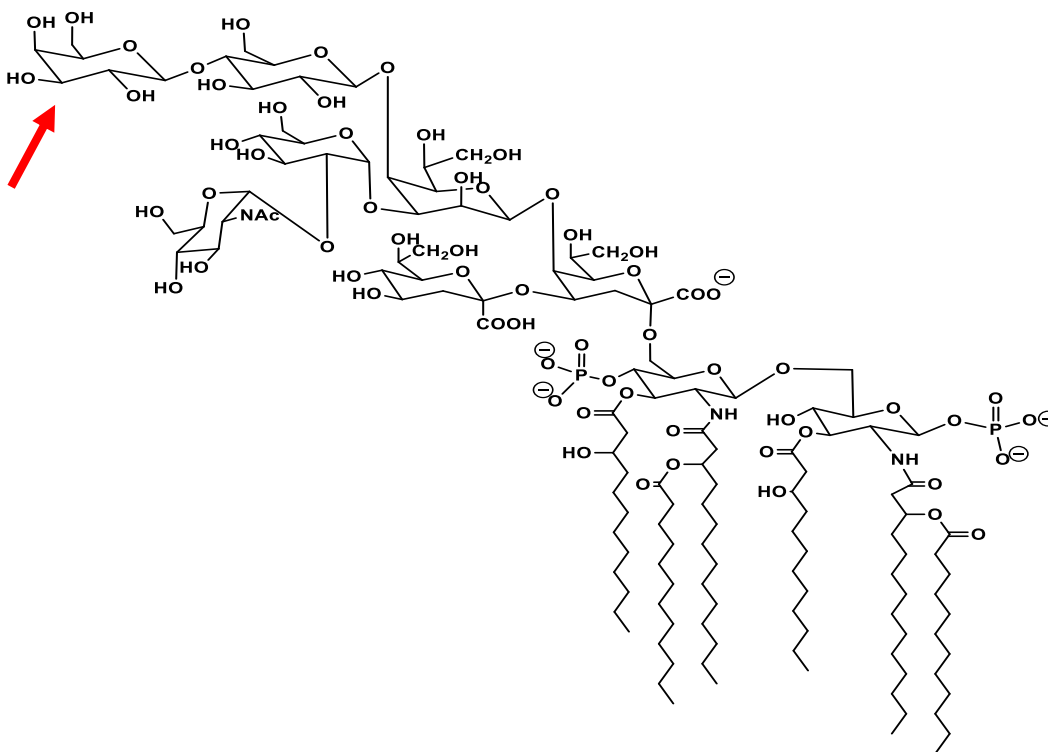


Figure 1.10. Δ lgtA truncated LOS structure. LgtE catalyzes the final step in the biosynthesis of this structure. The arrow indicates the galactosyl moiety transferred by LgtE.

LgtE is a member of the glycosyltransferase GT-A family based on predicted structure.¹² GT-A enzymes contain two domains positioned in close proximity to each other. Both domains have a Rossmann-like fold, consisting of an α helix/ β sheet/ α helix sandwich.⁵⁶ The Rossmann fold is characteristic of nucleotide binding proteins. One domain is attributed to the sugar nucleotide-binding cleft and the other is the acceptor-binding pocket.⁶ The central β sheet of one domain, together with a flanking β sheet from the other domain, forms the active site of the enzyme. Within the sugar nucleotide-binding domain of LgtE is the conserved DXD amino acid motif. This motif coordinates a divalent metal ion cofactor, Mn^{2+} , electrostatically stabilizing the increasing negative charge on the nucleotide diphosphate leaving group during the reaction.^{6, 14}

LgtE is further grouped into the β -1,4-galactosyltransferase subfamily GT-25. These enzymes have an additional conserved aspartic or glutamic acid residue in their active site that acts as a base which catalyzes the deprotonation of the acceptor substrate for a double displacement, S_N2 -type, nucleophilic attack at the C1 position of the nucleotide sugar donor (Figure 1.11).^{6, 14} Weijers *et al.* demonstrated that the transition state is an oxocarbenium ion-like intermediate formed by the donor sugar, the nucleotide diphosphate, and the acceptor moiety. The final product results from the addition of a monosaccharide to the acceptor substrate with the formation of a β -glycosidic bond.¹⁴

LgtE, along with the other enzymes involved in LOS biosynthesis, sequentially add sugars to the growing LOS molecule in a process analogous to an assembly line. LgtABCDE enzymes exist *in vivo* as an inner membrane protein complex,³⁹ noncovalently associated with the membrane *via* pairs of basic residues in the carboxyl-terminus.¹⁵ Lipid A of the nascent LOS molecule is also incorporated into the inner

membrane with the inner core sugars extending into the cytoplasm.³⁹ The physical proximity of the protein complex and nascent LOS molecule increases the effective acceptor substrate concentration, and may explain the high efficiency of glycosyltransferase activity observed *in vivo*⁴⁴ that is not observed *in vitro*.¹⁴

1.7 *Research Objectives*

Despite the ubiquity of carbohydrates in nearly all facets of life, to date a facile method of synthesizing complex carbohydrates and investigating their interactions with cognate glycan binding proteins has not been reported. To address this issue, the primary aim of this dissertation is to demonstrate that recombinant glycosyltransferases can synthesize glycans of known structure on a cationic surfactant vesicle platform, and that specific protein- glycan interactions can be examined in this context. This will form the basis for the development of high-throughput glycomic array technology, which is imperative for advancement in the field of glycomics. The work presented herein demonstrates that cationic surfactant vesicles are ideally suited to serve as the platform for the development of technology that will facilitate a mechanistic understanding of carbohydrate structure and function.

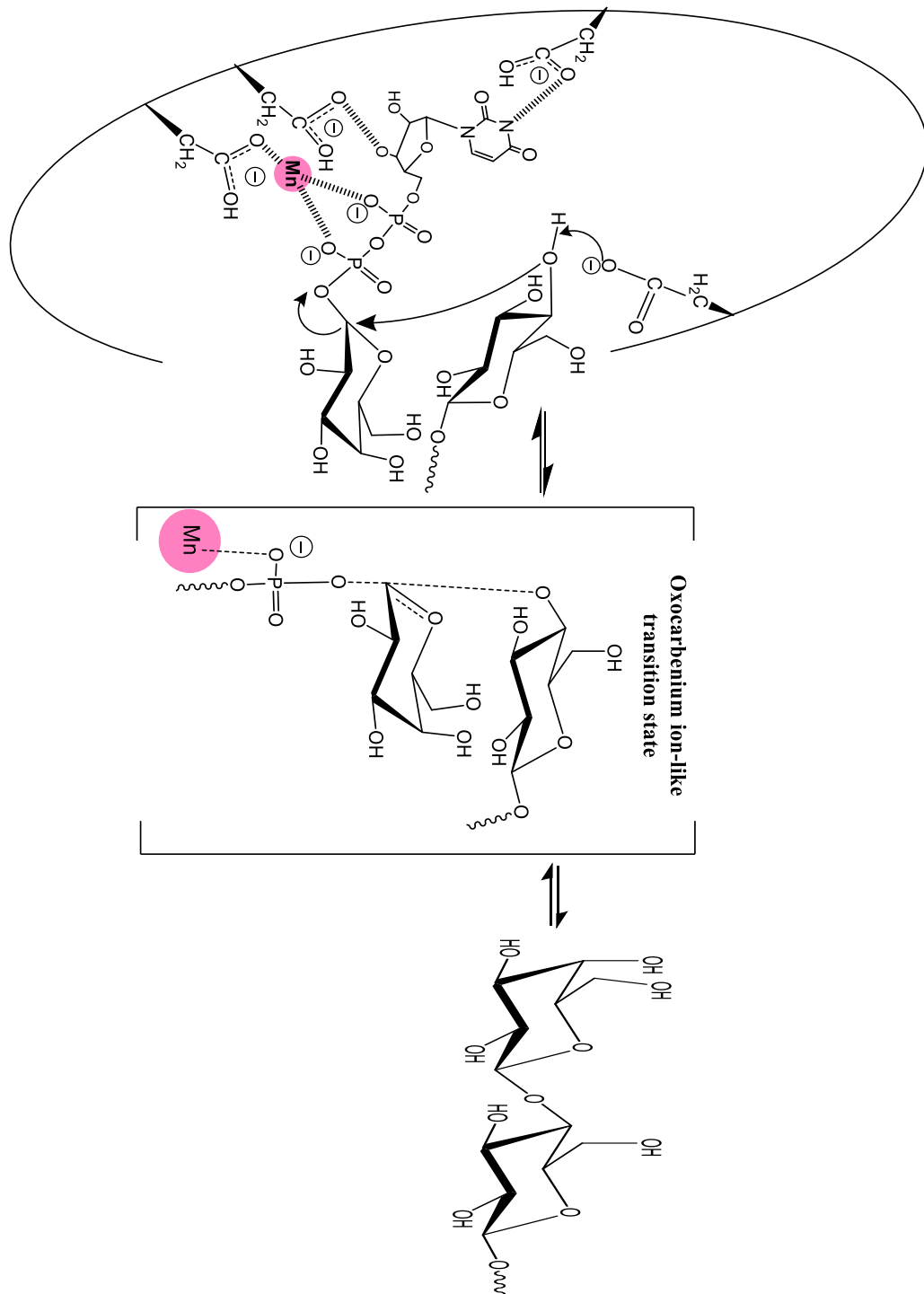


Figure 1.11. Proposed reaction mechanism of the inverting β -1,4-galactosyltransferase LgtE. Adapted from reference 13.

Chapter 2: Expression, Purification, and Characterization of LgtE

2.1 *Introduction*

Glycans are complex, three-dimensional structures that unlike proteins are not encoded for or synthesized from a template. Rather glycosyltransferases catalyze the transfer of monosaccharides onto an acceptor substrate. Glycan structural diversity is influenced by cellular metabolism,⁷ developmental stage,⁴ cell type,⁷ and nutrient availability,⁴³ and as such glycoconjugates are often isolated as heterogeneous glycan structures.⁵⁷

Low yields of coupling reactions and complications arising from effective control of regio- and stereoselectivity during glycan synthesis, in addition to the difficulty in isolating pure structures, results in a limited availability of homogenous glycoconjugates. The limited availability of ligands has significantly challenged investigations of protein-glycan interactions at a molecular level.¹⁷ Development of large-scale production techniques for complex carbohydrates is of critical importance in the field of glycomics. These techniques would facilitate further investigations into glycan structure, function, and recognition. Additionally, the facile synthesis of oligosaccharides of known structure would have a significant impact in the pharmaceutical industry, since therapeutic glycoproteins are commonly employed in the treatment of chronic and infectious diseases. However, manufacturers continue to have difficulty producing drugs with a homogenous glycan profile, as required by the U.S. Food and Drug Administration (FDA).⁵⁸ A recent report further highlighted the pressing need for a system that allows for the synthesis of homogenous glycans, with the revelation that three commercially

available glycoprotein drugs exhibit batch variation.⁵⁹ Owing to the diverse role glycans play in the biological functions of glycoproteins, this revelation raises serious regulatory concerns.

The *in vitro* utilization of purified bacterial glycosyltransferases is recognized as a potential method for the biosynthesis of complex oligosaccharides.^{15, 54}

Glycosyltransferases expressed in Gram-negative bacteria are an optimal choice as compared to their mammalian counterparts. The enzymes involved in LOS biosynthesis synthesize human glycoconjugates mimics¹⁰ but lack a N-terminal transmembrane domain.¹⁵ Therefore, bacterial enzymes are more soluble than their mammalian counterparts facilitating their expression and purification.¹⁵ Two previous studies provide evidence that *N. meningitidis* glycosyltransferases are amenable to the large-scale production of oligosaccharides.^{15, 54} In these *in vitro* studies, the β -1,4-galactosyltransferase, LgtB, the α -1,4-galactosyltransferase, LgtC, and the β -N-acetylglucosaminyltransferase, LgtA, were observed to modify a synthetic acceptor substrate and were not inhibited by nucleotide uridine-diphosphate (UDP), a reaction byproduct.

The previous research performed with *Neisseria* glycosyltransferases lends credence to the development a one-pot multi-enzyme system for the *in vitro* synthesis of oligosaccharides.⁶⁰ To fully synthesize the mimics of human glycans such as lacto-N-neotetraose, Gal- β -1,4-N-GlcNAc- β -1,3-Gal- β -1,4-Glc, or the P^k blood group trisaccharide, Gal- α 1,4-Gal- β -1,4-Glc, however, the enzyme responsible for the initial β -Gal addition must be obtained. Previous research provided biochemical evidence that the enzyme encoded by the *lgtE* gene was responsible for this initial β -1,4-

galactosyltransferase event in *Neisseria* LOS biosynthesis.² Piekarowicz and Stein provide direct evidence of the enzyme's *in vitro* activity and flexible acceptor substrate specificity on various LOS structures. Additionally, the study conducted by Piekarowicz and Stein contradicted the previous conclusion by Wakarchuk *et al.* that LgtE was unable to modify synthetic β -glycosyl acceptor substrates *in vitro*.⁶¹

2.2 *Specific Aims and Results*

Based on these contradictory findings, the goals of this thesis were:

1. To establish the conditions for the stable expression and purification of LgtE, and
2. To develop a high-throughput technique demonstrating the purified enzyme's β -1,4-galactosyltransferase activity. In the process of determining the appropriate conditions for expression, I also developed a novel method for the solubilization of membrane-associated macromolecules.

2.2.1 Optimization of LgtE Expression in *E. coli*

The glycosyltransferases involved in the biosynthesis of LOS, including LgtE, are predicted to be noncovalently associated, *via* pairs of dibasic residues in the C-terminus, with the periplasmic membrane *in vivo*.¹⁵ This property precludes the complete solubility of the full-length recombinant proteins. Previously, it was reported that the majority of LgtE was present in the insoluble fraction of the cell extract and that there were precipitated proteins present both before and after purification.² In an effort to increase protein solubility, the cell lysate was supplemented with the chaotropic agent, urea. Chaotropic agents disrupt inter- and intra-molecular noncovalent interactions, inducing

protein denaturation and facilitating solubilization. While the majority of the protein remained in the insoluble fraction under denaturing conditions, a significant amount was observed in the soluble fraction (Figure 2.1 lane 2 and Appendix A2).

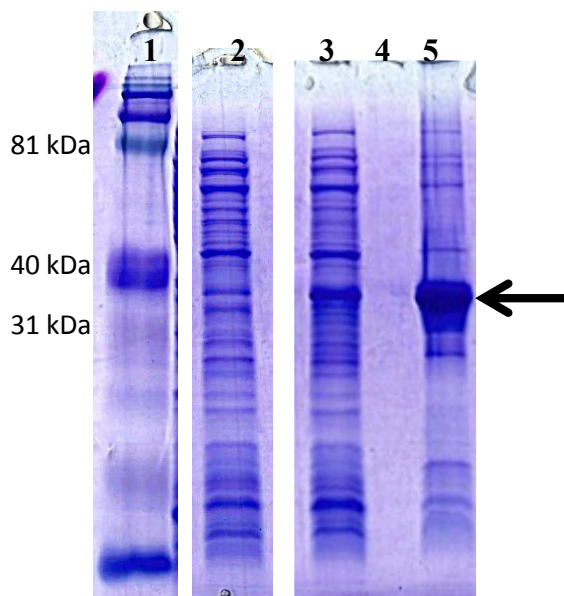


Figure 2.1. 15% Tris-HCl SDS-PAGE of 8M urea solubilized LgtE. *E. coli* cells were grown to mid-log phase and LgtE expression was induced by the addition of 1 mM IPTG. Lane 1: 7 μ l Kaleidoscope prestained standards (Bio-Rad Laboratories, Hercules, CA.). Lane 2: Soluble fraction uninduced. Lane 3: Soluble fraction with 8M urea treatment. Lane 4: Lysing buffer alone. Lane 5: Insoluble fraction with 8M urea treatment. LgtE is predicted to run at approximately 35 kDa², and is indicated by the arrow.

2.2.2 Purification of LgtE

The soluble fraction was applied to Ni²⁺-NTA resin (Qiagen) according to the manufacturer's instructions. Subsequently, the eluate was dialyzed to remove excess imidazole and reapplied onto the Ni²⁺-NTA column. Following this second round of purification, a single band of approximately 35 kDa was observed by SDS-PAGE analysis, indicating that purified protein was obtained (Figure 2.2 lane 1).

Despite the multiple rounds of purification, there remained a small amount of low molecular weight co-eluate, in fraction 4. At present, the identity of this band is unknown, however, it is likely that there was some proteolysis of the full length protein with the resultant polypeptide retaining the N-terminal hexahistadine tag.

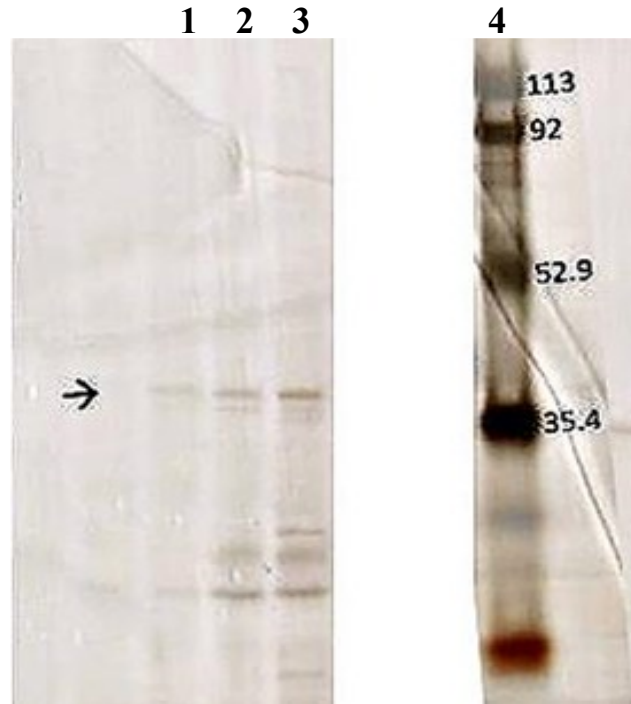


Figure 2.2. 15% Tris-HCl SDS-PAGE of purified LgtE. Following dialysis after the first Ni²⁺-NTA column purification, the recovered protein sample was re-purified on new resin. (From right to left) Lane 1: 11 μ l elution fraction 4; Lane 2: 11 μ l elution fraction 3; Lane 3: 11 μ l elution fraction 4; Lane 4: 7 μ l Kaleidoscope prestained standards. The arrow indicates the band corresponding to the purified protein.

2.2.3 Demonstration of *In Vitro* Glycosyltransferase Activity on Whole Cell *Gonococcus*

Following protein purification, the fractions containing purified protein were pooled and dialyzed against the dialysis buffer (Materials and Methods). Under these conditions there was no observed protein precipitation, indicating an improvement in the purification conditions as compared to previous work performed in our lab.² The purified enzyme was stored at -20 °C.

To confirm that LgtE had re-folded properly and that β -1,4-galactosyltransferase activity is maintained, I developed an indirect enzyme-linked immunosorbent assay (ELISA) procedure to detect LgtE catalyzed LOS modification on whole cell gonococcus. Figure 2.3 illustrates the method by which product formation is detected. 2-1-L8, a monoclonal antibody specific for LOS expressing a lactosyl α - chain structure,⁴⁰ is used as the capture antibody. The antibody will not bind the glucose terminal acceptor substrate (Figure 2.3A); however, following LgtE LOS modification, in which a galactosyl moiety is transferred to the terminal glucose residue, the whole cell gonococcus will now be retained by 2-1-L8 (Figure 2.3B).

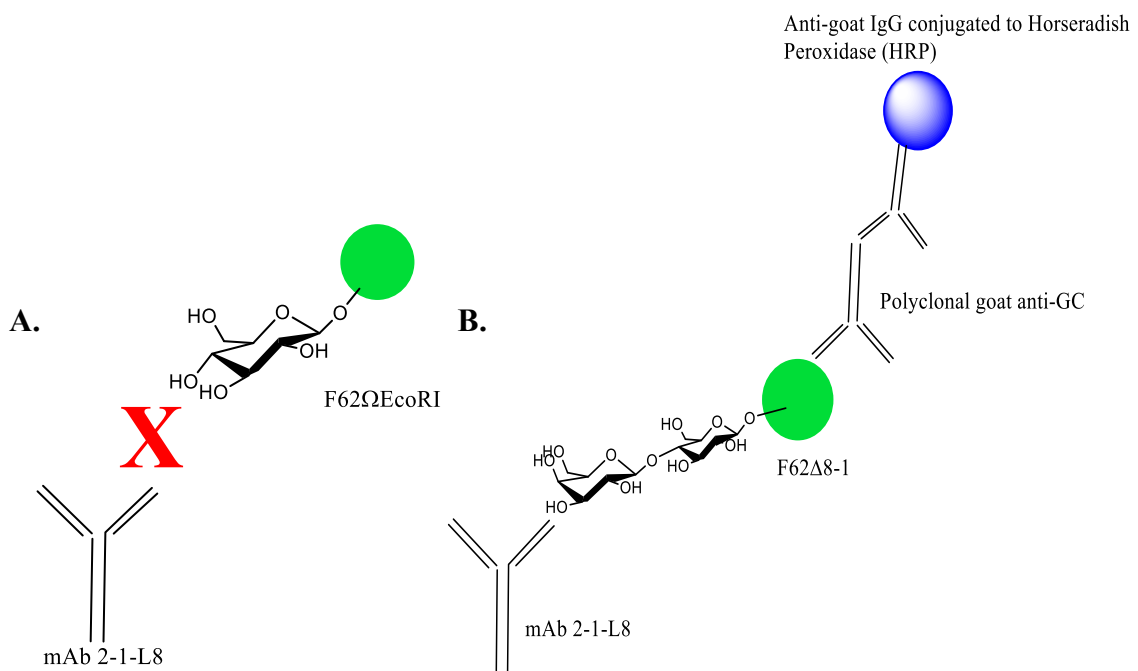


Figure 2.3. Schematic of the indirect ELISA experimental setup. **A.** Negative control: F62 Ω EcoRI will not bind to the capture antibody, as it expresses a glucose terminal LOS structure. **B.** Positive control: F62 Δ 8-1 expresses the lactose terminal LOS structure that is the epitope recognized by the capture antibody. This structure is the product of LgtE LOS modification.

LgtE was incubated in reaction buffer containing *N. gonorrhoeae* strain F62 Ω EcoRI. Strain F62 Ω EcoRI primarily expresses a LOS structure composed of a single glucose in the α -chain and a phosphate as the β -chain.^{43, 62} Incubation of whole cell F62 Ω EcoRI with LgtE increased retention by the capture antibody, indicating that LgtE mediated the transfer of galactose to the acceptor substrate (Figure 2.4).

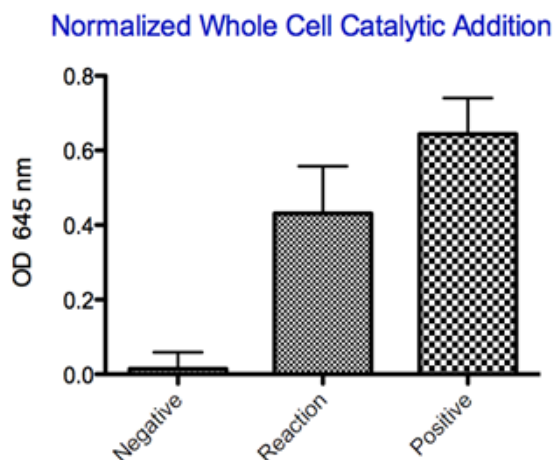


Figure 2.4. Quantification of LgtE catalyzed modification of whole cell LOS by indirect ELISA. Whole cell F62 Ω EcoRI serves as the negative control, and whole cell F62 Δ 8-1 serves as the positive control. The numbers depicted represent average values of four trials.

2.2.4 Novel Purification Technique Using Surfactant Vesicles

Our colleagues in the DeShong group have demonstrated that molecules associated with the membrane of whole cell bacteria will associate with SDBS-rich cationic surfactant vesicles. I sought to take advantage of this observation to increase the solubility of LgtE in *E. coli*. LgtE is presumed to associate with the inner membrane of *N. gonorrhoeae in vivo*. I hypothesized that the protein would preferentially associate with cationic vesicles. It appears in figure 2.5A lanes 6-8 that the band corresponding to the induced protein, LgtE, is associated with purified vesicles.

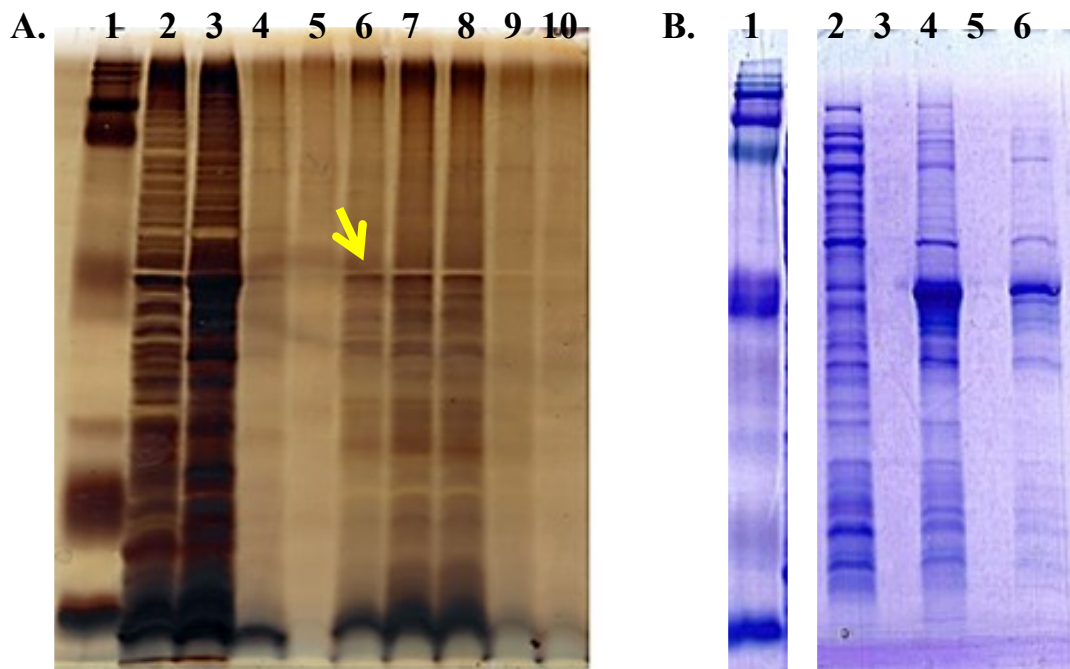


Figure 2.5. **A.** Vesicle extraction of membrane associated molecules. Silver stain of 10-20% Tris-HCl SDS-Page analysis of fractions collected from Sepharose 2B size exclusion column. *Lane 1:* Kaleidoscope protein ladder; *Lane 2:* Uninduced supernatant; *Lane 3:* Induced supernatant; *Lane 4:* Lysing buffer alone; *Lane 5:* Fraction 1; *Lane 6:* Fraction 2; *Lane 7:* Fraction 3; *Lane 8:* Fraction 4; *Lane 9:* Fraction 5; *Lane 10:* Fraction 6. Arrow indicates that band that corresponds to the apparent molecular weight of LgtE **B.** Vesicle extraction of insoluble molecules from the cell pellet. Coomassie Blue stain of 15% Tris-HCl SDS-Page analysis. From left to right: *Lane 1:* Kaleidoscope protein ladder; *Lane 2:* Supernatant under non-denaturing conditions; *Lane 3:* Lysing buffer alone; *Lane 4:* Pellet under non-denaturing conditions; *Lane 5:* Lysing buffer alone; *Lane 6:* Pellet from non-denaturing conditions re-solubilized with anionic surfactant vesicles.

Further, the vesicle extraction method was used to extract insoluble proteins from the cell pellet. The data presented in figure 2.5B lane 6 indicates that the vesicles selectively enrich for the induced protein, as there are less co-extracted proteins compared to the soluble fraction obtained under denaturing conditions. To account for potential misinterpretation based on variations in gel loading, the OD_{650} was monitored to ensure that the cell density under all conditions was consistent. Additionally, the pellet that was not solubilized by surfactant vesicles was re-suspended with the minimal amount of Triton-X 100 required to obtain a suspension in Laemmli buffer. Further work is

needed to determine if the extracted protein can be purified on a Ni²⁺-NTA column and if the protein is catalytically active following purification, but this preliminary data indicates that cationic surfactant vesicles may be used to enrich for insoluble proteins.

2.3 Discussion

The exploitation of glycosyltransferases for the large-scale production of oligosaccharides is worthy of further investigation. A major technical difficulty hindering the development of a “one pot” system is the low solubility of glycosyltransferases. Despite lacking the transmembrane domains of their mammalian counterparts, numerous reports have demonstrated that bacterial enzymes are fairly insoluble, consistent with the observations made in this study.^{2, 15, 54, 61} While it is possible to truncate the enzyme, the C-terminus is predicted to contain the domain responsible for acceptor substrate binding.¹² Therefore, removal of this flexible region may perturb the very same flexible substrate specificity that I hope to exploit for biosynthetic studies.¹⁵

This work aimed to increase the solubility and stability of the recombinant enzyme. Using the above outlined techniques, including urea solubilization and vesicle extraction, a variety of recombinant bacterial glycosyltransferases may be purified to a working concentration, and subsequently utilized for oligosaccharide biosynthesis *in vitro*.

2.4 Experimental

2.4.1 Bacterial Strains, Plasmids, Oligonucleotides, and Culture Conditions.

N. gonorrhoeae strain F62 wild-type was obtained from P. Fredrick Sparling, University of North Carolina, Chapel Hill. F62Δ8-1 has been previously characterized in

this laboratory.^{40, 63} *E. coli* strain BL21 (DE3) [*fhuA2 [lon] ompT gal (λ DE3) [dcm] ΔhsdS λ DE3 = λ sBamHI ΔEcoRI-B int::(lacI::PlacUV5::T7 gene1) i21 Δnin5*] was obtained from New England Biolabs (Ipswich, Mass.). Plasmid pET15b was obtained from Novagen (Madison Wis.). Cloning of *lgtE* into pET15b done by Dr. Piekarowicz and was previously described.²

Neisseria strains were grown in standard gonococcal medium (designated GCP if broth and GCK if agar) (Difco Laboratories) plus growth supplements.⁶⁴ The broth media is supplemented with 0.042% sodium bicarbonate for cultures grown under aerobic conditions, otherwise cultures were incubated at 37°C in a CO₂ incubator. *E. coli* strains were grown on Luria Bertani (LB) agar or in LB broth.⁶⁵ When antibiotic selection is necessary, ampicillin is used at a concentration of 50 µg/ml.

2.4.2 Chemicals, Reagents, Enzymes.

Restriction enzymes were purchased from New England Biolabs (Ipswich, Mass.). All chemicals used were reagent grade or better and were purchased from Sigma Chemical Co. (St. Louis Mo.) unless specified otherwise. 15% and 10-20% precast Tris-HCl gels were obtained from Bio-Rad Laboratories (Richmond, Calif.).

1x SDS-PAGE running buffer was made with 192 mM glycine, 25 mM Tris, and 0.1% SDS in Elix water. 3x Laemmli buffer was prepared with 10% glycerol, 1 M Tris-HCl pH 6.8, 2% SDS, 4% β-mercaptoethanol, and a pinch of bromophenol blue.⁶⁶ Coomassie Brilliant Blue stain was prepared by dissolving 0.25 grams Coomassie Brilliant Blue R-250 per 100 ml of 5:4:1 methanol: Elix water: acetic acid solution. Particulate matter was removed by vacuum filtration through a 0.22 µm bottle top filter

(Corning, Corning, NY). Coomassie Brilliant Blue destaining solution is the 5:4:1 methanol: Elix water: acetic acid solution.

Silver staining solutions were prepared as reported by Tsai *et al.*⁶⁷ The gel was fixed in 10:1 ethanol: acetic acid solution. The sensitization solution was prepared by dissolving 0.83 grams periodic acid in 100 ml Elix water. Silver-ammonia staining solution was prepared by adding 180 mM ammonia drop wise to 0.75% silver nitrate with 45 mM NaOH. Formaldehyde developer contains 200 mg/L citric acid and 0.1% formaldehyde.

2.4.3 Transformation

Plasmid pET15b-lgtE was transformed into *E. coli* strain BL21 (DE3), and a single colony was used to inoculate 25 ml of LB broth containing ampicillin. Cells were incubated with moderate shaking at 37°C until the optical density at 600 nm reached 0.6. 5 ml of the starter culture was then used to inoculate 250 ml of LB broth. Again, the cells were incubated with moderate shaking at 37°C until the optical density at 600 nm reached 0.6.

2.4.4 Induction and Expression of LgtE

Protein expression was induced by the addition of isopropyl β -D-1-thiogalactopyranoside (IPTG) to the culture. IPTG was added to a final concentration of 1 mM, and incubations were continued for 3 hours at 37°C. The cells were collected by centrifugation at 4°C and re-suspended. For purification under non-denaturing conditions, the cell pellet was re-suspended in a minimal volume of lysing buffer containing 50 mM NaH_2PO_4 , 300 mM NaCl, and 10 mM imidazole pH 8.0. Additionally for purification

under non-denaturing conditions, lysozyme to a final concentration of 100 µg/ml, 100 µM phenylmethylsulfonyl fluoride (PMSF), and 0.1% Triton X-100 were added to the re-suspended pellet. The mixture was incubated on ice for 60 minutes. For purification under denaturing conditions, the cell pellet was re-suspended in a minimal volume of lysis buffer containing 100 mM NaH₂PO₄, 10 mM Tris, and 8 M urea pH 8.0.

Cells were lysed by three cycles of freeze thawing at -80°C. To ensure complete lysis, the suspension was transferred to a glass tube and sonicated for a minimum of five pulses at 10 seconds each on ice. The cell extract was clarified by centrifugation for 30 minutes at 15,000 rpm at 4°C in a Sorvall SS34 rotor, and the supernatant containing the soluble fraction was separated from the insoluble pellet. Both the soluble fraction and the insoluble pellet were stored at 4°C, until further analysis or purification.

2.4.5 Protein Purification

All purification steps were performed at 4°C. The soluble fraction was then incubated with Ni²⁺-NTA resin (Qiagen), rocking, for a minimum of three hours. The protein-resin mixture was subsequently packed, according to manufacture instructions, in a column. The flow through was collected and reapplied to the column two times to ensure saturation of the Ni²⁺-NTA resin. The resin was then washed with 5 column volumes of denaturing wash buffer containing 100 mM NaH₂PO₄, 10 mM Tris, and 8M urea, 20 mM imidazole pH 8.0. The protein was eluted following application of the elution buffer containing 100 mM NaH₂PO₄, 10 mM Tris, and 8M urea, and 250 mM imidazole pH 8.0. All buffers were made fresh and equilibrated to a temperature of 4 °C.

Following the first round of purification the elute fractions that contained protein were determined by SDS-PAGE analysis. These fractions were dialyzed against the denaturing lysis buffer pH 8.0, overnight at 4 °C. The protein mixture was then applied to 3 ml of fresh Ni²⁺-NTA resin pre-packed in a clean column. Again, the collection volume was reapplied twice to ensure saturation. The column was washed and the bound protein was eluted, as previously described. The presence of purified protein was determined by SDS-PAGE.

The purified protein was refolded by overnight dialysis at 4°C against buffers containing a linear reduction in urea concentration (8M, 6M, 4M, 2M, 1M, 0.5M, and 0M). Additionally, dialysis buffers contained 20 mM HEPES pH 7.5, 10 mM β-mercaptoethanol, 0.5 mM PMSF, 50 mM glycine, 5 mM EDTA, and 20% glycerol. The enzyme was then stored at -20 °C.

2.4.6 SDS-PAGE Analysis

5 µl of the cell pellet solubilized with Triton X- 100 was added to 3x Laemmli lysing buffer. 5 µl (unless otherwise noted) of column fractions or the soluble fractions were added to 3x Laemmli buffer. The samples were run on a 10-20% Criterion™ Precast Tris-HCl gel in 1x Tris-glycine running buffer at 100 volts for approximately 2.5 hours.

Those gels analyzing whole cell lysates were stained with Coomassie Brilliant Blue. Staining followed the method outlined by Sambrook *et al.*⁶⁸ whereby following SDS-PAGE analysis the gel is incubated in Coomassie staining solution for 16 hours. The

next day, the stain was removed and protein bands were visualized by washing out excess Coomassie dye with de-staining solution.

To detect lower protein concentrations such as in fractions collected off the Ni²⁺-NTA column, gels were stained with silver salts.^{67, 68} The gel was fixed overnight in a solution of 40% ethanol- 5% acetic acid and then oxidized in 0.83% periodic acid for 5 minutes. The gel was washed for 2 hours in multiple changes of H₂O every 20 minutes, stained for 5 minutes in silver staining solution (22.5 mM NaOH, 0.42% NH₄OH, 47 mM AgNO₃), and rewashed for 2 hours in multiple changes of H₂O every 20 minutes. The gel was developed (100 ml of 0.005% citric acid-0.007% formaldehyde) until bands became visible. A digital image of the gel was then obtained on a flatbed scanner.

2.4.7 Construction of F62ΩEcoRI

N. gonorrhoeae strain F62ΩEcoRI was originally constructed by Dr. Derek Braun.⁴⁴ Following the defined protocol, *N. gonorrhoeae* strain F62 was transformed with the plasmid pLgtDEΩEcoRI. pLgtDEΩEcoRI has a spectinomycin-resistance (specR) Omega interposon cassette (Ω), flanked by rho-independent transcriptional terminators, inserted downstream of the putative promoter initiating lgtE transcription.

To verify that the Ω cassette had properly inserted into the *EcoRI* site 1% agarose gels were prepared in TBE buffer with 10 μl ethidium bromide (10 mg/ml). Agarose gel electrophoresis was performed at constant voltage (100 V) until the loading dye front had reached the bottom of the gel. Gels were visualized using a Gel Doc XR ultraviolet transilluminator (Biorad) and gel images were processed using Quantity One 1-D analytical software version 4.6.1 (Biorad).

The resulting LOS phenotype of the recombinant F62 Ω EcoRI strain is equivalent to the inactive LgtE, or Δ lgtE, LOS chemotype, as confirmed by SDS-PAGE analysis.

2.4.8 Galactosyltransferase Assay

Reactions were carried out in a total volume of 50 μ L. The reaction buffer contained 20 mM HEPES pH 7.5, 1 mM MnCl₂, 5 x 10⁶ whole cells, 1 μ g purified LgtE, and 1 mM UDP- α -D-galactose (Santa Cruz Biotechnology). The reaction was carried out for a minimum of 3 hours at 30 °C. Whole cell bacteria were killed by gentamicin sulfate (100 μ g/ml) treatment for 3 hours at 37 °C, prior to the reaction with LgtE. The controls contained all the components of the reaction buffer minus UDP-galactose.

2.4.9 ELISA

Monoclonal antibody 2-1-L8⁴⁰ was added undiluted to the wells of a 96 well microtiter plate (Corning, Corning, NY). The wells were then blocked with 0.1% blocking reagent (Roche Applied Science, Indianapolis, IN). Wells were washed with 0.1% PBS-Tween wash buffer pH 7.4. The control and reaction mixtures were incubated in the wells for a minimum of one hour, followed by PBS-Tween wash. Polyclonal goat anti-gonococcus antibody was then incubated in the wells. Following a wash step, donkey anti-goat IgG conjugated to horseradish peroxidase (Jackson ImmunoResearch Laboratories, West Grove, PA) was added to the wells. After a final wash step, 3,3',5,5'-tetramethylbenzidine (Sigma Aldrich, St. Louis, MO) liquid substrate was added to the wells and the plate was protected from light. The OD at 645 nm was measured with SpectraMax 190 Absorbance Plate Reader (Molecular Devices, Sunnyvale, CA), and data were acquired with SoftMax Pro Software (Molecular Devices, Sunnyvale, CA).

2.4.10 Surfactant Vesicle Solubilization

Sodium dodecylbenzenesulfonate (SDBS) was purchased from TCI America and was utilized without further purification. Cetyltrimethylammonium tosylate (CTAT) was purchased from Sigma and was recrystallized from ethanol-acetone to give a white powder. The purified solid was stored at room temperature in a desiccator containing Drierite. The cell pellet, with a wet mass of approximately 1.5 grams, was re-solubilized in 30 ml of Elix water and 21 mg of SDBS. The pellet-surfactant mixture was gently stirred, at 4 °C, for 16 hours. 9 mg of CTAT was then added to the mixture, for a total surfactant concentration of 1 wt %, and stirring continued for a minimum of 3 hours. The cell pellet was cleared by centrifugation, 2 ml of the pellet-surfactant mixture loaded on a Sephadex G-25M column, length 5.5 cm, diameter 5.5 cm, (GE Healthcare Biosciences, Pittsburg, PA) and centrifuged at 1000 rpm for 25 min in a Sorvall RC-3B centrifuge with an H-1000B swinging bucket rotor (Thermo Fisher Scientific).

Vesicles were then purified by size exclusion chromatography. The cleared cell lysate was loaded on to a Sepharose 2B column, length 5.5 cm and diameter 1.5 cm, (GE Healthcare Biosciences, Pittsburg, PA). The void volume of the Sepharose 2B column was determined by noting blue dextran elution in fractions 2-4. Vesicle solution (1 ml) was added to the column and collected as the first fraction. Fifteen 1.0 ml fractions were collected. The vesicles were observed to elute in fraction 2-4, in accordance with previous reports.³²

2.4.11 List of Bacterial Strains and Plasmids Used

Strain or plasmid	Description	Source or Reference
F62	Wild type <i>N. gonorrhoeae</i> strain	P. F. Starling (University of North Carolina, Chapel Hill)
pDCB19 Ω EcoRI	~4000-bp amplicon corresponding to bp 1650 to 2364 of the <i>lgtABCDE</i> region, cloned into the <i>EcoRI</i> and <i>BamHI</i> sites of pGEM7Zf(-). The Ω interposon is ligated into an engineered <i>EcoRI</i> site between <i>lgtD</i> and <i>lgtE</i> .	D.C. Braun
F62 Ω EcoRI	<i>N. gonorrhoeae</i> F62 strain transformed with pDCB19 Ω EcoRI. The LOS phenotype is equivalent to Δ <i>lgtE</i> .	This work.
F62 Δ 8-1	<i>N. gonorrhoeae</i> F62 strain with a 239-bp <i>ApoI</i> deletion in <i>lgtA</i> ; this strain produces L8+ LOS and is equivalent to Δ <i>lgtA</i> LOS phenotype.	W. Song
<i>E. coli</i> BL21(DE3)	F ⁻ <i>ompT gal dcm lon hsdS_B(r_B⁻ m_B⁻) λ(DE3 [lacI lacUV5-T7 gene 1 ind1 sam7 nin5])</i>	New England Biolabs (Ipswich, MA)
pET15b- <i>lgtE</i>	A fragment of F62 chromosomal DNA encoding the <i>lgtE</i> gene was cleaved with <i>NdeI</i> and <i>BamHI</i> and ligated into the expression vector pET15b that had been cleaved with the same enzymes. The ligation mixture was used to transform <i>E. coli</i> BL21(DE3).	A. Piekarowicz

Chapter 3: Demonstration of Oligosaccharide Biosynthesis by *N. gonorrhoeae* LgtE on Functionalized Catanionic Surfactant Vesicles

3.1 Introduction

Glycan binding proteins (GBPs) are found in both vertebrates and non-vertebrates and encompass families of lectins and anti-carbohydrate antibodies.⁶⁹ It is through the interactions with the cognate GBPs that carbohydrates mediate various cellular functions including adhesion, cellular signaling, tumor metastasis, inflammation, and immune responses.³ The ubiquity of glycan-protein interactions in biological processes underlies the need to develop a platform that would allow for the high-throughput analysis of these interactions at the molecular level.

Since 2002, when the first glycomic array was reported, numerous groups have developed a variety of techniques to conjugate glycans to a scaffold for high-throughput analysis.¹⁹ A major hindrance to the commercialization of any one glycomic array platform is the critical importance of spatial arrangement and density of the presented glycans. The need to control both the density and the display of glycans is necessitated by the multidentate binding characteristics of GBPs (Figure 3.1A). GBPs have low binding affinity for individual ligands, with dissociation constants in the millimolar to micromolar range, but can establish specificity and high affinity through multivalent binding.⁷⁰ Compounding the difficulty in obtaining reproducible data from different glycomic platforms, is the observation that not only can suboptimal ligand density affect GBP interactions, but also the glycan conjugated linker can have a significant impact on GBP binding.¹⁷ Gildersleeve and coworkers have demonstrated that variations in the density and the scaffold utilized for glycan presentation is responsible for variations in the glycan

binding profile of the same GBP.²⁴ There is evidence that optimal presentation of glycans is specific for each glycan binding protein, and the correct presentation is difficult to predict. Therefore, the appropriate scaffold, ligand density, and the orientation must be determined empirically for each glycan binding protein. In an effort to develop a platform in which glycan density can be easily varied in a controlled fashion, our collaborators in the DeShong laboratory have focused on functionalized cationic surfactant vesicles.

As described in detail above, cationic vesicles were initially characterized by Kaler and coworkers in 1989.³¹ These colloidal aggregates form spontaneously upon mixing the cationic surfactant CTAT with a molar excess of the anionic surfactant SDBS. The vesicles form a unilamellar bilayer and, with an excess of SDBS, have an overall surface charge of approximately -55 millivolts (mV), comparable to the surface charge of a Gram-negative bacterium.³⁷

Our collaborators have demonstrated that cationic vesicles can be functionalized with glycoconjugates and that the resulting vesicles can be utilized for the study of lectin binding. The glycoconjugates carrying a hydrophobic C₁₂ tail spontaneously insert into the vesicle leaflet through hydrophobic interactions and are bioavailable, as observed in solution with lectin induced agglutination (Figure 3.1B).³² Thomas and coworkers demonstrated that the concentration of the incorporated glycoconjugates could be controlled by simply adding more or less to the preparation, and that the spatial distribution of the glycans could be determined by lectin mediated aggregation kinetics studies.³² We have observed that LOS extracted from *N.*

gonorrhoeae spontaneously incorporates into the vesicle bilayer through hydrophobic interactions *via* the lipid A moiety.³⁷

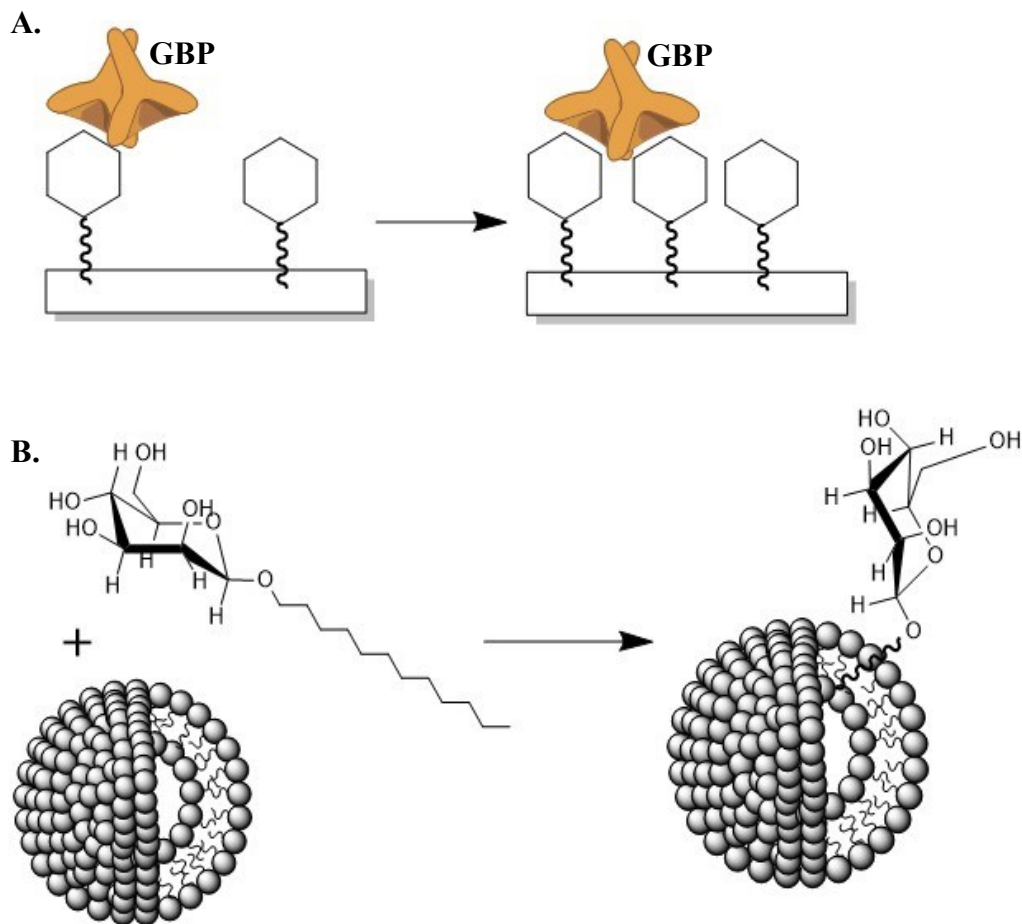


Figure 3.1. Glycan density and spatial arrangement have a significant influence carbohydrate binding protein affinity. **A.** Low glycan density attenuates GBP affinity for the cognate ligand by reducing the probability of formation of multivalent binding complexes **B.** Catanionic vesicles can be functionalized with glycoconjugates, such that the density of the surface exposed glycan can be readily varied. GBP- Glycan Binding Protein.

Due to the low-cost of the individual surfactants, the facile preparation and long-term stability of the vesicles, and based on previous reports suggesting the ability to immobilize functionalized catanionic vesicles on a variety of surfaces, glycan-functionalized catanionic surfactant vesicles may be an ideal scaffold for the development of a glycomic array.

3.2 *Specific Aims and Results*

The primary aim of this research is to demonstrate the utility of cationic vesicles as a platform for the *in vitro* synthesis of oligosaccharide structures. Enzymatic modification of functionalized SDBS-rich vesicles is demonstrated by a variety of analytical techniques. Herein, evidence is provided of the bioavailability of the functionalized moiety, and the results are proof-of-principle that recombinant *N. gonorrhoeae* glycosyltransferases can be employed in an enzymatic toolkit for the *in vitro* synthesis of glycans on this novel platform.

3.2.1 Demonstration of LgtE Glycosyltransferase Activity on Whole Cells and on Functionalized Surfactant Vesicles

Piekarowicz and Stein previously reported that LgtE catalyzes the transfer of multiple galactose residues to an LOS substrate, when the enzyme is present in excess, and this transformation could be visualized as multiple bands by SDS-PAGE.² This observation indicated that LgtE had relaxed acceptor substrate specificity and could function as a poly-galactosyltransferase.

To determine the galactosyltransferase activity of the enzyme on whole cell LOS and on LOS functionalized vesicles, LgtE was incubated in reaction buffer containing donor substrate and either LOS functionalized vesicles or whole cells as the acceptor substrate. The data presented in figure 3.2 indicate that LgtE transferase activity is maintained on whole cell *N. gonorrhoeae* strain F62 Ω EcoRI LOS, the natural acceptor for the enzyme, with the appearance of multiple higher molecular weight bands (lanes 1 versus lane 2). Under the experimental conditions employed, each band corresponds to a LOS structure of a molecular weight that is one galactose larger than the band below it.

Following incubation of cationic vesicles functionalized with Δ lgtE LOS (Figure 3.2, lane 3), LOS isolated from these vesicles produced multiple higher molecular weight bands, indicating that LgtE is able to modify LOS functionalized surfactant vesicles (Figure 3.2, lane 4). Taken together the data in figure 3.2 indicate that the purified galactosyltransferase is active *in vitro* on acceptor substrates presented both in a whole cell and in a cationic surfactant vesicle background.

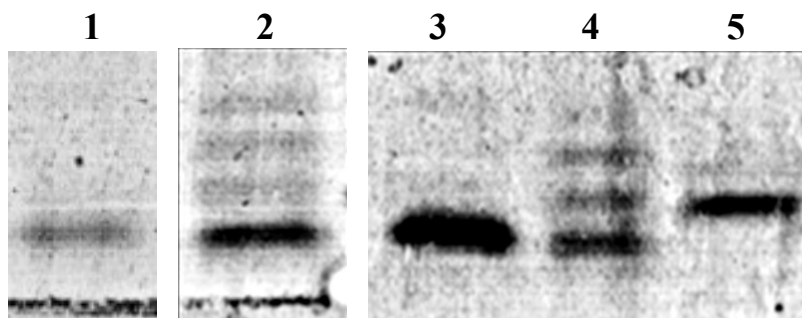


Figure 3.2. SDS-PAGE of whole cell LOS and LOS functionalized vesicles following LgtE modification. *Lane 1:* 1:10 dilution of F62 Ω EcoRI whole cell LOS. *Lane 2:* F62 Ω EcoRI whole cell LOS following LgtE reaction. *Lane 3:* Δ lgtE LOS vesicles. *Lane 4:* Δ lgtE LOS vesicles following reaction with LgtE. *Lane 5:* Δ 8-1 LOS vesicles.

To quantitatively assess LgtE transferase activity on functionalized surfactant vesicles, the amount of product observed in figure 3.2 was determined using image analysis software.¹ Figure 3.3 is a profile plot of the relative pixel density in each band observed in lane 4 of figure 3.2. Integration of the individual peaks quantifies the degree of product formation. Gel analysis indicates that LgtE converted approximately 54% of the glucose terminal LOS functionalized vesicles into either mono- or di-galactosyl terminal structures (Table 3.1). Based on the apparent higher density of the Gal- β 1,4-Gal- β 1,4-Glc LOS band as compared to the Gal- β 1,4-Glc LOS band, it appears that LgtE preferentially catalyzes the addition of a galactose molecule onto galactose terminal LOS structure. This observation may be explained by the fact that under the conditions of this

assay, where UDP-galactose is present at saturating concentrations and LOS is limiting, diffusion dictates the frequency of collisions between LOS molecules in the vesicles and the enzyme, and therefore random interactions with unmodified LOS are less probable than random interactions with previously modified LOS.

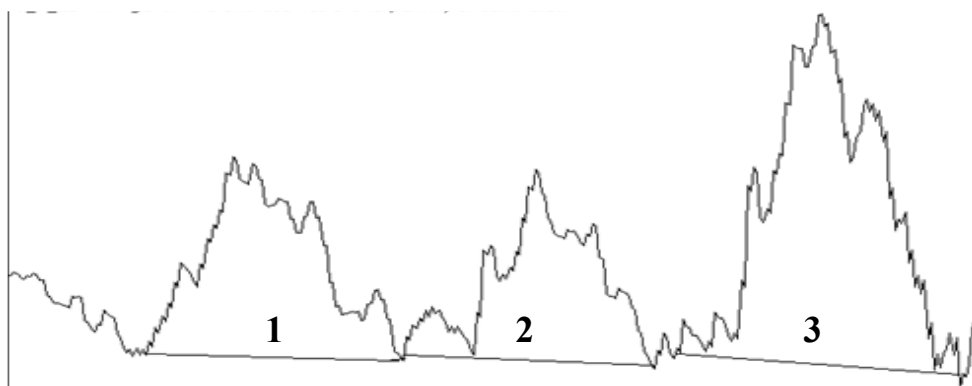


Figure 3.3. Gel analysis of LOS functionalized cationic surfactant vesicles following reaction with LgtE. *Peak 1* corresponds to the highest molecular weight band, presumed to be the Gal- β 1,4-Gal- β 1,4-Glc LOS structure. *Peak 2* corresponds to the middle molecular weight band, presumed to have an LOS structure of Gal- β 1,4-Glc. *Peak 3* corresponds to the unmodified Glucose terminal LOS structure. Peaks were obtained using ImageJ software.¹

	Area (pixels ²)	Percent	Relative Density
Glc LOS	26311.4	46.1	1
Gal- β 1,4-Glc LOS	13738.6	24.1	0.52
Gal- β 1,4-Gal- β 1,4-Glc LOS	16974.04	29.8	0.64

Table 3.1. Quantification of gel analysis on LOS functionalized vesicles following incubation with LgtE. The area of each band is expressed in square pixels. The relative density is determined by dividing the percent of each product band by the percent of the unreacted substrate band. Data were obtained using ImageJ software.¹

3.2.2 Differential Lectin Binding Demonstrates the Diversity of Glycoconjugates on Bacterial Cells

The data presented above indicate that LgtE mediates the transfer of a galactosyl group to both glucose and galactose terminal LOS presented on a whole cell or cationic

vesicle. SDS-PAGE analysis, however, does not provide specific information on the composition of the product LOS structure. As an alternative approach to demonstrating LgtE activity on whole cells and vesicles, the differential binding of labeled lectins was assayed.

I developed a quantitative assay demonstrating lectin binding to whole cell gonococcus and to functionalized surfactant vesicles. Flow cytometry was determined to be an ideal method that could be adapted for this purpose. Initially, I investigated LgtE modification of whole cell LOS. The acceptor substrate, glucose terminal LOS expressed on F62 Ω EcoRI, was labeled with Concavalin A (ConA), as depicted in figure 3.4A. ConA specifically recognizes α -D-mannopyranosyl, β -D-glucopyranosyl, and β -D-fructofuranosyl moieties. Quantification of product formation, galactose terminal LOS,

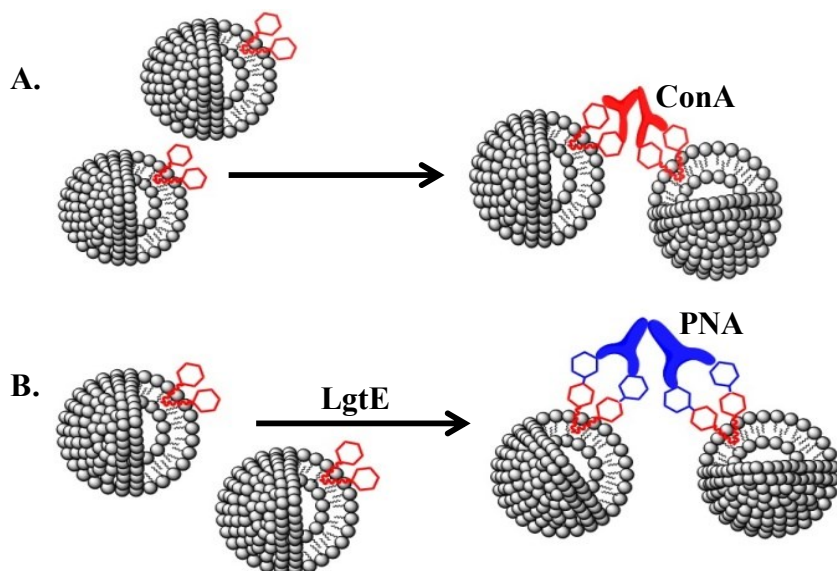


Figure 3.4. Schematic of differential lectin binding as assessed by flow cytometry. The unmodified acceptor substrate is a glycoconjugate expressing a terminal glucosyl moiety (A). This structure is preferentially bound by the lectin ConA. Following LgtE mediated galactose addition, the glycoconjugate no longer binds ConA. Rather, the galactosyl structure now preferentially binds PNA (B). This figure is meant to depict ligand binding in either a whole cell or a cationic vesicle background.

was assessed with labeled peanut agglutinin (PNA), a lectin specific for terminal β -galactosyl residues (Figure 3.4B).

Incubating LgtE with whole cells decreases the binding of ConA by approximately 1.5 fold, as is depicted in the comparison of figures 3.5A and 3.5B and is further quantified in figure 3.5E. In figure 3.5F it is also apparent that incubating the whole cells with LgtE decreases the forward-scattered light, which is proportional to size, of the detected events. This decrease in size can be explained by decreased agglutination of the whole cells by ConA following LgtE modification.

Unexpectedly, *N. gonorrhoeae* strain F62 Ω EcoRI bound a significant concentration of labeled PNA despite numerous washing steps. Pre-absorbing the whole cells with unlabeled PNA reduces the background binding, and it is apparent in figures 3.5D and 3.5E that LgtE transferase activity increases the mean fluorescence of the events by approximately twofold (quantified in Figure 3.5E). Further, in figure 3.5F it is evident that the average size of the events increases following LgtE modification. Taken together the data indicate that LgtE maintains transferase activity *in vitro* on F62 Ω EcoRI LOS, and that the activity can be assessed with labeled lectins by flow cytometry. Additionally, the data demonstrate that there are numerous glycosylated molecules other than LOS on the surface of the gonococcus to which PNA can bind.^{71, 72} The high background of glucosyl-terminated glycans on the cell surface precludes the use of this assay for quantification purposes, and emphasizes the necessity in the field of glycomics for system in which a carbohydrate of interest can be investigated devoid of other glycosylated molecules.

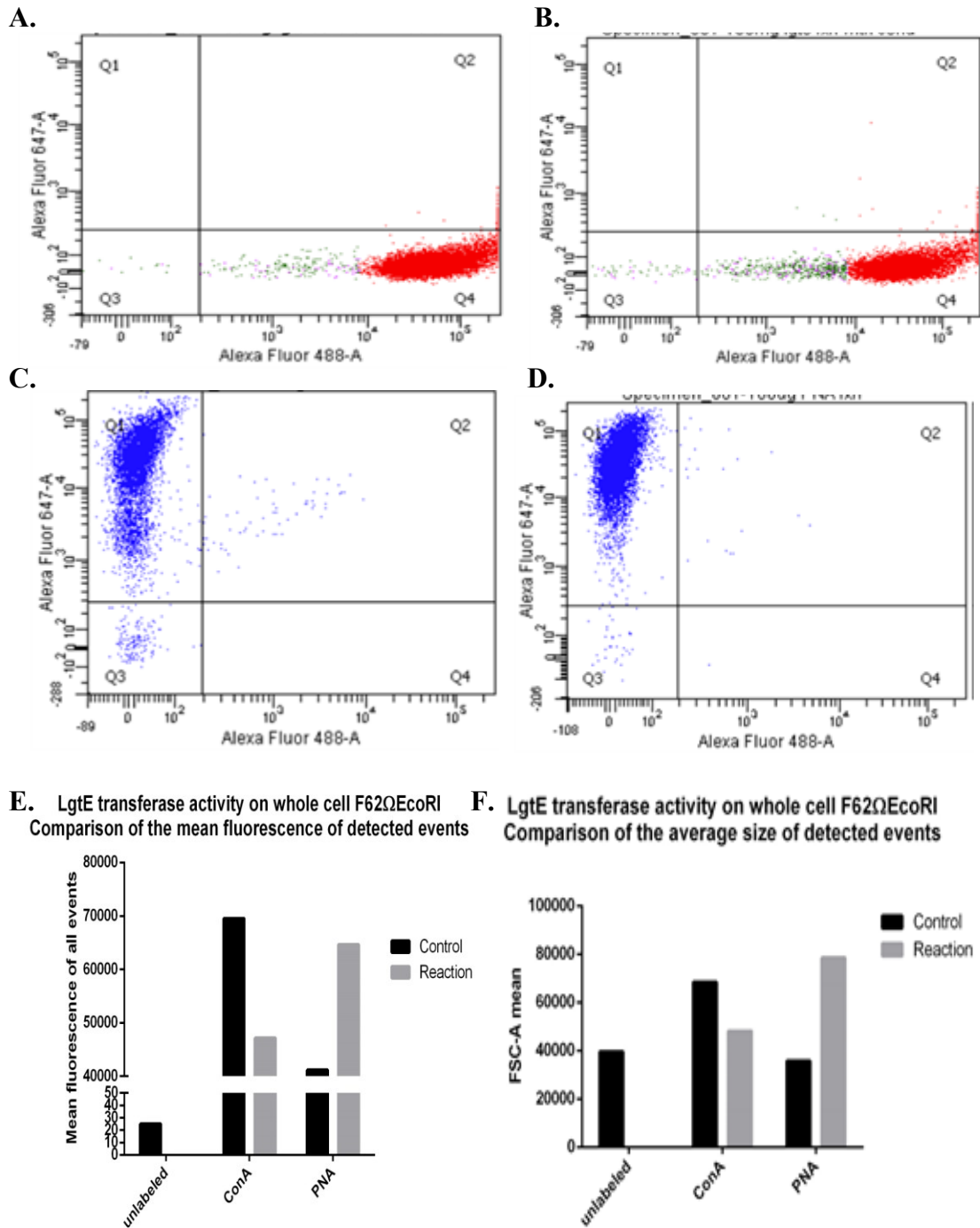


Figure 3.5. LgtE mediates the transfer of a galactosyl group, *in vitro*, to whole cell F62ΩEcoRI. **A.** F62ΩEcoRI with ConA (positive control) **B.** F62ΩEcoRI with ConA following incubation with 1 μM LgtE. **C.** F62ΩEcoRI with PNA (negative control). **D.** F62ΩEcoRI with PNA following incubation with LgtE. **E.** Quantification of mean fluorescence depicted in panels a-d, respectively. **F.** Quantification of the average FSC-A for each condition depicted in panels a-d. Forward-scattered light (FSC-A) is proportional to the size of the detected events.

3.2.3 LgtE Transferase Activity is Maintained on LOS Functionalized Vesicles

The transferase activity of LgtE on functionalized surfactant vesicles was also analyzed. Initially, LgtE activity on Δ lgtE LOS functionalized cationic vesicles was assayed. Under the experimental conditions employed, as demonstrated in figures 3.6A

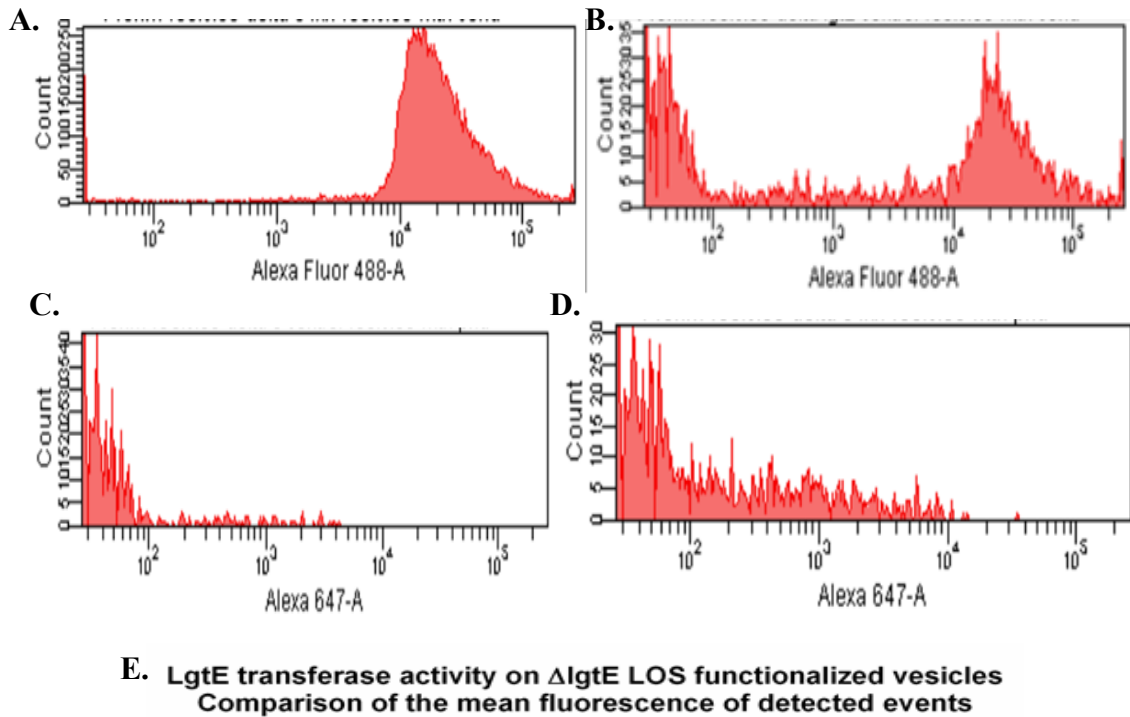


Figure 3.6. LgtE mediates the transfer of a galactosyl moiety to Δ lgtE LOS functionalized vesicles. **A.** ConA incubated with Δ lgtE LOS functionalized vesicles. **B.** ConA incubated with Δ lgtE LOS functionalized vesicles following reaction with LgtE. **C.** PNA incubated with Δ lgtE LOS functionalized vesicles. **D.** PNA incubated with Δ lgtE LOS functionalized vesicles following reaction with LgtE. **E.** Quantification of the mean fluorescence for all events depicted in panels a-d, respectively.

and 3.6B, LgtE mediated a twofold reduction in ConA binding to Δ lgtE LOS functionalized vesicles. Additionally, PNA binding was observed to increase by approximately tenfold following incubation of the vesicles with LgtE (Figures 3.6C and 3.6D). The data quantified in figure 3.6E indicate that LgtE mediates the transfer of a galactosyl group to LOS functionalized cationic surfactant vesicles.

3.2.4 LgtE is Active on a Synthetic Substrate Incorporated into Surfactant Vesicles

An aim of this study is to exploit the relaxed substrate specificity of LgtE to create glycans of defined structure and composition, employing acceptor substrates not necessarily derived from *Neisseria* LOS. To investigate the feasibility of exploiting LgtE for the modification of a diverse array of glucose terminal structures, I sought to demonstrate the activity of LgtE on C₁₂-glucose functionalized surfactant vesicles (Figure 3.7). In this experiment, it is hypothesized that transfer of a galactosyl residue to the glucopyranosyl-functionalized cationic vesicle would result in a decrease in the ability of ConA to bind to the vesicle and a corresponding increase in the binding of PNA to the vesicle.

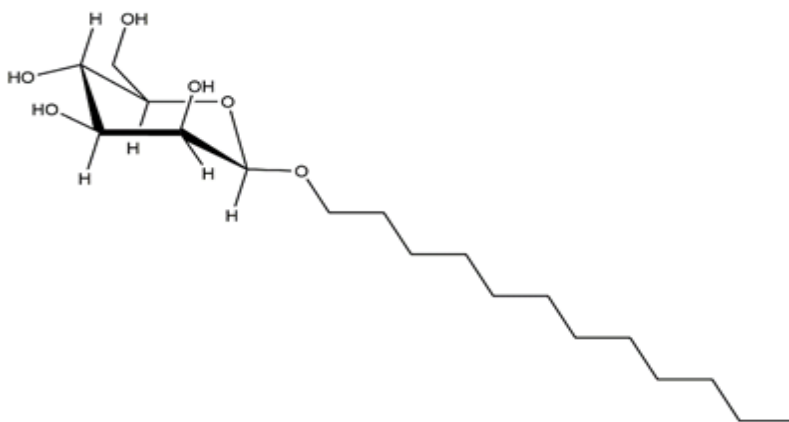


Figure 3.7. Structure of *n*-Dodecyl- β -glucopyranoside, or C₁₂-glucose.

As depicted in figures 3.8A and 3.8B and quantified in figure 3.8E, ConA binding was reduced twofold following reaction with LgtE. Figure 3.8E also indicates an approximately tenfold increase in PNA binding (depicted in Figures 3.8C and 3.8D).

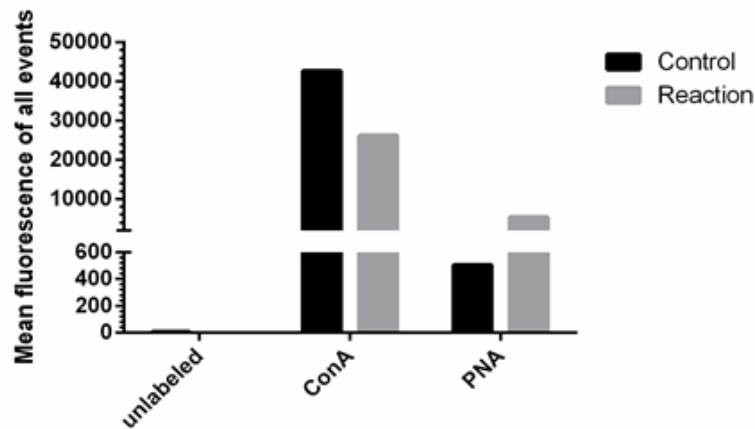
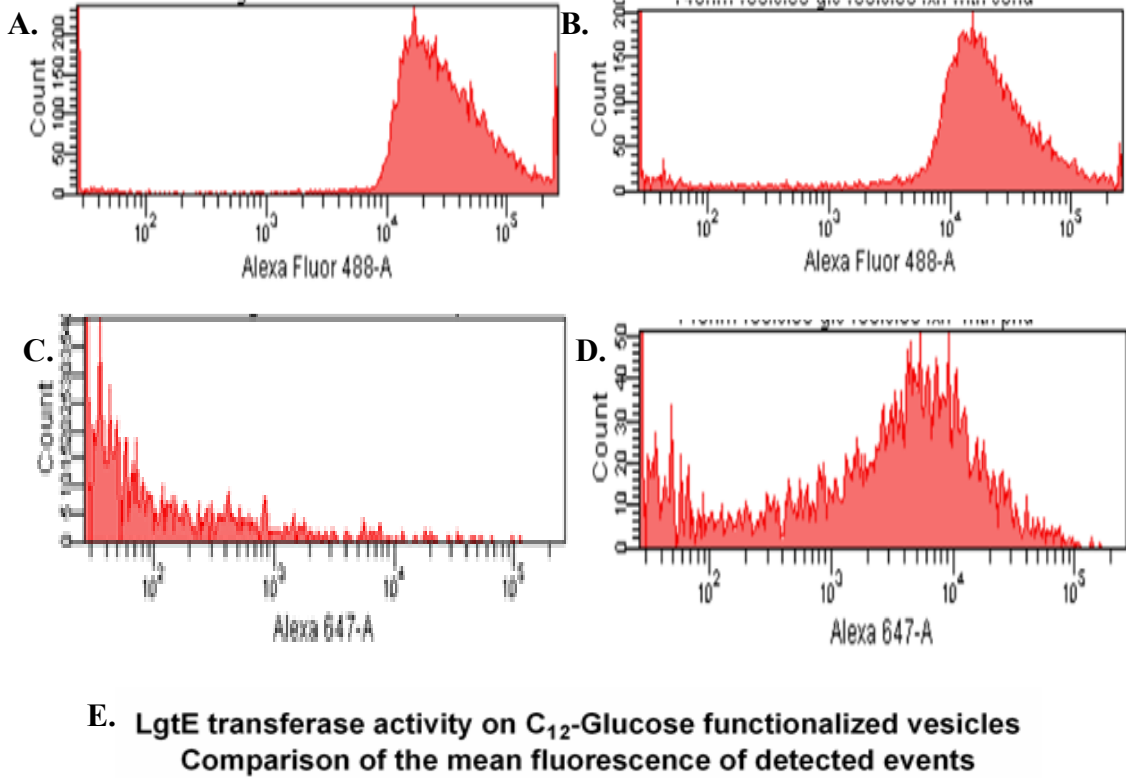


Figure 3.8. LgtE mediates the transfer of a galactosyl moiety to C₁₂-Glucose functionalized vesicles. **A.** ConA incubated with C₁₂-Glucose functionalized vesicles. **B.** ConA incubated with C₁₂-Glucose functionalized vesicles following reaction with LgtE. **C.** PNA incubated with C₁₂-Glucose functionalized vesicles. **D.** PNA incubated with C₁₂-Glucose functionalized vesicles following reaction with LgtE. **E.** Quantification of the mean fluorescence for all events depicted in panels a-d, respectively.

Taken together, the data presented in figures 3.6 and 3.8 indicate that LgtE performs galactosyltransferase reactions, *in vitro*, on functionalized surfactant vesicles, independent of glycan origin.

3.2.5 Vesicle Integrity is Maintained Following Enzymatic Synthesis

The lectin binding data presented above indicate that LgtE glycosyltransferase activity is maintained on LOS incorporated in SDBS-rich cationic surfactant vesicles. To confirm that enzymatic synthesis did not disrupt the integrity of the vesicles, the reaction buffer containing vesicles was applied to a Sepharose 2B column. Previous studies have reported that intact vesicles can be separated from free surfactant molecules and free glycans on a similar size exclusion matrix.³² Functionalized vesicles elute in the void volume, whereas free glycans and free LOS are retarded due to their small size and shape, thus eluting in later fractions.³² 1 ml Fractions were collected, and the LOS species in fractions 2-4 were visualized by SDS-PAGE. Figure 3.9 (lanes 2-4) indicates that the vesicles are present in the void volume, with the majority in fraction 3 (lane 3).

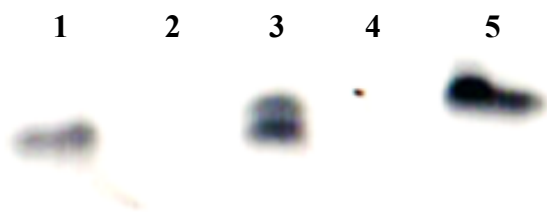


Figure 3.9. Vesicles are intact following enzymatic synthesis. 16.5% Tris-Tricine gel. Lane 1: Δ lgtE vesicles (negative control). Lanes 2-4 are Δ lgtE vesicles following reaction with LgtE. Lane 2: Fraction 2. Lane 3: Fraction 3. Lane 4: Fraction 4. Lane 5: Δ lgtA vesicles (positive control).

Additionally, a higher molecular weight band is present in the lane containing the reaction product that is not present in the negative control (lane 3 vs lane 1 Figure 3.9).

The data in figure 3.9 indicate that the vesicles are intact following enzymatic synthesis

and further confirm that LgtE glycosyltransferase activity is maintained on functionalized cationic vesicles.

3.3 Discussion

Numerous studies have demonstrated the utility of cationic surfactant vesicles for both *in vitro* investigations of glycan presentation.^{32, 37, 38} Our collaborators previously demonstrated that cationic surfactant vesicles are particularly well suited for investigating protein: carbohydrate interactions because of the ease at which glycan density can be varied.³² The investigation of diverse glycan structures in this context is limited, however, by the requirement that a glycan must be conjugated to a hydrophobic moiety for incorporation into the vesicle bilayer.

One possible method for broadening the scope of presented glycans is employing glycosyltransferases to synthesize oligosaccharides on the surface of vesicles. The work presented here indicates that *N. gonorrhoeae* β -1,4-galactosyltransferase LgtE biosynthesizes diverse glycans incorporated into cationic surfactant vesicles. Significantly, it is observed from the data in figure 3.5 and 3.6 that LgtE mediates the transfer of a galactosyl group not only to glycans of neisserial origin, but also, as shown in figure 3.8, catalyzes the transfer of a galactosyl moiety to a synthetic glucose terminal substrate. Taken together, the data indicate the potential of bacterial glycosyltransferases for the chemo-enzymatic synthesis of diverse oligosaccharide structures. Recombinant glycosyltransferases, therefore, have enormous potential for use in biomedical engineering. For example, by modifying glycans found on the surface of human erythrocytes, one could make it possible for an individual with type A blood (α -1,3-

GalNAc) to receive a transfusion of type B (α -1,3-Gal) donor blood, simply by incubating the cells with a specific recombinant glycosyltransferase.

The data presented in figures 3.5, 3.6, and 3.8 also demonstrate that glycan binding protein recognition of incorporated glycans is maintained, and that these interactions can be investigated by a variety of analytical techniques, including FACS analysis. Flow cytometry is currently used in a number of laboratories for a variety of analyses including measuring a patient's T-cell count or determining a patient's antibody panel. The techniques developed in this dissertation facilitate the development of a new vesicle based platform in which a patient's serum can be analyzed by standard flow cytometry techniques for the presence of antibodies against diverse carbohydrate antigens.

Taken together, the data presented in this chapter provides a proof-of-concept that recombinant glycosyltransferases synthesize oligosaccharides, *in vitro*, on functionalized cationic surfactant vesicles. Further, the data indicate that cationic vesicles may be utilized as a platform for the investigation of protein-glycan interactions, and should be considered for development of glycomic array technologies.

3.4 *Experimental*

3.4.1 Chemicals, Reagents, Lectins, and Antibodies

All chemicals were reagent grade or better from Sigma Aldrich Co. (St. Louis, Mo.) unless specified otherwise. Cetyltrimethylammonium tosylate, sodium dodecylbenzenesulfonate, *n*-dodecyl β -D-glucopyranoside (C₁₂-glucose), and proteinase

K were obtained from Sigma Aldrich Co. (St. Louis, Mo.). Tris-Tricine gels (16.5%) and running buffer were obtained from Bio-Rad Laboratories (Richmond, CA).

MAb 2-1-L8 was graciously provided by Wendell Zollinger (Walter Reed Army Institute of Research, Washington, DC). Alexa Fluor® goat anti-mouse IgG (H+L), Concavalin A Alexa Fluor® 488 conjugate (Molecular Probes®), and peanut agglutinin Alexa Fluor® 647 (Molecular Probes®) were purchased from Invitrogen Corp. (Carlsbad, CA).

3.4.2 Preparation of Vesicles

Functionalized cationic vesicles were prepared by members of the DeShong group. Sodium dodecylbenzenesulfonate (SDBS) was purchased from TCI America and was used without further purification. Cetyltrimethylammonium tosylate (CTAT) was purchased from Sigma and was recrystallized from ethanol-acetone to give a white powder. The purified solid was stored at room temperature in a desiccator containing Drierite.

Cationic vesicles were prepared from SDBS and CTAT, with molar excess of SDBS. Anionic vesicles were prepared with 1 wt% of total surfactant by combining 70.0 mg (200 μmol) of SDBS and 30.0 mg (65.8 μmol) of CTAT. Millipore water 18 Ω (9.90 ml) was added to the mixture of surfactants, and the resulting solution was stirred for 24 hours. Cationic vesicles formed within 1 hour of mixing, based on the turbidity of the solution, and have an average diameter of 140 ± 30 nm, as measured by dynamic light scattering (DLS).

Vesicles were purified by size exclusion chromatography. A column (5.5 cm height, 1.5 cm diameter) was packed with Sephadex G-100 (Sigma). Vesicle solution (1 ml) was added to the column and collected as the first fraction. This was followed by the addition of 1 ml aliquots of water. Each 1 ml aliquot was collected in a separate vial. A total of 14 fractions were collected and the vesicles were observed in fractions 3 and 4. The presence of vesicles in fractions 3 and 4 was confirmed by dynamic light scattering (DLS). DLS measurements were performed by Dr. Neeraja Dashaputre in the DeShong lab. Based on a phenol-sulfuric acid based colorimetric assay these vesicle-containing fractions were observed to contain carbohydrate incorporated in them.³⁷ Hence these two fractions were combined and used experimentally.

All glycan-functionalized cationic vesicles were prepared and characterized by Dr. Neeraja Dashaputre. The results from these studies are reported here to provide complete experimental information regarding these materials. Glucose functionalized vesicles were prepared by combining 0.1 mole fraction of glycoconjugate with SDBS (mole fraction 70%) and CTAT (mole fraction 30%) in 9.9 ml of water. The solution was stirred for 24 hours.

LOS functionalized vesicles were prepared by combining 1.00 mg purified lyophilized LOS in 10 ml preformed 1% SDBS rich vesicle solution. The resulting vesicle preparation was purified as described above.

3.4.3 LOS Purification for Functionalized Vesicles

LOS was purified from broth-grown cells with acetone-powdered organisms by the hot phenol-water method.^{73,32} LOS was extracted with hot phenol-water and

concentrated by lyophilization. Extractions were continued until the purified LOS gave a minimal absorbance when measured at 200 nm, ensuring minimal nucleic acid contamination.

3.4.4 LOS SDS-PAGE Analysis

Whole cell gonococcal LOS was prepared from plated cultures as described by Hitchcock and Brown⁷⁴ and diluted 1:25 in 1x Laemmli buffer. The suspension was heated to 65 °C for a minimum of 10 minutes. Reactions and vesicles were diluted and heated in the same manner. 20 µl of each sample were loaded onto a 16.5% Criterion™ Tris- Tricine Precast gel (Bio-Rad Laboratories Inc.). The gel was run at a constant current of 3 milliamphere (mA), on ice, for approximately 8 hours, or until the dye front reached the bottom of the gel.

After electrophoresis, the gel was fixed overnight in a solution of 40% ethanol-5% acetic acid and then oxidized in 0.83% periodic acid for 5 minutes. The gel was washed for 2 hours in multiple changes of H₂O every 20 minutes, stained for 5 minutes in silver staining solution (22.5 mM NaOH, 0.42% NH₄OH, 47 mM AgNO₃), and rewashed for 2 hours in multiple changes of H₂O every 20 minutes. The gel was developed (100 ml of 0.005% citric acid-0.007% formaldehyde) until bands became visible.

A digital image of the gel was obtained on a flatbed scanner. Subsequently, the gel was analyzed with ImageJ software (Rosband W. U.S. National Institutes of Health, Bethesda, MD. <http://imagej.nih.gov/ij/>).

3.4.5 Flow Cytometry Analysis on Whole Cell *Gonococcus*

Pilin and Opa dual negative colonies of F62 Δ 8-1 and F62 Ω EcoRI strains were selected and passaged. Bacterial cells were suspended in 20 mM HEPES pH 7.5 to an OD₆₅₀ of 0.6. The cells were pelleted and fixed by re-suspension in 4% paraformaldehyde (PFA). Fixation proceeded for 10 minutes at room temperature with moderate shaking, and subsequently washed three times with 20 mM HEPES pH 7.5. Bacterial cells were fixed again for 10 minutes, and then washed five times with 20 mM HEPES pH 7.5. Fixed bacteria were stored in HEPES buffer at 4 °C.

8×10^5 bacteria were incubated with ConA Alexa Fluor® 488 conjugate in buffer (20 mM HEPES pH 7.5, 150 mM NaCl, 1 mM CaCl₂, 1 mM MnCl₂, and 1 mM MgCl₂) or with PNA Alexa Fluor® 647 conjugate in buffer (20 mM HEPES pH 7.5, 150 mM NaCl, 1 mM CaCl₂, and 1 mM MgCl₂) for 1 hour at room temperature with moderate shaking. The suspensions were washed three times with 20 mM HEPES, and re-suspended in 500 μ l 20 mM HEPES. Bacteria were subjected to FACS analysis using FACSCanto II (BD Biosciences) flow cytometer. Data were analyzed with FACSDiva (BD Biosciences software).

3.4.6 Flow Cytometry Analysis on Functionalized Surfactant Vesicles

100 μ M Δ lgtE LOS vesicles or C₁₂-glucose functionalized vesicles were incubated in 50 μ l reaction buffer (20 mM HEPES pH 7.5, 1 mM MnCl₂, 1 μ M LgtE) with or without 1 mM UDP-galactose, at 30 °C for a minimum of 2 hours. The vesicles were centrifuged at 800 RPM for 10 minutes at room temperature, and re-suspended in 100 μ l 2% BSA. The solution was incubated for 1 hour at room temperature with

moderate shaking. The vesicle solutions were centrifuged again and re-suspended in 50 μ l 20 mM HEPES pH 7.5. The vesicles were incubated with ConA Alexa Fluor® 488 conjugate in buffer (20 mM HEPES pH 7.5, 150 mM NaCl, 1 mM CaCl₂, 1 mM MnCl₂, and 1 mM MgCl₂) or with PNA Alexa Fluor® 647 conjugate in buffer (20 mM HEPES pH 7.5, 150 mM NaCl, 1 mM CaCl₂, and 1 mM MgCl₂) for 1 hour at room temperature with moderate shaking, followed by an overnight incubation at 4 °C. The vesicle-lectin complexes were subsequently washed three times with 20 mM HEPES pH 7.5. Labeled vesicles were subjected to FACS analysis using FACS Aria (BD Biosciences) flow cytometer. Data were analyzed with FACSDiva (BD Biosciences software).

3.4.7 Vesicle Integrity Assay

100 μ M Δ lgtE LOS vesicles were incubated in 150 μ l reaction buffer (20 mM HEPES pH 7.5, 1 mM MnCl₂, 1 μ M LgtE, 1 mM UDP-galactose), at 30 °C for a minimum of 2 hours. The vesicle containing solution was then directly applied to a column (length 5.5 cm, diameter 1.5 cm) containing Sepharose 2B (GE Health Sciences) for size exclusion chromatography. The samples were run with Blue Dextran (Sigma) as a marker. 15 fractions of 1.0 ml were collected, with the vesicles eluting primarily in fractions 2 and 3.

To confirm the presence of the vesicles, 15 μ l of each fraction was mixed with 5 μ l 3x Laemmli buffer and then subjected to SDS-PAGE analysis. The fractions were run on a 16% Criterion™ Tris-Tricine Precast gel (Bio-Rad Laboratories Inc.). The gel was run at a constant current of 3 mA, on ice, for approximately 8 hours, or until the dye front

reached the bottom of the gel. The gel was then fixed and silver-stained as described above.

Chapter 4: Utility of Catanionic Surfactant Vesicles as a Novel Glycomic Array Platform

4.1 Introduction

The previous chapter presented evidence of glycosyltransferase mediated oligosaccharide chemo-synthesis on functionalized cationic surfactant vesicles. These observations led to hypothesis that functionalized surfactant vesicles could be used as a platform for high-throughput investigations of carbohydrate-active enzymes and lectin binding.

Of the more than 60,000 putative glycosyltransferases in the CAZy database, the enzymatic activity of only a small subset has been demonstrated and characterized.^{75, 76} There is an increased interest in the field of glycobiology to develop a quantitative and qualitative assay in which enzymatic activity can be assessed on an array of glycan structures. Ban *et al.* developed a high-throughput label-free assay in which acceptor glycans are covalently immobilized in monolayers on gold plates. Acceptor substrates were modified with azide group and were linked to the monolayer through a terminal alkyne group (Figure 4.1A).¹⁹ Following an enzymatic reaction, changes in the mass of the acceptor substrate were determined using self-assembled monolayers with matrix-assisted laser desorption-ionization mass spectrometry (SAMDI-MS).⁷⁶ This methodology allows for the rapid screening of diverse carbohydrate-active enzymes, however, the authors make the assumption that the chemical characteristics of the linker moiety do not have an influence on enzymatic activity. However, Lairson and coworkers observed that the reaction rate of *N. meningitidis* galactosyltransferase LgtC was reduced two to four- fold depending on the structure of the linker.⁷⁷ Clearly, the length of the

linker and its ability to display the glycan acceptor in a “biologically-relevant manner” had been compromised. Presumably, either the density of the glycan presented, or its orientation in space, cannot be controlled adequately by this technique. Moreover, the necessity for highly specialized instruments limits the general use of the SAMDI-MS assay.

Another assay recently reported for the investigation of carbohydrate-active enzymes employs flow cytometry analysis and glycans covalently coupled to microspheres.⁷⁸ For this assay, glycans are functionalized on the reducing end with a linker containing a terminal amine group. The functionalized glycan substrates are then conjugated to carboxyl polystyrene microspheres by carbodiimide-based amide coupling (Figure 4.1B).⁷⁸ While it is possible to demonstrate the analysis of multiple enzyme activities simultaneously,⁷⁸ functionalized microsphere synthesis is a time-consuming and labor-intensive process, limiting the applicability of the technique. In addition, this method, much like the method described above, does not allow for control of either the density of the glycan or the presentation of the glycan on the surface of the bead. Accordingly, the relevance of the results of this assay to “biologically-relevant” events cannot be assessed.

These two reports highlight the necessity for the development of an array platform in which glycan substrates can be easily incorporated, immobilized with control of density and presentation of the glycan, and analyzed in high-throughput manner. The development of a platform for the high-throughput analysis of glycans will enhance

investigations of not only carbohydrate-active enzymes but also other carbohydrate binding proteins.

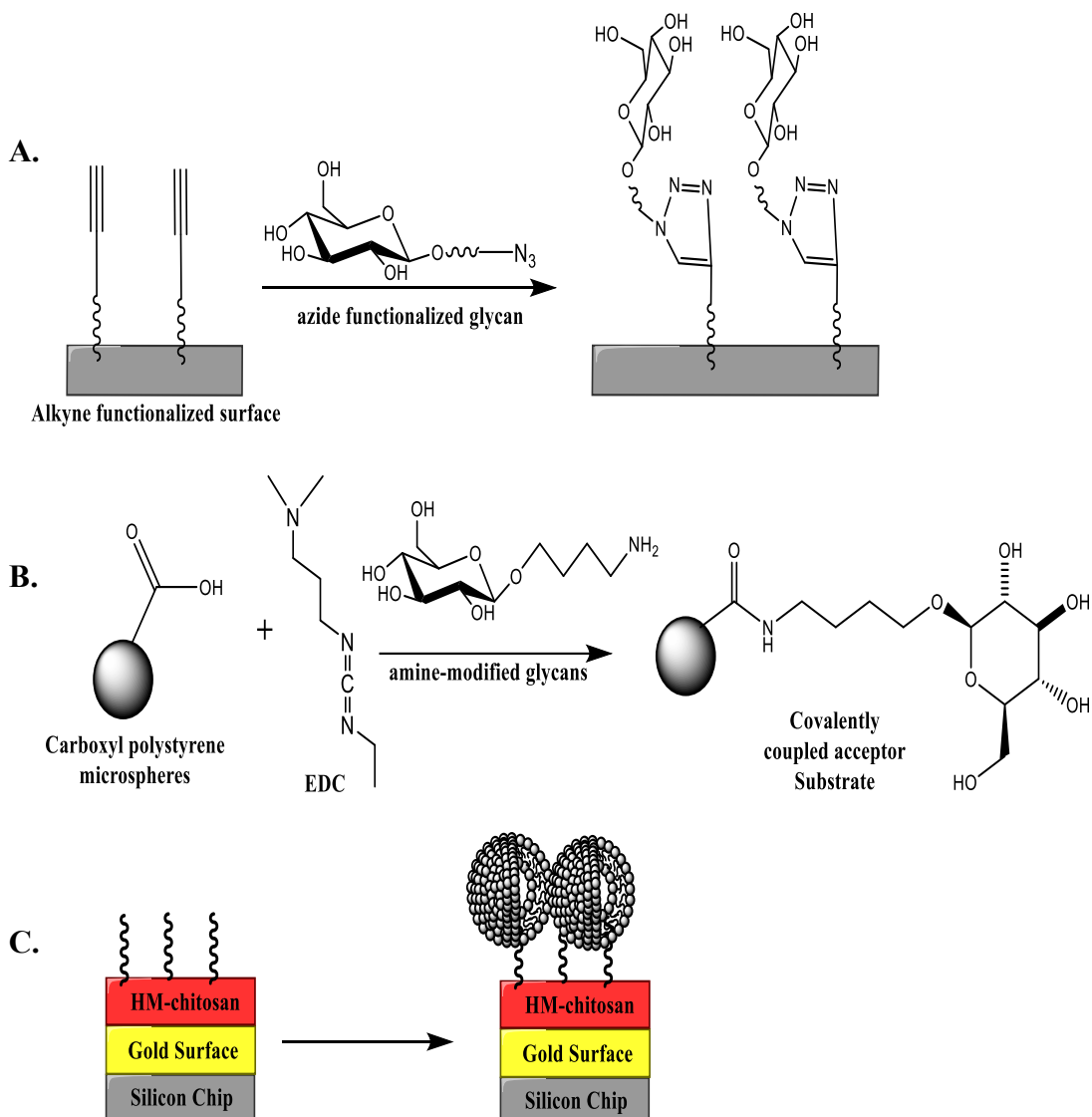


Figure 4.1. Methodology of glycan immobilization. **A.** Click chemistry reaction of alkyne functionalized surface with azide functionalized glycan, resulting in covalent coupling of the glycan to the functionalized surface. **B.** Carboxyl polystyrene microspheres are activated with EDC (N-(3-Dimethylaminopropyl)-N'-ethylcarbodiimide) forming the unstable intermediate, O-acylisourea, which directly reacts with primary amines. The amine-modified glycan forms an amide bond with the activated carboxyl. **C.** HM-chitosan retention of cationic surfactant vesicles.

Studies have previously demonstrated that the physical properties of cationic surfactant vesicles could be exploited for the development of a novel glycomic array

platform. Dowling *et al.* demonstrated that intact cationic surfactant vesicles are immobilized by hydrophobically modified chitosan.⁷⁹ The authors functionalized the biopolymer chitosan with aliphatic chains, and electrodeposited the functionalized biopolymer onto gold electrodes. The amphiphilic biopolymer interacts noncovalently with cationic vesicles in solution, capturing vesicles by insertion of the hydrophobic tails into the vesicle bilayer (Figure 4.1C). Importantly, the authors demonstrated that the retained vesicles are intact and that capture could be spatially controlled.⁷⁹ This study suggests that hydrophobically modified chitosan could serve as a tether to immobilize vesicles functionalized with glycoconjugates in the development of a high-throughput glycomic array.

Pond *et al.* reported that cationic surfactant vesicles are retained on nitrocellulose-coated glass slides.³⁸ The utility of this alternative vesicle immobilization method was illustrated by the construction of a glycomic array prototype. The authors demonstrated that lectins recognized glycoconjugates incorporated into SDBS-rich cationic surfactant vesicles, and that the binding profiles were influenced by carbohydrate density.³⁸ The authors concluded that the vesicles remain intact and that this nitrocellulose-based platform could be employed in development of a high-throughput platform. These works provide the first experimental evidence that cationic surfactant vesicles can be immobilized and remain structurally intact on a “hard” surface.

4.2 *Specific Aims and Results*

The aim of this work is to demonstrate that functionalized cationic vesicles are an ideal platform for high-throughput investigations of carbohydrate-active enzymes and glycan binding proteins. The data presented herein provide evidence that LgtE enzyme

kinetics are equivalent on LOS presented on a whole cell to that of LOS presented on a cationic surfactant vesicle.

4.2.1 LgtE Transferase Activity

The SDS-PAGE analysis presented in the previous chapter indicates that LgtE may have a higher transfer efficiency on LOS functionalized cationic vesicles compared to LOS presented in a whole cell background. To quantitatively determine the validity of this observation, the binding parameters of the enzyme's *in vitro* activity on whole cell *N. gonorrhoeae* F62 Ω EcoRI LOS were determined, and compared to LgtE activity on LOS functionalized vesicles. To accomplish this aim, a series of western blot analyses were performed using the monoclonal antibody 2-1-L8⁴⁰ to quantify product formation. This technique was chosen over other biochemical assays because of the exquisite substrate specificity of the antibody. It was apparent from flow cytometry analysis, presented in the previous chapter, that there are numerous glycosylated species expressed on the surface of whole cell bacteria. Depending on structure, each of these species could potentially be modified by LgtE, and consequently lead to misinterpretation when comparing the catalytic efficiency on whole cells to functionalized cationic surfactant vesicles. Utilization of the western blot technique facilitated the discrimination of LOS from other glycosylated membrane macromolecules.

Enzymatic transferase activity could be determined from an *in vitro* reaction assay adapted from Musumeci *et al.*⁸⁰ The reaction was allowed to proceed under steady-state conditions, in which the donor substrate, UDP-Galactose, was added at saturating concentrations. The enzyme's cofactor, manganese (Mn²⁺), concentration was carefully

controlled to ensure linear enzyme reaction velocity, but limiting the concentration so as to not disrupt the electrostatic forces that maintain cationic vesicle stability. To establish this critical concentration of manganese, turbidity studies of the vesicle solution were performed as a function of manganese concentration (Figure 4.2A). This assay, adapted from Thomas *et al.*,³² correlates an increase in absorbance at 450 nm to an

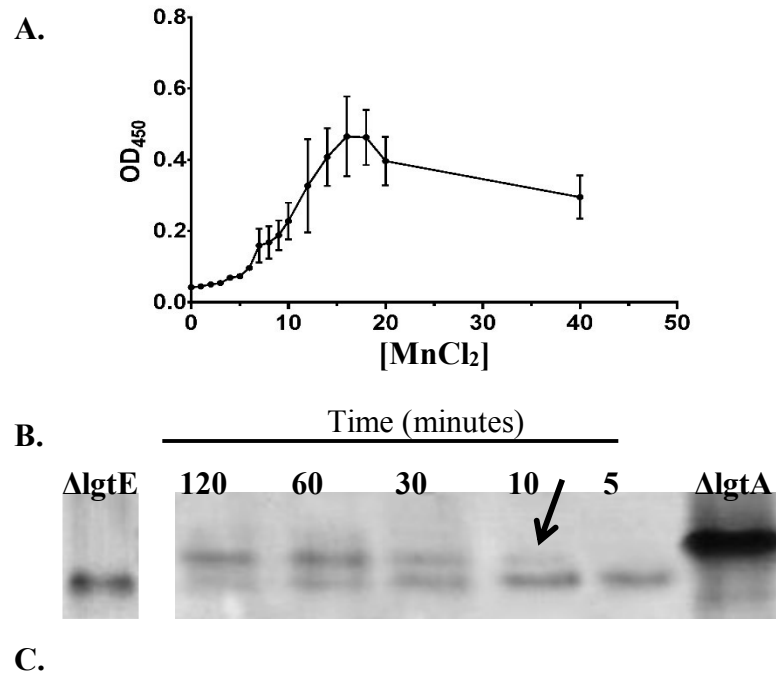
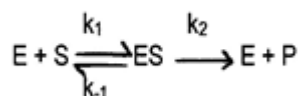


Figure 4.2. Steady-state conditions for in vitro activity assay. **A.** Surfactant vesicle stability with varying concentrations of MnCl₂. The spike in absorbance, which indicates an increased light scattering at 7 mM MnCl₂, is indicative of vesicle disruption with subsequent precipitation. **B.** SDS-PAGE time course analysis of 1.5 μM LgtE in vitro activity on whole cell LOS. Control LOS structures are indicated. Formation of the glycosylated product is indicated by the appearance of a higher molecular weight band at the later time points (black arrow). **C.** Relative glycosylation product band intensity as a function of time.

increase in turbidity, which in turn is proportional to the extent of vesicle aggregation. Moreover, a time course analysis was performed to establish the optimal time point at which the enzyme catalyzed reaction's initial velocity is linear with respect to enzyme concentration and time (Figure 4.2B and 4.2C).

The data in figure 4.2A indicate that the vesicles are stable in conditions up to 5 mM MnCl₂. Accordingly, subsequent kinetic studies were conducted at 5mM MnCl₂. The time course depicted in figure 4.2B and quantified in 4.2C indicates that a reaction with 1.5 μM LgtE, at the time point of 30 minutes, is linear with respect to time. Therefore, 30 minutes was chosen for steady-state kinetic analysis. Based on the linearity of figure 4.2C at this point, it can be assumed that at an enzyme concentration of 1.5 μM, LgtE is saturated with substrate and the rate of product formation is directly proportional to the initial velocity of the enzyme-catalyzed reaction. Under these conditions, the reaction is considered to be in steady-state. This relationship of product formation to reaction velocity is the basis of the Michaelis-Menten equation. The Michaelis-Menten equation can be applied to describe a single site enzyme catalyzed reaction shown as:



(Scheme 4.1)

The enzyme velocity (v_o) equals the amount of product produced per unit time. Based on our model, $v_o = k_2[ES] = k_{cat}[ES]$, where $[ES]$ is the concentration of enzyme bound to substrate and k_{cat} is the catalytic turnover rate. Therefore, $[ES]$ governs the rate of the reaction. $[ES]$ in turn is governed by two factors: the rate of ES formation ($=k_1[E][S]$) and

the rate of ES breakdown ($=k_{-1}[ES]+k_2[ES]$). For the steady state assumption to hold true, the rate of ES formation must equal the rate of ES breakdown:

$$k_1[E][S] = (k_{-1} + k_2)[ES]$$

(Equation 4.1)

Thus, for the enzyme reaction to be at steady-state, the condition of $[S]_{\text{total}} \gg [E]_{\text{total}}$ must be true. At time points on the linear part of the graph (Figure 4.2C), such as from 10-60 minutes where the rate of $[ES]$ change is equal to zero, the rate of product formation is directly proportional to time. Under constant $[ES]$, i.e. steady-state conditions, it can be assumed that the reaction is not inhibited by such factors as substrate depletion, production inhibition, or enzyme inactivation, simplifying kinetic analysis.

After determining the steady-state parameters, enzymatic activity was assayed. To ensure that the observed concentration of product formation accurately reflected LgtE activity and was not an artifact of loading, the volume of the acceptor substrate added to the reaction mixture was held constant while varying the total reaction volume. All other reactant concentrations were adjusted accordingly. Additionally, to correct for any variations in antibody binding, a standard curve of F62 Δ 8-1 LOS was probed simultaneously and under the same conditions as each experimental blot, the signal detected from the blots was then normalized to the standard curve.

Figures 4.3 and 4.4 depict the progression of LgtE galactosyltransferase activity at varying concentrations LOS presented as an integral component of the bacterial cell membrane or incorporated into surfactant catanionic vesicles, respectively. Band intensity was quantified as previously described.

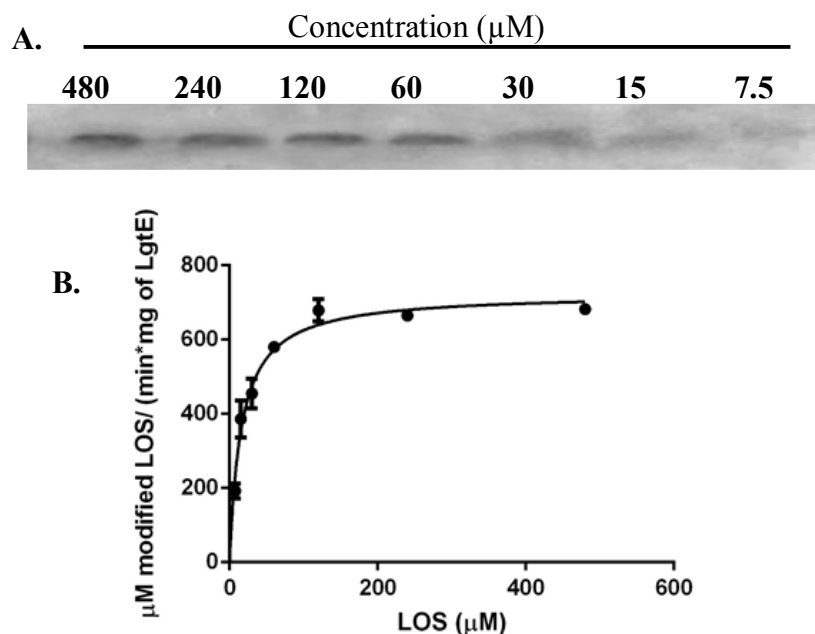


Figure 4.3. Activity of LgtE on whole cell *N. gonorrhoeae* F62 Δ EcoRI. **A.** Western blot analysis of the *in vitro* glycosylation assays. The observed signals correspond to the formation of L8+ glycoform (detected by the MAb 2-1-L8) **B.** Plot of LgtE activity as a function of acceptor substrate concentration. Values reflect the average of 3 independent experiments.

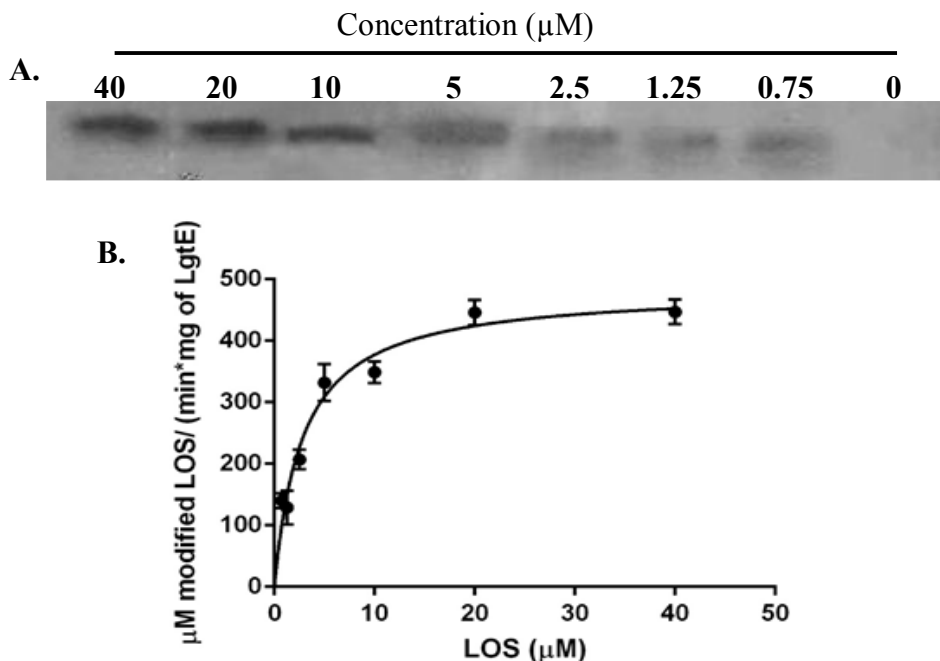


Figure 4.4. Activity of LgtE on Δ lgtE LOS functionalized cationic surfactant vesicles. **A.** Western blot analysis of the *in vitro* glycosylation assays. The observed signals correspond to the formation of L8+ glycoform **B.** Plot of LgtE activity as a function of acceptor substrate concentration. Values reflect the average of 3 independent experiments.

4.2.2 Interfacial Catalysis

LgtE is a peripheral membrane protein *in vivo*, and while the enzyme-membrane dynamics have not been fully elucidated, the enzyme is thought to be transiently associated with the membrane *via* pairs of dibasic residues in the C-terminus.^{12, 15, 39} Based on the knowledge that lipooligosaccharide is synthesized on a lipid carrier in the inner membrane³⁹ it is reasonable to assume that *in vivo* LgtE must first form a complex with membrane prior to participating in LOS biosynthesis. Therefore, the catalytic behavior of LgtE may in part be determined by the organization and dynamics of enzyme at the inner membrane: cytosol interface, and as such LgtE catalysis should be described by an interfacial catalysis kinetic model.⁸¹

Interfacial catalysis involves a series of steps that require consideration to elucidate a complete kinetic description.^{81, 82} The simplest model incorporating each step of interfacial catalysis is illustrated in figure 4.5. Based on the model, LgtE in the aqueous phase (E) binds to the interface (E*). The intrinsic equilibrium interfacial binding step is described by the equilibrium dissociation constant, K_s . The bound enzyme then forms the Michaelis complex (E*S) with surface exposed LOS, described by the

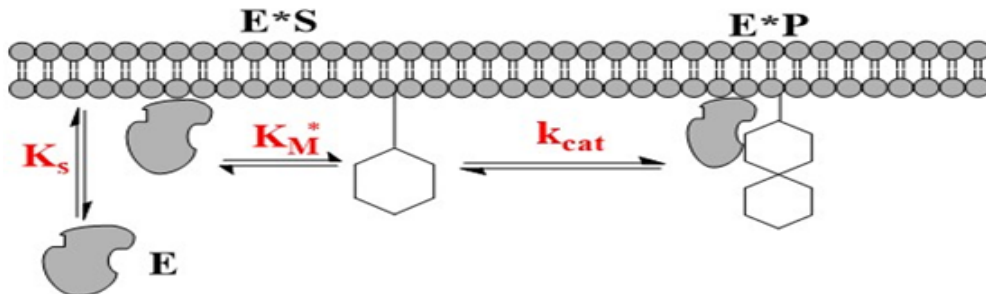


Figure 4.5. Model of LgtE interfacial catalysis. E: enzyme (LgtE); S: substrate (Δ lgtE terminal LOS); P: product (Δ lgtA terminal LOS). During steady state the enzyme in the aqueous phase (E) is in equilibrium with the enzyme at the interface (E*). Figure adapted from reference 81.

interfacial Michaelis constant, K_M^* . LgtE subsequently mediates galactosyl group transfer (E*P) described by the maximal velocity per enzyme molecule, k_{cat} . The glycan can then be further modified by downstream enzymes.

While figure 4.5 allows for an appreciation of the increased complexity of interfacial catalysis by incorporating an interfacial binding step, the dynamics of the enzyme-membrane complex must also be considered in order to completely describe the kinetics of LgtE catalysis at an interface. Enzyme dynamics can be described by one of two models depicted in figure 4.6. If the enzyme “hops” from vesicle to vesicle during catalysis, the rate of desorption and adsorption of the enzyme from the interface will be a part of the overall rate of catalytic turnover, complicating kinetic studies (Figure 4.6A). If, however, the enzyme remains tightly anchored to the vesicle, the enzyme operates in a “processive” mechanism in which multiple catalytic cycles take place prior to enzyme dissociation (Figure 4.6B). This processive mechanism is referred to as “scooting mode.” In the scooting model, the kinetics of interfacial binding step (E to E*) are not considered in the overall steady state reaction kinetics, simplifying kinetic analysis.

For simplicity, LgtE can be assumed to adhere to the scooting mechanism depicted in figure 4.6B. This assumption is reasonable based on the relatively similar structural features of the interfacial binding domain of LgtE and phospholipase A2, a well-studied interfacial catalyst.^{81, 82} LgtE is presumed to associate with the inner membrane *via* the C-terminus, which contains numerous non-polar and basic residues, both of which may contribute to the stabilization of the enzyme: membrane complex.^{12, 15} The structure of phospholipase A2 also contains a region of non-polar and basic residues, the interfacial recognition site, however this region is located at the N-terminus of the

enzyme structure.⁸³ Therefore, based on structural similarity of the interfacial binding domain, the kinetic model in figure 4.5, can be analyzed in the steady-state to give the rate of product formation.⁸²

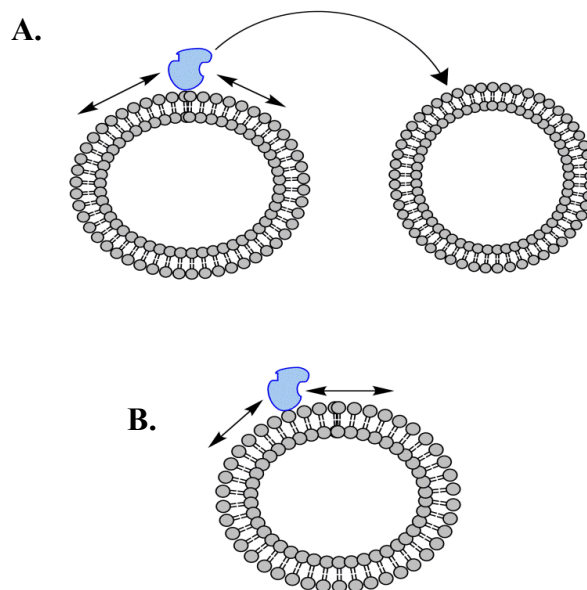


Figure 4.6. Hopping and scooting model describing enzyme dynamics in a membrane. The enzyme is depicted in blue. **A.** Hopping mechanism. **B.** Scooting mechanism. Figure adapted from reference 81.

However, in order to investigate this steady-state reaction under initial velocity conditions, a number of assumptions must be made. The first assumption is that either the binding/dissociation of enzyme to interface is slow, or that the individual surfactant vesicles are not in flux with free surfactant in solution, such that ES from figure 4.5 is not in equilibrium with E*S. Based on this assumption, the only steady-state fluxes that occur are in the chemical reaction, and therefore k_{cat} is the rate-limiting step. With this assumption in mind, the expression for the rate of product formation per enzyme molecule can be derived;⁸²

$$v_o^0 = \frac{k_{cat}[S^*] + k_{cat}^{aq}K_M^*K_d \left(\frac{K_S}{K_M}\right)}{[S^*](1 + K_M^*) + K_dK_M^* \left(1 + \frac{K_S}{K_M}\right)}$$

(Equation 4.2)

where K_S is the dissociation constant for the substrate in the interface, k_{cat} and k_{cat}^{aq} describe the maximal velocity per enzyme molecule at the interface and in the aqueous phase respectively, K_d describes the equilibrium dissociation constant for the substrate, and K_M and K_M^* describe the apparent Michaelis constants in the aqueous phase and at the interface, respectively. Note that the concentration of the substrate $[S^*]$ is expressed in mole fraction because this concentration represents the concentration of substrate that E^* sees at the interface, not the concentration of S in the bulk phase, $[S]$, expressed in molarity (M).

Here k_{cat} and K_M^* account for all the kinetic constants that involve reactions at the interface, and similarly k_{cat}^{aq} and K_M in the aqueous phase, also

$$K_M = K_S \left(1 + \frac{k_{cat}^{aq}}{k_{-1}}\right)$$

(Equation 4.3)

Where k_{-1} is described in equation 4.1 and

$$K_M^* = K_S \left(1 + \frac{k_{cat}}{k_{-1}^*}\right)$$

(Equation 4.4)

Therefore equation 4.2 can be rewritten as:

$$v_o^0 = \frac{V_M^{app}[S^*] + V_{mono}K_M^{app}}{[S^*] + K_M^{app}}$$

(Equation 4.5)

where the reaction velocity at the interface, V_M^{app} , is described by,

$$V_M^{app} = \frac{k_{cat}}{1 + K_M^*}$$

(Equation 4.6)

The apparent Michaelis constant, K_M^{app} , which incorporates both the reaction at the interface and the reaction in bulk solution is described by,

$$K_M^{app} = \frac{K_d K_M^*}{1 + K_M^*} \left(1 + \frac{K_S}{K_M} \right)$$

(Equation 4.7)

And the reaction velocity on the substrate in bulk solution, V^{mono} , which is in equilibrium with the substrate at the interface, is described by,

$$V^{mono} = \frac{k_{cat}^{aq} K_S'}{K_S + K_M}$$

(Equation 4.8)

V_M^{app} , V^{mono} , and K_M^{app} are determined from curve fitting of initial rate vs [LOS] in figures 4.3 and 4.4 to equation 4.5.⁸²

The reaction progress curves in figures 4.3 and 4.4, however, could not be reasonably fit to equation 4.5 (Appendix A4 and A5), rather the shape of the curves reflected the standard Michaelis-Menten enzyme kinetics (Scheme 4.1), indicating that the interfacial binding step (K_M^*) does not contribute to the steady state rate of LgtE catalysis. Nonlinear regression fit to the standard Michaelis-Menten equation is confirmed to be reasonable based on the goodness of fit, $r^2 > 0.94$ for the whole cell reaction and $r^2 > 0.96$ for the vesicle reaction, and visual inspection of the residual plots (Appendix A6).

Our model, describing LgtE as a freely diffusible enzyme in solution (Figure 4.7), is corroborated by prior investigations into the unique properties of the cationic vesicle system.^{36, 84} Specifically, CTAT/SDBS vesicles, with a molar excess of SDBS in the outer leaflet, are extremely stable for long periods of time. Stability was assessed by monitoring the hydrodynamic radius of vesicles in solution, which is a good indicator of structural rearrangements.⁸⁴ Danoff *et al.* conducted dynamic light scattering (DLS) experiments to determine the hydrodynamic radii of cationic vesicles at different time points and with buffers of different ionic strength.⁸⁴ SDBS-rich vesicles were determined to have a hydrodynamic radii of 70 ± 25 nm. However, following size exclusion chromatography (SEC) purification the hydrodynamic radii increased to 98 nm,⁸⁴ and the measured radii remained consistent for at least two months.³² This lack of deviation from the initial time point indicates that the vesicles are equilibrium structures, i.e. there is a stabilizing balance of attractive hydrophobic forces of the alkyl tail groups and the repulsive electrostatic forces of the polar head groups. Further, the authors observed that cationic vesicles efficiently capture and retain cationic dyes for up to 2 months, without any measurable leaching.⁸⁴ Taken together these results suggest that the additive attractive hydrophobic and repulsive electrostatic interactions stabilize the unilamellar

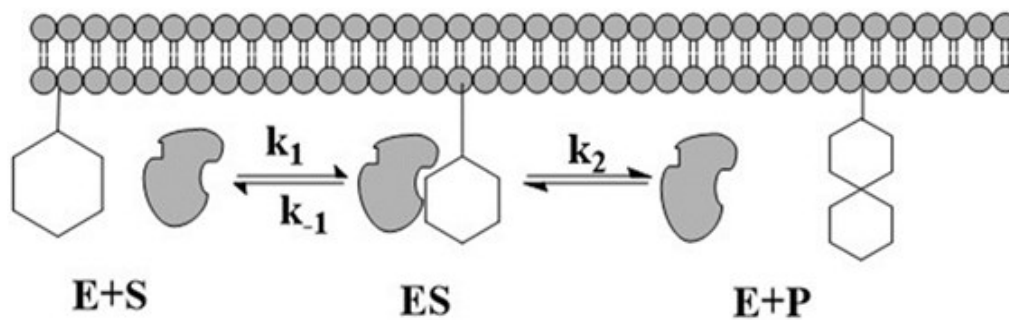


Figure 4.7. Proposed model of LgtE catalysis, in which there is no interfacial binding step.

vesicle structure despite changes in the solvent environment. Therefore, LgtE intercalation into the bilayer is unlikely as it is predicted to disrupt vesicle stability.

Further supporting our model, the ionic strength of the reaction buffer may influence the electrostatic interactions of the dibasic C-terminus residues of LgtE and the outer monolayer of the vesicle membrane, which has a zeta potential of approximately -50 mV.³² The reaction buffer consist of 20 mM HEPES pH 7.4, and 5 mM MnCl₂ (see experimental methods). The ionic strength of the buffer can be calculated from equation 4.9:

$$I = \frac{1}{2} \sum_{i=1}^n c_i z_i^2 \quad (\text{Equation 4.9})$$

where c_i is the concentration of the ionic species, i , and z_i is the valence of the ion. The total ionic strength of the solvent (I) is the sum of the all the ions in solution. From equation 4.9, the ionic strength of the reaction buffer is determined to be 10 mM. Ions in solution will screen the charges on the enzyme and the vesicle respectively, reducing the distance over which the attractive electrostatic forces are significant. The Debye length, κ^{-1} , describes the range and magnitude of these electrostatic interactions. For a 2:1 divalent ion such as Mn²⁺ at a total concentration, of 5mM at 30 °C, the Debye length, expressed in nanometers, can be determined from equation 4.10:⁸⁵

$$\kappa^{-1} = \sqrt{\frac{\epsilon \epsilon_o k_B T}{2 N_A e^2 I}} \quad (\text{Equation 4.10})$$

where ϵ_o is the permittivity of free space, ϵ is the dielectric constant of the medium, k_B is the Boltzmann constant, T is the temperature in Kelvin, N_A is the Avogadro number, and

e is the elementary charge. The screening length of the LgtE reaction buffer is 3.1 nm. As a result, when LgtE is more than 3.1 nm away from the vesicle surface, electrostatic attractive forces become negligible. Considering that the average carbon-carbon bond in the glucose ring is approximately 0.15 nm,⁸⁶ it can be reasonably assumed that the surface exposed LOS molecules extend to a distance at which the electrostatic forces between the two molecules is reduced (Figure 1.9). Moreover, negatively charged KDO sugars and phosphorylethanolamine (PEtN) modification of LOS inner core residues may also attenuate the attractive electrostatic force between the enzyme and the vesicle surface.

Based on previous evidence describing the unique stability of the cationic vesicle system, and taking into consideration the screening effects of the buffer, LgtE affinity for LOS can be described by the Michaelis constant (K_M), defined mathematically as:

$$K_M = \frac{k_{-1} + k_2}{k_1} \quad (\text{Equation 4.11})$$

for the simple enzyme catalyzed reaction scheme:



If the binding of S to E is rapidly reversible relative to catalysis, i.e. $k_{-1} \gg k_2$, K_m is determined from the relationship:

$$K_M = \frac{k_{-1}}{k_1} = \frac{[E][S]}{[ES]}$$

(Equation 4.12)

which is the mathematical expression for the thermodynamic dissociation constant (K_D). K_M therefore, under conditions where $k_{-1} \gg k_2$, represents a measure of affinity of an enzyme for a substrate. In cases where $k_{-1} \leq k_2$, the K_M is greater than the dissociation constant, and the experimentally determined K_M is only an approximate measure of affinity.

The kinetic parameters presented in table 4.1 indicate that the K_M of the LgtE catalyzed reaction is increased approximately eightfold on LOS presented on functionalized cationic surfactant vesicles as compared to LOS presented in a whole cell background. Further, the k_{cat}/K_M is increased approximately fivefold, supporting the data presented in the previous chapter that indicated that LgtE catalyzed LOS modification occurs more efficiently on vesicles as compared to whole cell bacteria. The observed increase in activity may be a result of the inherent heterogeneity of whole cell bacterial membranes, which is in sharp contrast to the homogeneity of the vesicle surface. The three-dimensional macromolecular structure of LOS is dynamic, a consequence of the numerous hydroxyl groups and the free rotation permitted about the glycosidic bond.⁸⁷ Weak interactions between LOS and integral proteins of the bacterial cell membrane, mediated by electrostatic forces, hydrogen bonding, and hydrophobic interactions, can modulate LOS conformation and therefore also influence the efficiency of enzymatic modification. Functionalized surfactant vesicles only incorporate LOS into the outer membrane, reducing the probability that LOS presentation will be altered by these noncovalent interactions. Therefore, the probability that LOS will be presented in

an accessible conformation for LgtE recognition is greater for LOS functionalized catanionic vesicles, than in whole cell membranes.

Acceptor	K_M (μM)	k_{cat} (1/min)	k_{cat}/K_M (1/min* μM)
Δ lgtE Whole Cell LOS	18 \pm 2	75 \pm 2	4.3
Δ lgtE LOS vesicles	2.4 \pm 0.5	50 \pm 3	20.4

TABLE 4.1. Kinetic parameters of LgtE catalyzed LOS modification. Values reflect the average of 3 independent experiments.

4.2.3 Proof of Principle: Functionalized Catanionic Vesicle- Based Glycomic Array

To investigate the feasibility of exploiting LgtE and other recombinant enzymes in developing a glycomic array, we utilized a technology advanced by the DeShong group.³⁷ Neeraja Dashaputre in the DeShong lab demonstrated that functionalized vesicles are retained on electrodes coated with hydrophobically modified chitosan (HM-chitosan), and that the vesicles could be visualized by microscopy on this platform. Figure 4.8 depicts the experimental set up. Initially, the electrodes were prepared by printing gold onto silicon wafers in a specific pattern (Figure 4.8A). HM-chitosan was then electrodeposited on the electrodes such that a thin film coated the surface of the electrode (Figure 4.8B step 1). The enzymatic reaction with LgtE and Δ lgtE terminal LOS functionalized vesicles was performed in solution, and then I spotted the reaction mixture onto the HM-chitosan coated electrode (Figure 4.8B step 2). Product formation was detected by the monoclonal antibody 2-1-L8, which is specific for the lactosyl α -chain LOS structure (Figure 4.8B step 3). Finally the presence of bound monoclonal

antibody was detected by Alexa Fluor® 568 goat anti-mouse IgG (H+L) antibody (Molecular Probes®).

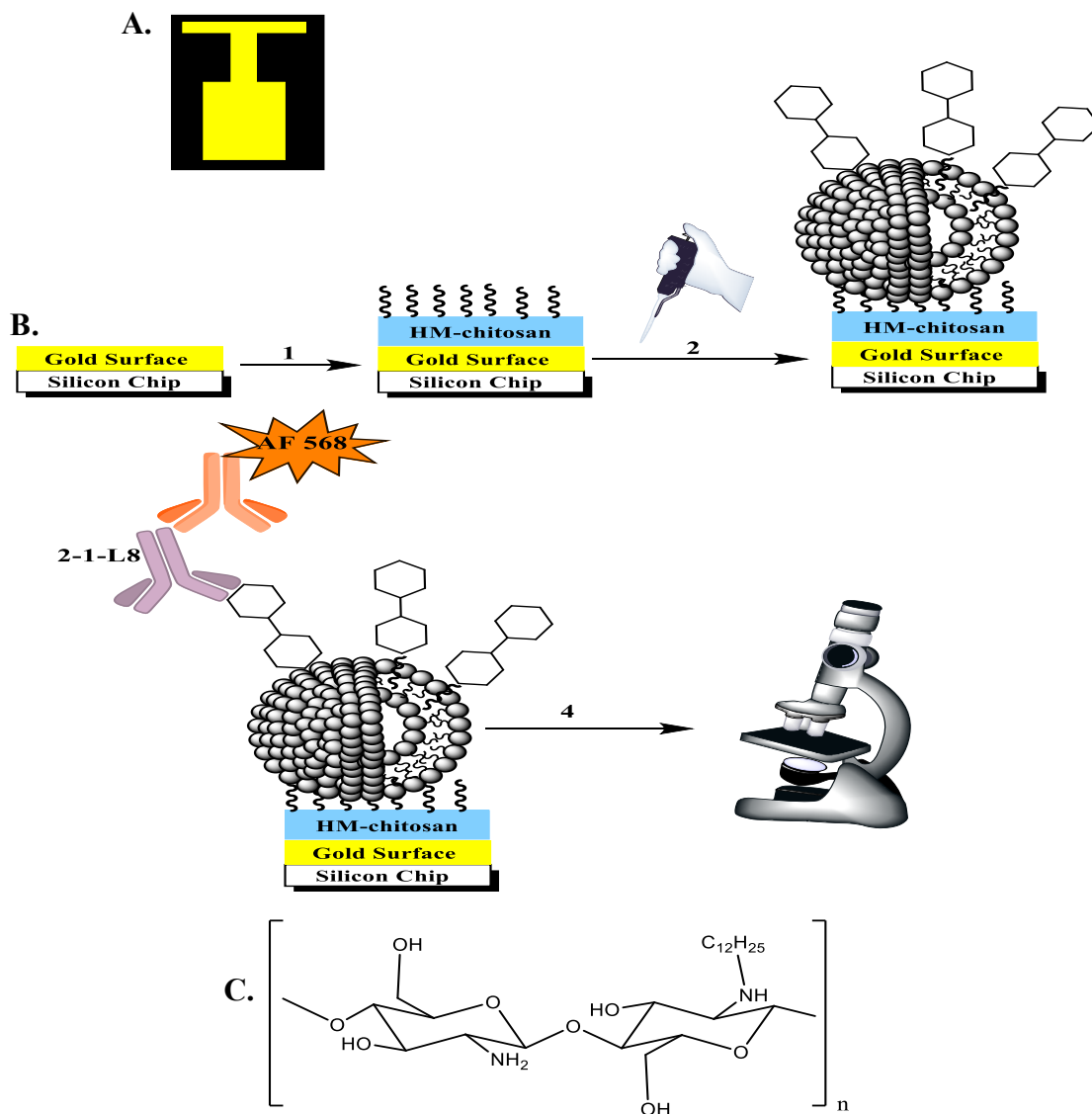


Figure 4.8. Schematic of the preparation of carbohydrate microarrays using HM-chitosan and SDBS-rich functionalized vesicles. **A.** Representation of the electrode. The yellow represents the printed gold surface on which HM-chitosan is electrodeposited. Blue areas represent the silicon wafer on which a specific pattern of gold is printed. **B.** Preparation of the electrode. *Step 1:* HM-chitosan is electrodeposited onto the gold surface *via* a pH dependent mechanism. *Step 2:* HM-chitosan inserts aliphatic chains into the catanionic vesicle bilayer, absorbing intact vesicles on the surface. *Step 3:* The surface of the vesicles is probed with the primary monoclonal antibody. The presence of the bound primary antibody is detected by a fluorescently labelled secondary antibody. *Step 4:* Electrodes were visualized under a fluorescent microscope **C.** Chemical structure of HM-chitosan. The *n*-dodecyl tails were covalently attached to the amine groups of chitosan *via* reductive amination (Figure adapted from Dr. Neeraja Dashaputre's dissertation).

Figure 4.9 presents the results of the experiment outlined in figure 4.8B. I visualized the electrodes on a fluorescent microscope (see experimental methods for more detail) and the representative images of each condition are shown. Figure 4.9C demonstrates that incubating Δ lgtE LOS functionalized vesicles with the purified enzyme enhances antibody binding above the background signal observed in figure 4.9B.

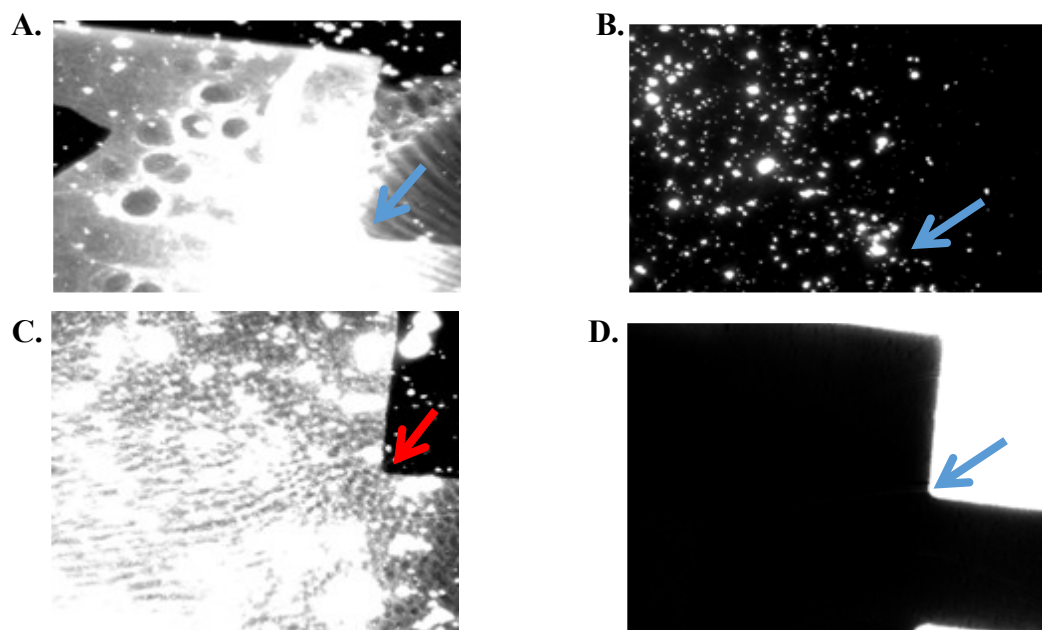


Figure 4.9. Visualization of LgtE mediated, catalytic modification on functionalized vesicles by fluorescently labelled antibodies. From left to right, **A.** Positive control: Δ lgtA LOS functionalized vesicles **B.** Negative control: Δ lgtE LOS functionalized vesicles **C.** Reaction electrode: Δ lgtE LOS functionalized vesicles coated on the electrode. 1.5 μ g purified LgtE, UDP-galactose, together with reaction buffer are spotted on the coated electrode and incubated overnight at 30 °C. **D.** Brightfield image of electrode. The arrows indicate the right angle formed by the stem of the electrode.

Figure 4.9C confirms that LOS-functionalized cationic vesicles are retained by the amphiphilic biopolymer, and that chemo-enzymatic synthesis is achieved. Figure 4.9 also demonstrates that glycan binding proteins specifically recognize functionalized cationic surfactant vesicles. Importantly, the data builds on previous studies providing experimental evidence for the utility of glycan-functionalized surfactant vesicles as a platform in investigations of carbohydrate-active enzymes and glycan binding proteins.

4.3 Discussion

Carbohydrate-active enzymes are among the most abundant biocatalysts found in nature. However, their functional characterization has been limited, in part, due to the lack of a platform that allows for the characterization of a variety of enzymes on a diverse array of acceptor substrates. The data presented above demonstrate that glycans incorporated into cationic surfactant vesicles are modified by a recombinant glycosyltransferase with similar efficiency as glycans presented on whole cell bacteria. This result is surprising, but can be explained by the physical properties of the cationic surfactant system. In particular, functionalized SDBS-rich cationic surfactant vesicles possess a zeta potential that is equivalent to the phospholipid bilayer of a Gram-negative bacterium. Therefore, the acceptor glycan is presented in background that mimics the *in vivo* environment in which the acceptor substrate encounters the glycosyltransferase. Additionally, the data outlined in this chapter suggest that the bioavailability of the substrate is enhanced when presented on the surfactant vesicle.

Based on the kinetic parameters defined above, functionalized cationic surfactant vesicles are ideal platforms for characterization of carbohydrate-processing enzymes. Further, data presented herein, demonstrating the retention and screening of functionalized vesicles on a “hard” surface, supports the utility of these vesicles in constructing a high-throughput array. This work represents a significant step towards the development of glycomic array technology and will facilitate future investigations not limited to the characterization of carbohydrate-active enzymes, but also into the binding characteristics of glycan binding proteins.

4.4 *Experimental*

4.4.1 Time Course LOS SDS-PAGE Analysis

Whole cell gonococcal LOS was prepared from plated cultures as described by Hitchcock and Brown⁷⁴ and diluted 1:25 in 3x Laemmli buffer. The suspension was heated to 65 °C for a minimum of 10 minutes. Reactions and vesicles were diluted and heated in the same manner. 20 µl of each sample were loaded onto a sodium dodecyl sulfate-polyacrylamide gel electrophoresis (SDS-PAGE) gel. After electrophoresis, the gel was fixed overnight in a solution of 40% ethanol- 5% acetic acid and then oxidized in 0.83% periodic acid for 5 minutes. The gel was washed for 2 hours in multiple changes of H₂O every 20 minutes, stained for 5 minutes in silver staining solution (22.5 mM NaOH, 0.42% NH₄OH, 47 mM AgNO₃), and rewashed for 2 hours in multiple changes of H₂O every 20 minutes. The gel was developed (100 ml of 0.005% citric acid-0.007% formaldehyde) until bands became visible.

A digital image of the gel was obtained on a flatbed scanner. Subsequently, the gel was analyzed with ImageJ software (Rosband W. U.S. National Institutes of Health, Bethesda, MD. <http://imagej.nih.gov/ij/>).

4.4.2 Enzymatic Assays

The concentration of the acceptor substrate present on the surface of both vesicles and on whole cells was determined indirectly by the exoglycosidase activity of $\beta(1\rightarrow4)$ glucosidase (from almonds Sigma-Aldrich, St. Louis, MO). The glucosidase reaction was allowed to go to completion overnight at 37 °C.

The concentration of liberated glucose was then determined with a glucose oxidase assay kit (Sigma-Aldrich, St. Louis, MO). This quantitative, enzymatic assay determines the amount of glucose present in a solution *via* glucose oxidation to gluconic acid and hydrogen peroxide by glucose oxidase. The hydrogen peroxide byproduct reacts with *o*-dianisidine in the presence of peroxidase to form a pink colored product. The intensity of the color is quantified on a UV/Visible spectrophotometer (Ultrospec 2000, Pharmacia Biotech) at 540 nm and is proportional to the original glucose concentration. Thus, by comparison to a standard curve the concentration of glucose cleaved by $\beta(1 \rightarrow 4)$ glucosidase from the surface can be inferred.

Purified LgtE enzyme concentration was calculated based on absorbance readings by a Nano-drop UV/Visible spectrophotometer (Thermo Fischer Scientific, Wilmington, DE). The extinction coefficient, $23045 \text{ M}^{-1} \text{ cm}^{-1}$, of the enzyme was calculated in water based on the amino acid sequence (ExpASy, SIB Swiss Institute of Biotechnology).

LgtE galactosyltransferase activity was determined in reaction buffer (20 mM HEPES [pH 7.5], 1 mM UDP- α -D-galactose, 5 mM MnCl_2) containing 1.5 μM LgtE and 40, 20, 10, 5, 2.5, 1.25, 0.75, and 0 μM Δ lgtE LOS incorporated into functionalized vesicles, or 480, 240, 120, 60, 30, 15, 7.5, and 0 μM Δ lgtE LOS expressed on the surface of F62 Ω EcoRI whole cells. To normalize for SDS-PAGE visualization, the volume of the reaction mixture was varied such the total volume of the donor substrate remained the same for each concentration point. The reaction mixtures were incubated at 30 °C for 30 minutes and then terminated by adjusting the reaction mixture volumes to a single maximum volume, followed by centrifugation and re-suspension in 20 μl of 3x Laemmli buffer. 10 μl aliquots were then subjected to SDS-PAGE analysis. Following SDS-

PAGE separation, LOS were electro-transferred onto Immobilon-P membrane (EMD Millipore Corp., Billerica, MA.) in a Tris-Tricine-methanol buffer (10 mM Tris [pH 8.3], 10 mM Tricine, 20% methanol) at a constant voltage of 100 V for 20 minutes. The membrane was then incubated in buffer (1x PBS, 0.05% Tween-20, 5% dry milk) to block nonspecific sites. The monoclonal antibody 2-1-L8, previously described by O'Connor et al.,⁴⁰ served as the primary antibody, and was incubated with the membranes for a minimum of 1.5 hours at room temperature. Following a second block step, bound antibody was detected by incubation with horseradish peroxidase-conjugated goat anti-mouse IgG (H+L) (Jackson ImmunoResearch Laboratories, West Grove, PA) for a minimum of one hour at room temperature. The intensity of signal corresponding to product formation was quantified by ImageJ software at each substrate concentration. The amount of product formation was calculated, per time unit and μM LgtE, from a standard curve of known concentrations of ΔlgtA terminal LOS structures blotted simultaneously. The experimental data were fit to obtain V_{max} and K_M using GraphPad Prism version 6.0 for Windows considering a Michaelis-Menten model (GraphPad Software, Inc., La Jolla, CA, www.graphpad.com)

4.4.3 Vesicle Visualization on HM-Chitosan Coated Electrode

Dr. Neeraja Dashaputre of the DeShong group prepared the electrodes. Briefly, chitosan of medium molecular weight (190-310K) and Brookfield viscosity of 286 cps was purchased from Sigma-Aldrich, which had a degree of deacetylation about 80%. It was dissolved in 0.2 M acetic acid (pH < 6.5). Hydrophobically modified (HM) chitosan was prepared by reductive amination of chitosan with dodecylaldehyde by the method reported in her dissertation.³⁷ The degree of hydrophobic modification was 2.5 mol %

based on monomer. The method involves the following steps. Chitosan (2.00 g) was dissolved in 100 ml water, and glacial acetic acid was added drop wise (0.2 ml with stirring). The resulting suspension was stirred for 16 h. Ethanol (100 ml) was added to this solution and stirred for 15 min. Dodecyl aldehyde (0.057 g) dissolved in 5 ml ethanol was added to the chitosan solution drop wise, while stirring the chitosan solution vigorously. After 30 min, a solution of 0.78 g of NaCNBH₃ dissolved in 10 mL ethanol was added thrice (2.34 g total) at intervals of 2 h. The solution was stirred for 24 h after the final addition of NaCNBH₃. NaOH (100 ml, 0.1 M) was added to neutralize the solution. Formation of a white precipitate was observed as NaOH was added. NaOH (15 ml of 1 M) was added drop wise to complete precipitation of HM chitosan. The resulting precipitate was washed with water until the pH of the supernatant was pH 7, and dissolved in 0.2 M acetic acid. The solution was poured onto non-stick baking pans and dried for 3 days to cast films of HM chitosan. HM chitosan was dissolved in water, with drop wise addition of acetic acid to prepare 1 wt % solution (pH 5.5). Later synthesis of HM chitosan involved drying the HM chitosan directly without dissolving it in acetic acid. This resulted in a better control of pH of HM chitosan solution, thus resulting in better, more even electrodeposition of HM chitosan. Fluorescently-labeled chitosan and HM chitosan were obtained from Professor Gregory Payne's lab. These were synthesized by reacting the polymers with NHS-fluorescein, as previously reported in the literature.³⁸

100 μ M LOS functionalized vesicles were incubated in reaction buffer (20 mM HEPES pH 7.5, 1 mM MnCl₂, 1 μ M LgtE) with or without 1 mM UDP- α -D-galactose, at 30 °C for a minimum of 2 hours. Subsequently, the reaction mixture was spotted onto the functionalized electrodes, and then washed 3 times with 1x PBS pH 7.2. Monoclonal

antibody 2-1-L8 was then applied to the electrodes for a minimum of one hour. Following a wash step, Alexa Fluor® 568 goat anti-mouse IgG (H+L) antibody (Molecular Probes®) in 20 mM HEPES pH 7.5 was applied to the electrode. A final wash step was performed and the electrodes were visualized on a Zeiss Axio Imager.Z1 fluorescent microscope (Carl Zeiss) through a EC Plan-Neofluor 10x objective in bright field and fluorescence using filter set 43HE (excitation wavelength 550/25 nm and emission wavelength 605/70 nm; Zeiss). Photographs were taken with a mounted AxioCam MR3 (Zeiss), and the images were analyzed using AxioVision Rel. 4.8.2 software (Zeiss).

Chapter 5: Conclusions and Prospectus

From xenotransplantation to vaccination,⁸⁸ to more recently the treatment of traumatic brain injury,⁸⁹ glycosylation is increasingly recognized as a critical component of pharmacology and an essential consideration in clinical innovations. Glycan-functionalized cationic surfactant vesicles are an established platform for investigations into carbohydrate binding proteins, and more recently are being utilized for targeted drug delivery and vaccine development.⁸⁸ The work of this dissertation presents novel applications for functionalized cationic surfactant vesicles. First, I demonstrate that under the appropriate conditions, surfactant vesicles can be utilized for enrichment of insoluble species associated with cell membranes, such as bacterial glycosyltransferases. In conjunction with our collaborator's unpublished data demonstrating the ease and efficiency by which surfactant molecules can be separated from proteins and LOS incorporated in vesicles, this novel application of cationic vesicles has the potential of facilitating macromolecule purification from membrane structures.

Second, this study presents a novel demonstration of *Neisseria* glycosyltransferase LgtE activity on whole cell LOS. While *in vitro* activity of the enzyme has been previously demonstrated, previous reports utilized free LOS, which lacks true physiological relevance. Subsequently, LgtE activity was demonstrated on LOS functionalized and C₁₂-glucose functionalized cationic surfactant vesicles by flow cytometry analysis. The data presented in chapter three is the first report utilizing flow cytometry techniques to assess enzymatic modification of functionalized cationic surfactant vesicles.

This study also expands on previous work demonstrating the utility of functionalized cationic surfactant vesicles in investigations of ligand recognition and catalysis by glycan binding proteins.^{19, 32} The data presented in chapter three demonstrate that enzymatic activity of a galactosyltransferase is maintained in the presence of cationic vesicles, and that the galactosyltransferase activity is not limited to glycans of bacterial origin. Moreover, as discussed in chapter four, the kinetics of glycan enzymatic modification is modestly improved on cationic vesicles as compared to whole bacterial cells. Based on the data presented in chapters three and four, glycan-functionalized cationic surfactant vesicles may serve as a platform expediting, for example, the synthesis of inhibitors to galectin-3 (gal-3), a lectin that recognizes beta-galactoside terminating glycoconjugates and has an active role in cancer progression and metastasis.⁹⁰ This example of vesicle utility is particularly promising as studies conducted by the Stein and DeShong groups indicate that the cationic surfactant vesicles can be modified to target hyper-proliferative cells (Dr. Lenea H. Stocker's dissertation). Therefore, this work could be expanded such that specific recombinant glycosyltransferases biosynthesize carbohydrates of known structure, *in vitro*, on cationic vesicles. These vesicles could subsequently be administered as part of a chemotherapy regime (Figure 5.1).

Finally, this dissertation provides the basis for a variety of future technological advances in the field of glycomics. Specifically, by providing evidence of the utility of cationic vesicles as a platform for the development of a glycomic array to profile the human glycome. Data is presented in chapter four indicating that following enzymatic modification, vesicles are retained on a "hard" surface and that the modified glycans are

bioavailable, as demonstrated by differential antibody binding. This data, together with the FACS analysis in chapter three, confirms that functionalized cationic vesicles have the potential to serve as a scaffold to probe differential lectin or antibody binding.

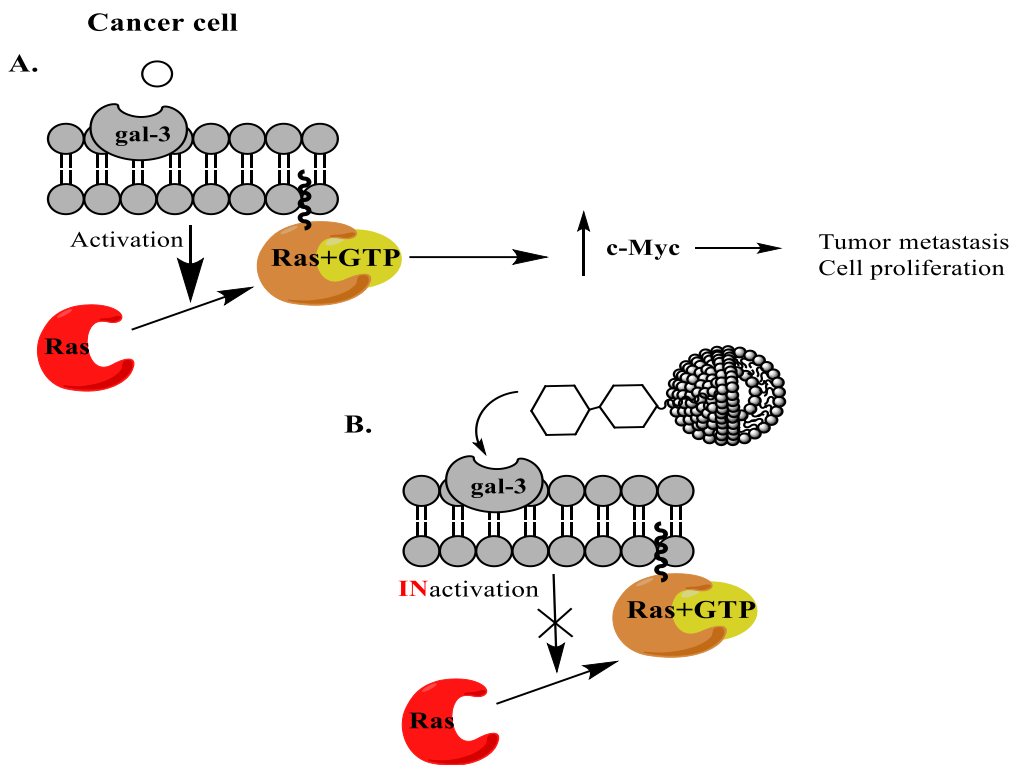


Figure 5.1. Galectin-3 overexpression mediates tumor metastasis and proliferation. **A.** Gal-3 activation recruits Ras+GTP to the plasma membrane inducing downstream signaling. Ultimately, expression of the transcription factor c-Myc is increased, leading to increased cellular proliferation and tissue invasion. **B.** The work of this dissertation may lead to the synthesis of glycans that selectively inhibit gal-3 activation, potentially reducing the incidence of metastatic disease.

The clinical implications of the data presented in chapters three and four are significant. According to the American Cancer Society, in 2014 alone there will be an estimated 1,665,540 new cancer cases diagnosed and 585,720 cancer deaths in the United States. It is well established that altered protein glycosylation in cancer cells is a key characteristic of malignant transformation.^{91,92} Within the field of cancer research, there is a great interest to exploit the cancer glycome as source of biomarkers. However, the discovery of disease markers has been limited by the inherent diversity and complexity of

tumor specific glycans, and a lack of quantitative techniques to detect subtle changes in glycan structure.⁹² Recent evidence presented by Fry *et al.* and Blixt *et al.* has reinvigorated the idea that lectin or antibody profiling, respectively, could be utilized to detect tumor specific antigens and determine disease progression.^{92, 91} Fry and colleagues employed a commercially available lectin microarray glass slide as a platform, and applied formalin-fixed paraffin-embedded metastatic and non-metastatic breast tissue, as well as serum and urine from patients with metastatic breast cancer to the slide, to investigate lectin binding profiles (Figure 5.2).⁹² The authors concluded that there are subtle distinctions in the glycan expression profile of metastatic and non-metastatic breast cancer, and a lectin microarray could be used to detect these glycan biomarkers. There are limitations to this methodology, however, a consequence of covalently coupling lectins to slides. Significantly, structural flexibility may be restricted and the orientation of the immobilized lectins is random, both of which influence lectin binding properties.⁹²

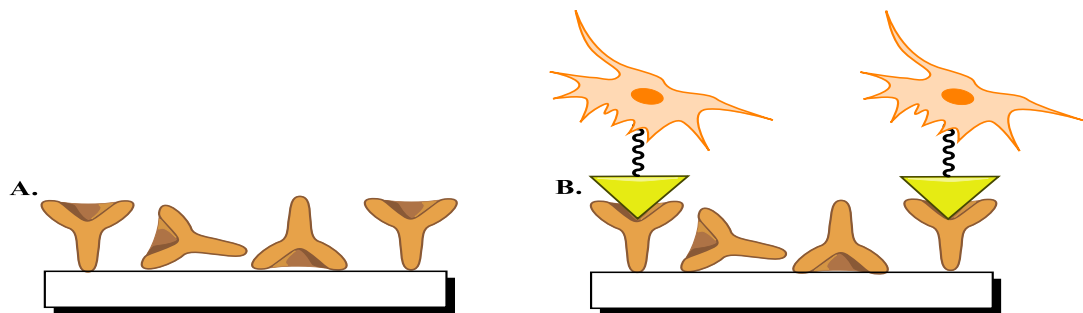


Figure 5.2. Lectin microarray profiling of cancer tissue. **A.** Covalently coupled lectins are immobilized on a glass slide. In the process of immobilization, the orientation of the coupled lectins is random, which may result in discrepancies in the observed binding profiles. **B.** Metastatic tissue, urine, or serum from patients with breast cancer are applied to the slide, and a glycomic profile is obtained.

Blixt *et al.* took a different approach toward investigating the cancer glycome.

Previously, it was reported that there is a positive correlation of the mucin-type O-glycan Tn (GalNAc α 1-O-Ser/Thr) in primary tumors with lymph node metastasis.⁹² Moreover,

the authors found that the sera of patients diagnosed with breast, ovarian, and rectal cancer all demonstrated reactivity with immobilized peptides expressing the Tn antigen.⁹¹ Expanding on the work of Blixt *et al.*, the data presented in this dissertation demonstrate that recombinant glycosyltransferases chemo-enzymatically synthesize structurally defined glycans on the surface of functionalized cationic surfactant vesicles. Cationic vesicles, therefore, have the potential to serve as a novel platform for the immobilization of diverse glycan biomarkers onto an array platform, which could be probed by a patient's serum or urine for identification of tumor specific antibodies, autoantibodies associated with autoimmune diseases, or to determine an individual's antibody titer (Figure 5.3).⁹¹ Further, this dissertation demonstrates that the presentation of glycans on the vesicle surface does not influence protein binding, indicating that the proposed methodology circumvents the limitations inherent to lectin microarrays. Chemo-enzymatic synthesis is a desired means of obtaining glycan-based antigens, as numerous studies have highlighted the heterogeneity of glycan expression *in vivo*, complicating simple isolation techniques.^{44,93} The methodology proposed in figure 5.3,

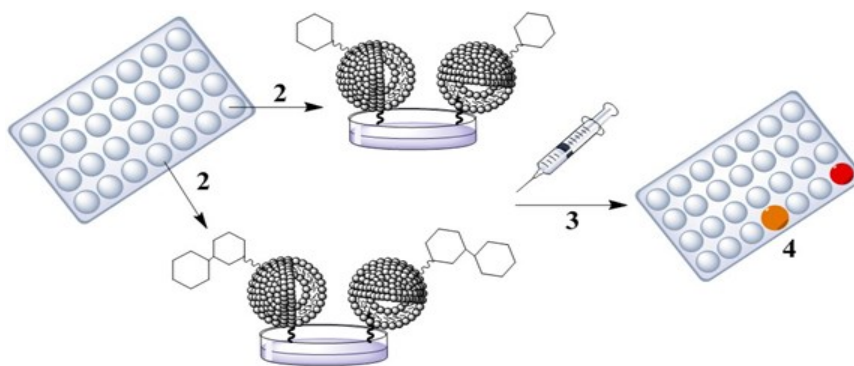


Figure 5.3. The work of this dissertation provides proof-of-concept that cationic surfactant vesicles along with recombinant glycosyltransferases can be utilized to develop diagnostic tool for immunoprofiling. *Step 1* (not shown): glycosyltransferases modify functionalized vesicles, biosynthesizing glycans of defined structure. Vesicles are applied and retained in wells of a microtiter plate, coated with HM-chitosan (step 2). Serum is applied (step 3), and the presence of antibody binding is detected (step 4).

therefore, has the potential to provide a patient with a quick and reliable diagnosis and to provide an indication of disease progression.

Currently, progress in the field of glycomics is limited by the absence of a standard platform on which glycans can be modified and investigated. Based on the work outlined in this dissertation, glycan-functionalized cationic surfactant vesicles should be considered to fulfill this role. In conclusion, cationic surfactant vesicles are a novel platform that could serve as a transformative tool for probing protein-glycan interactions in simple or complex mixtures and for the chemo-enzymatic synthesis of glycan-defined bioconjugates.

Appendices

Appendix 1: Characterization of *N. gonorrhoeae* Strain F62 Ω EcoRI

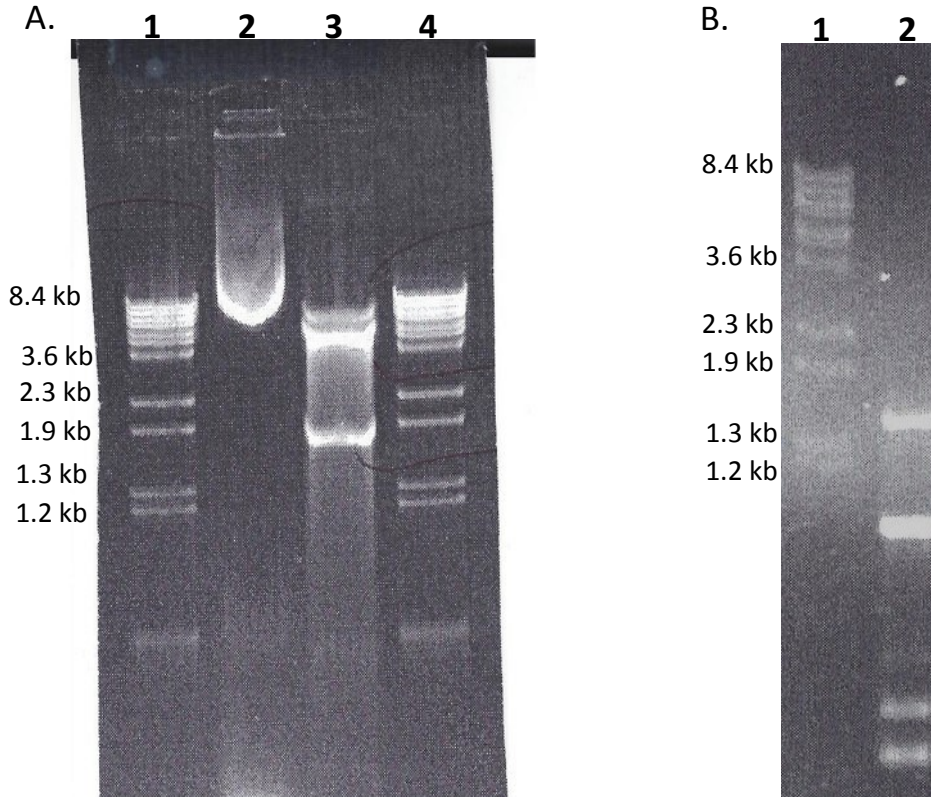


Figure A1. **A.** Confirmation that the Ω interposon of pLgtDE Ω EcoRI is located in the expected region. *Lane 1:* Lambda DNA ladder, digested with BstEII. The molecular weights are indicated on the left side in kilo-base pairs (kb). *Lane 2:* Undigested supercoiled pLgtDE Ω EcoRI. *Lane 3:* pLgtDE Ω EcoRI digested with EcoRI for ~2.5 hours at 38 °C. The Ω cassette liberated from the plasmid has an electrophoretic profile, as expected, of approximately 2082 kb. The digested plasmid has the expected profile of approximately 4 kb, and the residual undigested plasmid can be observed as the largest molecular weight band. *Lane 4:* Lambda DNA ladder, digested with BstEII. **B.** Verification of the proper insertion of the Ω cassette. *Lane 1:* Lambda DNA ladder, digested with BstEII. *Lane 2:* PCR amplification of *N. gonorrhoeae* strain F62 chromosomal DNA using a forward primer that binds within the Ω cassette at approximately 780 base pairs, and the reverse primer DA5, which binds 858 base pairs into the lgtE coding sequence. The resultant amplicon is expected to be 1638 base pairs. The additional lower molecular weight bands are most likely the result of aberrant primer binding due to the high degree of sequence homology within the *lgtBE* genes.

Appendix 2: 15% Tris-HCl SDS-PAGE of 8M urea solubilized LgtE (complete gel)

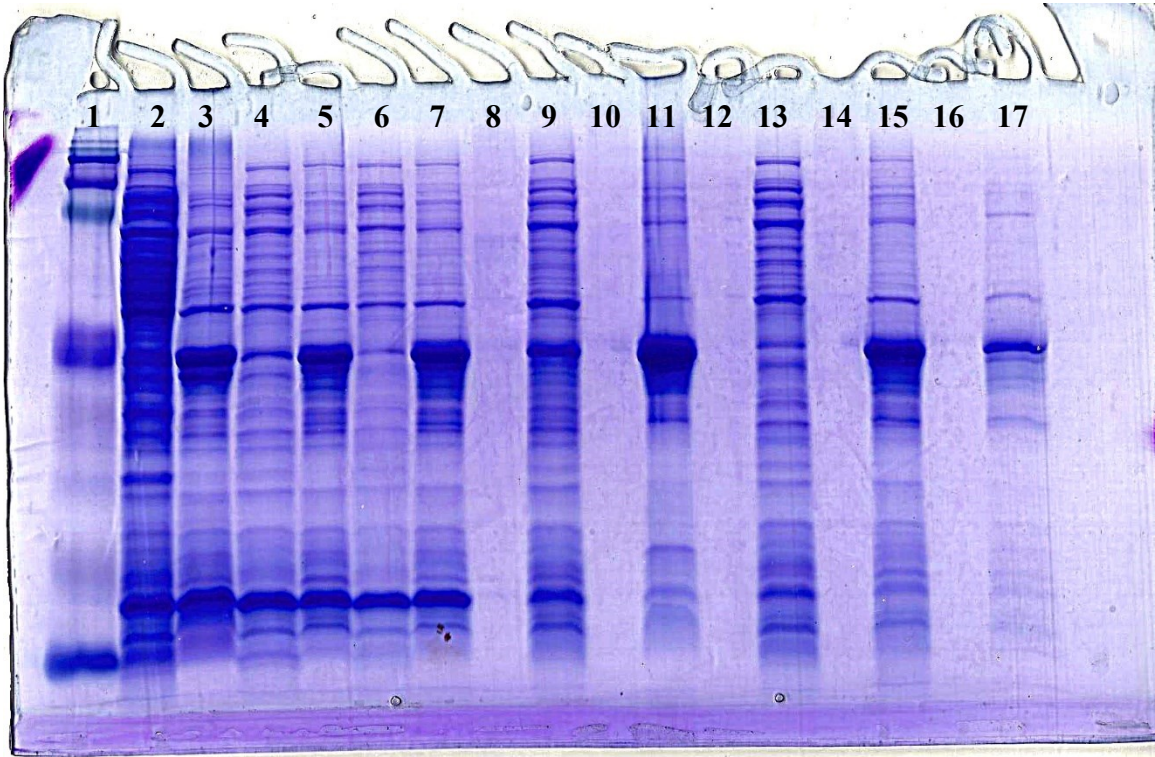


Figure A2. Coomassie Blue stain of 15% Tris-HCl SDS-PAGE analysis. From left to right: Lane 1- Kaleidoscope protein ladder Lane 2- Uninduced supernatant; Lane 3- Uninduced pellet; Lane 4- 30 °C induction supernatant; Lane 5- 30 °C induction pellet; Lane 6- 37 °C induction supernatant; Lane 7- 37 °C induction pellet; Lane 8- Lysing buffer alone; Lane 9- Supernatant under denaturing conditions (8M urea added prior to sonication); Lane 10- Lysing buffer alone; Lane 11- Pellet under denaturing conditions; Lane 12- Lysing buffer alone; Lane 13- 1:10 Uninduced supernatant; Lane 14- Lysing buffer alone; Lane 15- Pellet under non-denaturing conditions; Lane 16- Lysing buffer alone; Lane 17- Pellet from non-denaturing conditions resolubilized with anionic surfactant vesicles; Lane 18- Lysing buffer alone.

Appendix 3: Calculation of Interfacial Catalysis Parameters

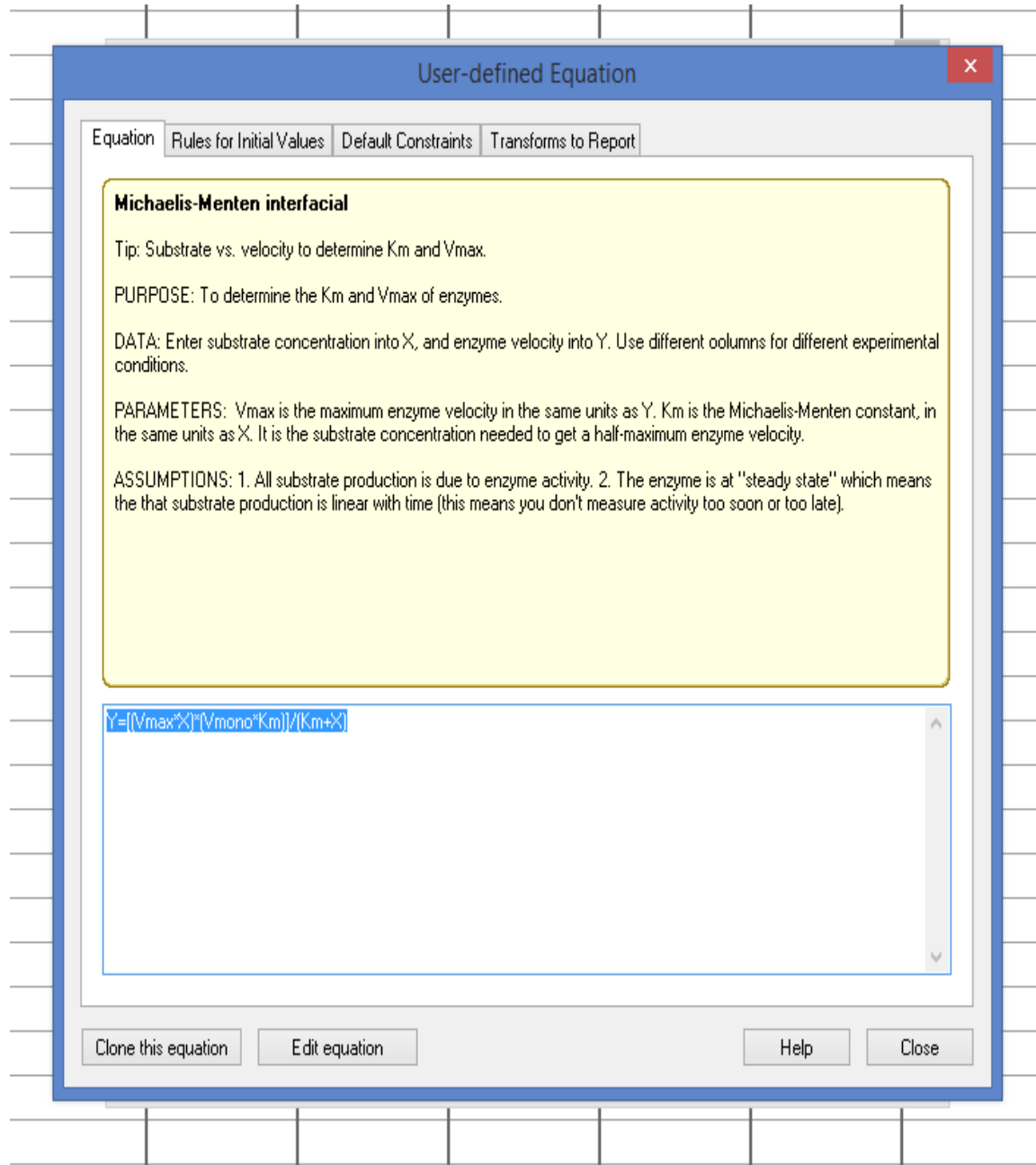


Figure A3. Equation 4.5 from text as a user-defined equation in GraphPad Prism. Vmax represents V_M^{app} ; Km represents K_M^{app} ; X is the substrate concentration at the interface in mole fraction; and Y is the measured rate of the reaction.

Appendix 4: Nonlinear Regression of Kinetic Rates on Whole Cells Using Interfacial Catalysis Model

Nonlin fit		A
		Data Set-A
		Y
1	Michaelis-Menten interfacial	Ambiguous
2	Best-fit values	
3	Vmax	~ 13.39
4	Vmono	~ 2.609
5	Km	17.54
6	Std. Error	
7	Vmax	~ 6.593e+011
8	Vmono	~ 1.285e+011
9	Km	5.382
10	95% Confidence Intervals	
11	Vmax	(Very wide)
12	Vmono	(Very wide)
13	Km	2.597 to 32.49
14	Goodness of Fit	
15	Degrees of Freedom	4
16	R square	0.9418
17	Absolute Sum of Squares	10129
18	Sy,x	50.32
19	Constraints	
20	Km	Km > 0.0
21		
22	Number of points	
23	Analyzed	7
24		
25		
26		
27		
28		
29		
30		
31		
32		
33		

Figure A4. Tabulated results of fitting the whole cell reaction initial rates versus [LOS] to equation 4.5. Note the wide confidence intervals and ambiguous fit. The 95% confidence interval describes a range of values which may reasonably contain the true value. The confidence intervals reflect the precision of the fit, in other words the likelihood that if the data were obtained under the same conditions that the same values of V_M^{app} and V^{mono} would be obtained.

Appendix 5: Nonlinear Regression of Kinetic Rates on Vesicles Using Interfacial Catalysis Model

Nonlin fit		A
		Data Set-A
		Y
1	Michaelis-Menten interfacial	Ambiguous
2	Best-fit values	
3	Vmax	~ 27.51
4	Vmono	~ 7.414
5	Km	2.437
6	Std. Error	
7	Vmax	~ 7.438e+011
8	Vmono	~ 2.004e+011
9	Km	0.6507
10	95% Confidence Intervals	
11	Vmax	(Very wide)
12	Vmono	(Very wide)
13	Km	0.6307 to 4.244
14	Goodness of Fit	
15	Degrees of Freedom	4
16	R square	0.9656
17	Absolute Sum of Squares	4424
18	Sy.x	33.26
19	Constraints	
20	Km	Km > 0.0
21		
22	Number of points	
23	Analyzed	7
24		
25		

Figure A5. Tabulated results of fitting the vesicle reaction initial rates versus [LOS] to equation 4.5. Note the wide confidence intervals and ambiguous fit.

Appendix 6: Residual plot of nonlinear regression fit to the standard Michaelis-Menten equation

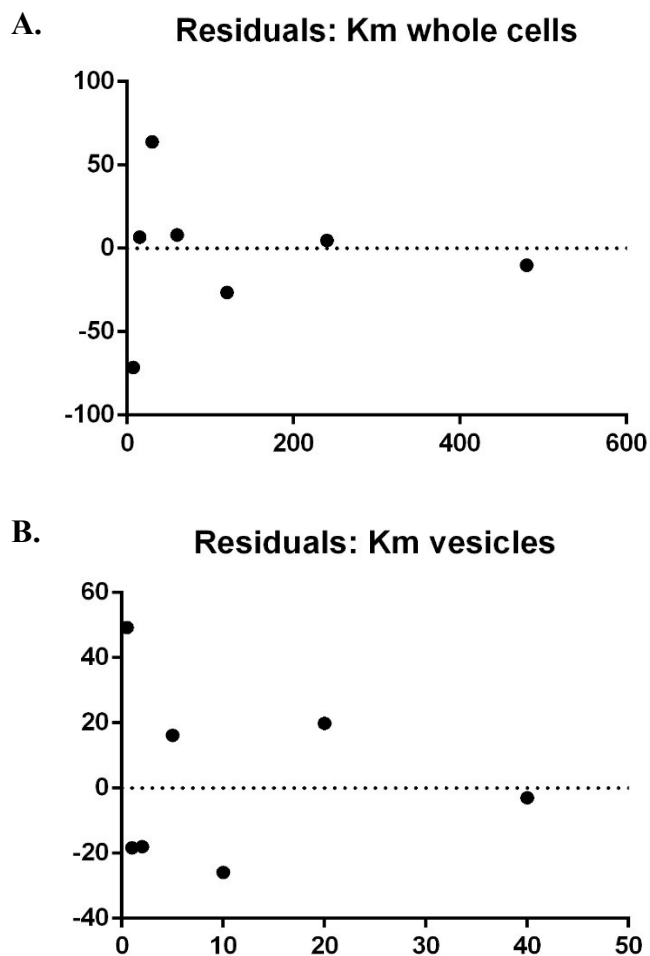


Figure A6. **A.** Residual plot of the nonlinear regression fit of LgtE activity on the surface of whole cell bacteria (figure 4.2) and **B.** on functionalized cationic vesicles (figure 4.3).

Appendix 7: Contribution to published works

a. Adriana LeVan, Lindsey I. Zimmerman, **Amanda C. Mahle**, Karen V. Swanson, Philip DeShong, Juhee Park, Vonetta L. Edwards, Wenxia Song, and Daniel C. Stein. (2012), Construction and Characterization of a Derivative of *Neisseria gonorrhoeae* Strain MS11 Devoid of All *opa* Genes. J. Bacteriol. 194:23 6468-6478. doi:10.1128/JB.00969-1

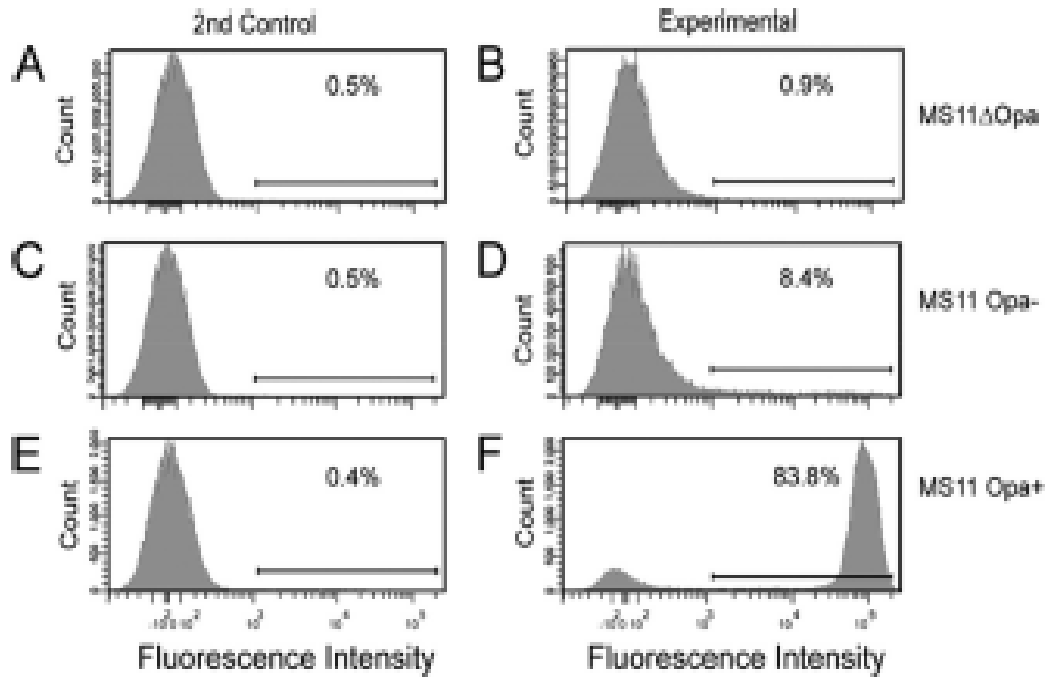


Figure 4. Flow cytometry analysis of Opa expression. Gonococcal MS11Δopa (A and B), phenotypically Opa-negative MS11 (C and D), and Opa- expressing MS11 (E and F) cells were stained with (B, D, and F) or without MAb 4B12 followed by Alexa-Fluor 405- conjugated goat anti-mouse IgG. The bacteria were analyzed by using flow cytometry. Shown are representative histograms from three independent experiments. The bar in the figure represents the gate used to measure Opa expression. The number in each figure corresponds to the percentage of the population that was expressing Opa.

b. Hurley, M. T., Wang, Z., **Mahle, A.**, Rabin, D., Liu, Q., English, D. S., Zachariah, M. R., Stein, D. and DeShong, P. (2013), Synthesis, Characterization, and Application of Antibody Functionalized Fluorescent Silica Nanoparticles. *Adv. Funct. Mater.*, 23: 3335–3343. doi: 10.1002/adfm.201202699

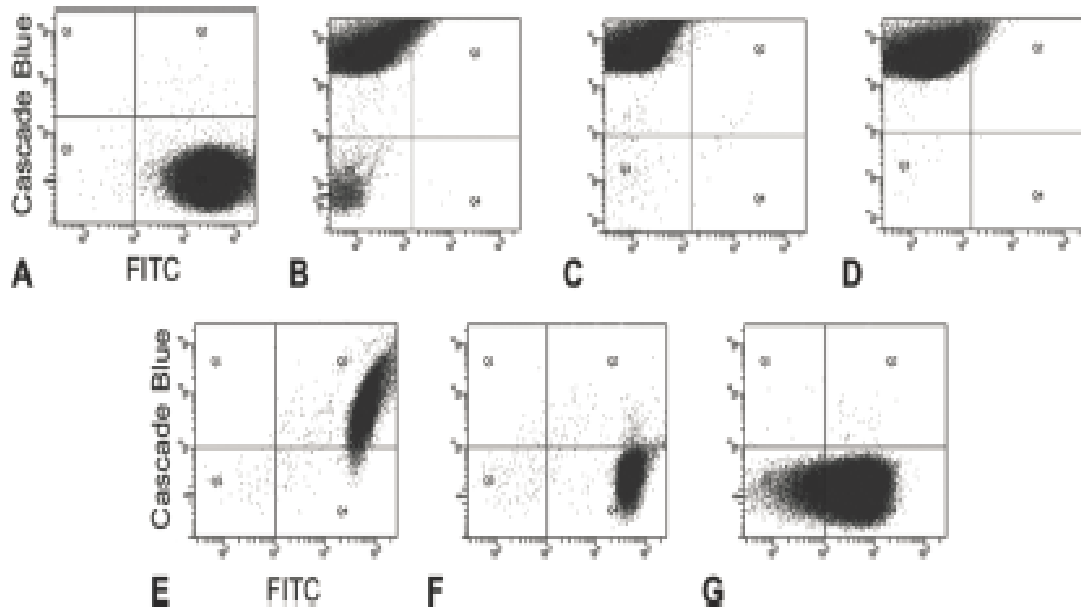


Figure 11. Flow cytometry using anti-gonococcal IgG FSNs A) FITC labelled GC. B) Non-functionalized Cascade Blue FSNs. C) PEG functionalized Cascade Blue FSNs. D) Anti-gonococcal IgG functionalized Cascade Blue FSNs. E) Anti-gonococcal IgG functionalized Cascade Blue FSNs with FITC labeled *E. Coli*. F) PEG functionalized Cascade Blue FSNs with FITC labeled Gonococci. G) Anti-gonococcal IgG functionalized Cascade Blue FSNs with FITC labeled *E. coli*. The voltage of the photomultiplier tube (PMT) utilized for the particles alone was 445 and for particles with bacteria it was 588. This discrepancy in detector voltage was due to the observed quenching of Cascade Blue by FITC. The profiles were gated on aggregates, eliminating cellular debris and background noise. Panel G was gated on all events due to the lack of *E. coli* aggregation.

Bibliography

1. Schneider, C. A.; Rasband, W. S.; Eliceiri, K. W., NIH Image to ImageJ: 25 years of image analysis. *Nat. Methods.* **2012**, *9*, 671-675.
2. Piekarowicz, A.; Stein, D. C., Biochemical properties of *Neisseria gonorrhoeae* LgtE. *J. Bacteriol.* **2002**, *184*, 6410-6416.
3. *Essentials of Glycobiology*. 2nd ed.; Cold Spring Harbor Laboratory Press: Cold Spring Harbor, NY, 2009.
4. 2nd ed.; Ajit Varki, R. D. C., Jeffrey D Esko, Hudson H Freeze, Pamela Stanley, Carolyn R Bertozzi, Gerald W Hart, and Marilynn E Etzler, Ed. Cold Spring Harbor Laboratory Press: Cold Spring Harbor (NY), **2009**.
5. Toone Eric, J.; Whitesides George, M., Enzymes as Catalysts in Carbohydrate Synthesis. *Enzymes in Carbohydrate Synthesis*, American Chemical Society: **1991**; *466*, 1-22.
6. Lairson, L.; Henrissat, B.; Davies, G.; Withers, S., Glycosyltransferases: structures, functions, and mechanisms. *Annu. Rev. Biochem.* **2008**, *77*, 521-555.
7. Kiessling, L. L.; Grim, J. C., Glycopolymer probes of signal transduction. *Chem. Soc. Rev.* **2013**, *42*, 4476-4491.
8. Apicella, M. A.; Mandrell, R. E.; Shero, M.; Wilson, M. E.; Griffiss, J. M.; Brooks, G. F.; Lammel, C.; Breen, J. F.; Rice, P. A., Modification by sialic acid of *Neisseria gonorrhoeae* lipooligosaccharide epitope expression in human urethral exudates: an immunoelectron microscopic analysis. *J. Infect. Dis.* **1990**, *162*, 506-512.

9. Hakomori, S. I.; Cummings, R. D., Glycosylation effects on cancer development. *Glycoconj. J.* **2012**, *29*, 565-566.
10. Preston, A.; Mandrell, R. E.; Gibson, B. W.; Apicella, M. A., The lipooligosaccharides of pathogenic gram-negative bacteria. *Crit. Rev. Microbiol.* **1996**, *22*, 139-180.
11. van Kooyk, Y.; Rabinovich, G. A., Protein-glycan interactions in the control of innate and adaptive immune responses. *Nat. Immunol.* **2008**, *9*, 593-601.
12. Zhu, P.; Boykins, R. A.; Tsai, C. M., Genetic and functional analyses of the *lgtH* gene, a member of the beta-1,4-galactosyltransferase gene family in the genus *Neisseria*. *Microbiology* **2006**, *152*, 123-134.
13. Robyt, J. F., *Essentials of carbohydrate chemistry*. Springer: New York, 1998;
14. Weijers, C. A.; Franssen, M. C.; Visser, G. M., Glycosyltransferase-catalyzed synthesis of bioactive oligosaccharides. *Biotechnol. Adv.* **2008**, *26*, 436-456.
15. Wakarchuk, W. W.; Cunningham, A.; Watson, D. C.; Young, N. M., Role of paired basic residues in the expression of active recombinant galactosyltransferases from the bacterial pathogen *Neisseria meningitidis*. *Protein Eng.* **1998**, *11*, 295-302.
16. Cantarel, B. L.; Coutinho, P. M.; Rancurel, C.; Bernard, T.; Lombard, V.; Henrissat, B., The Carbohydrate-Active EnZymes database (CAZy): an expert resource for Glycogenomics. *Nucleic Acids Res.* **2009**, *37*, 233-238.
17. Oyelaran, O.; Gildersleeve, J. C., Glycan arrays: recent advances and future challenges. *Curr. Opin. Chem. Biol.* **2009**, *13*, 406-413.

18. Wu, C. Y.; Liang, P. H.; Wong, C. H., New development of glycan arrays. *Org. Biomol. Chem.* **2009**, *7*, 2247-2254.
19. Park, S.; Gildersleeve, J. C.; Blixt, O.; Shin, I., Carbohydrate microarrays. *Chem. Soc. Rev.* **2013**, *42*, 4310-4326.
20. Tang, P. W.; Gool, H. C.; Hardy, M.; Lee, Y. C.; Feizi, T., Novel approach to the study of the antigenicities and receptor functions of carbohydrate chains of glycoproteins. *Biochem. Biophys. Res. Commun.* **1985**, *132*, 474-480.
21. Consortium for Functional Glycomics (CFG).
<http://www.functionalglycomics.org/static/consortium/resources.shtml>.
22. Fukui, S.; Feizi, T.; Galustian, C.; Lawson, A. M.; Chai, W., Oligosaccharide microarrays for high-throughput detection and specificity assignments of carbohydrate-protein interactions. *Nat. Biotechnol.* **2002**, *20*, 1011-1017.
23. Zhang, Y.; Gildersleeve, J. C., General procedure for the synthesis of neoglycoproteins and immobilization on epoxide-modified glass slides. *Methods Mol. Biol.* **2012**, *808*, 155-165.
24. Oyelaran, O.; McShane, L. M.; Dodd, L.; Gildersleeve, J. C., Profiling human serum antibodies with a carbohydrate antigen microarray. *J Proteome Res* **2009**, *8*, 4301-10.
25. Israelachvili, J. N., Intermolecular and surface forces. 2nd ed.; Academic Press: London ; San Diego, 1991.
26. Israelachvili, J. N., Intermolecular and surface forces. 3rd ed.; Elsevier. **2011**.

27. Bangham, A. D.; Horne, R. W., Negative staining of phospholipids and their structural modification by surface-active agents as observed in the electron microscope. *J. Mol. Biol.* **1964**, *8*, 660-668.
28. Deamer, D. W., From "banghasomes" to liposomes: a memoir of Alec Bangham, 1921-2010. *FASEB J.* **2010**, *24*, 1308-1310.
29. Bangham, A. D., Lipid bilayers and biomembranes. *Annu. Rev. Biochem.* **1972**, *41*, 753-776.
30. Szoka, F.; Papahadjopoulos, D., Comparative properties and methods of preparation of lipid vesicles (liposomes). *Annu Rev Biophys Bioeng* **1980**, *9*, 467-508.
31. Kaler, E. W.; Murthy, A. K.; Rodriguez, B. E.; Zasadzinski, J. A., Spontaneous vesicle formation in aqueous mixtures of single-tailed surfactants. *Science* **1989**, *245*, 1371-1374.
32. Thomas, G. B.; Rader, L. H.; Park, J.; Abezgauz, L.; Danino, D.; DeShong, P.; English, D. S., Carbohydrate modified cationic vesicles: probing multivalent binding at the bilayer interface. *J. Am. Chem. Soc.* **2009**, *131*, 5471-5477.
33. Koehler, R. D.; Raghavan, S. R.; Kaler, E. W., Microstructure and Dynamics of Wormlike Micellar Solutions Formed by Mixing Cationic and Anionic Surfactants. *J. Phys. Chem. B.* **2000**, *104*, 11035-11044.
34. Ragev, O.; Khan, A., Alkyl chain symmetry effects in mixed cationic anionic surfactant systems. *Journal of Colloid Interface Science* **1996**, *182*, 95-109.
35. Safran, S. A.; Pincus, P.; Andelman, D., Theory of spontaneous vesicle formation in surfactant mixtures. *Science* **1990**, *248*, 354-356.

36. Wang, X.; Danoff, E. J.; Sinkov, N. A.; Lee, J. H.; Raghavan, S. R.; English, D. S., Highly efficient capture and long-term encapsulation of dye by cationic surfactant vesicles. *Langmuir* **2006**, *22*, 6461-6464.
37. Dashaputre, N.; Mahle, A. C.; Javvaji, V.; Payne, G. F.; Raghavan, S. R.; Stein, D. C.; DeShong, P., A New Type of Glycan Microarray Using Immobilized Cationic Vesicles Functionalized with Glycolipids. **2013 In Preparation.**
38. Pond, M. A.; Zangmeister, R. A., Carbohydrate-functionalized surfactant vesicles for controlling the density of glycan arrays. *Talanta* **2012**, *91*, 134-139.
39. Raetz, C. R.; Whitfield, C., Lipopolysaccharide endotoxins. *Annu. Rev. Biochem.* **2002**, *71*, 635-700.
40. O'Connor, E. T.; Swanson, K. V.; Cheng, H.; Fluss, K.; Griffiss, J. M.; Stein, D. C., Structural requirements for monoclonal antibody 2-1-L8 recognition of neisserial lipooligosaccharides. *Hybridoma (Larchmt)* **2008**, *27*, 71-79.
41. Cullen, T. W.; Giles, D. K.; Wolf, L. N.; Ecobichon, C.; Boneca, I. G.; Trent, M. S., *Helicobacter pylori* versus the host: remodeling of the bacterial outer membrane is required for survival in the gastric mucosa. *PLoS Pathog.* **2011**, *7*, e1002454.
42. Goldberg, J. B.; Pler, G. B., *Pseudomonas aeruginosa* lipopolysaccharides and pathogenesis. *Trends Microbiol.* **1996**, *4*, 490-494.
43. Braun, D. C.; University of Maryland (College Park Md.). Department of Cell Biology and Molecular Genetics. Transcriptional analysis of the *lgtABCDE* gene locus of *Neisseria gonorrhoeae*. Thesis (Ph.D.), University of Maryland, College Park, **2002**.

44. Braun, D. C.; Stein, D. C., The *lgtABCDE* gene cluster, involved in lipooligosaccharide biosynthesis in *Neisseria gonorrhoeae*, contains multiple promoter sequences. *J. Bacteriol.* **2004**, *186*, 1038-1049.
45. Gotschlich, E. C., Genetic locus for the biosynthesis of the variable portion of *Neisseria gonorrhoeae* lipooligosaccharide. *J Exp Med* **1994**, *180*, 2181-2190.
46. Edwards, J. L.; Apicella, M. A., The molecular mechanisms used by *Neisseria gonorrhoeae* to initiate infection differ between men and women. *Clin. Microbiol. Rev.* **2004**, *17*, 965-981.
47. Arking, D.; Tong, Y.; Stein, D. C., Analysis of lipooligosaccharide biosynthesis in the *Neisseriaceae*. *J. Bacteriol.* **2001**, *183*, 934-941.
48. Harvey, H. A.; Jennings, M. P.; Campbell, C. A.; Williams, R.; Apicella, M. A., Receptor-mediated endocytosis of *Neisseria gonorrhoeae* into primary human urethral epithelial cells: the role of the asialoglycoprotein receptor. *Mol. Microbiol.* **2001**, *42*, 659-672.
49. Rice, P. A.; McCormack, W. M.; Kasper, D. L., Natural serum bactericidal activity against *Neisseria gonorrhoeae* isolates from disseminated, locally invasive, and uncomplicated disease. *J. Immunol.* **1980**, *124*, 2105-2109.
50. Estabrook, M. M.; Griffiss, J. M.; Jarvis, G. A., Sialylation of *Neisseria meningitidis* lipooligosaccharide inhibits serum bactericidal activity by masking lacto-N-neotetraose. *Infect. Immun.* **1997**, *65*, 4436-4444.
51. Persson, K.; Ly, H. D.; Dieckelmann, M.; Wakarchuk, W. W.; Withers, S. G.; Strynadka, N. C., Crystal structure of the retaining galactosyltransferase LgtC

- from *Neisseria meningitidis* in complex with donor and acceptor sugar analogs. *Nat. Struct. Biol.* **2001**, *8*, 166-175.
52. Burch, C. L.; Danaher, R. J.; Stein, D. C., Antigenic variation in *Neisseria gonorrhoeae*: production of multiple lipooligosaccharides. *J. Bacteriol.* **1997**, *179*, 982-986.
53. Tong, Y.; Arking, D.; Ye, S.; Reinhold, B.; Reinhold, V.; Stein, D. C., *Neisseria gonorrhoeae* strain PID2 simultaneously expresses six chemically related lipooligosaccharide structures. *Glycobiology* **2002**, *12*, 523-533.
54. Blixt, O.; van Die, I.; Norberg, T.; van den Eijnden, D. H., High-level expression of the *Neisseria meningitidis* *lgtA* gene in *Escherichia coli* and characterization of the encoded N-acetylglucosaminyltransferase as a useful catalyst in the synthesis of GlcNAc beta 1-->3Gal and GalNAc beta 1-->3Gal linkages. *Glycobiology* **1999**, *9*, 1061-1071.
55. Nothaft, H.; Szymanski, C. M., Protein glycosylation in bacteria: sweeter than ever. *Nat. Rev. Microbiol.* **2010**, *8*, 765-778.
56. Breton, C.; Snajdrová, L.; Jeanneau, C.; Koca, J.; Imberty, A., Structures and mechanisms of glycosyltransferases. *Glycobiology* **2006**, *16*, 29-37.
57. Wang, L. X.; Lomino, J. V., Emerging technologies for making glycan-defined glycoproteins. *ACS Chem. Biol.* **2012**, *7*, 110-122.
58. Hossler, P.; Khattak, S. F.; Li, Z. J., Optimal and consistent protein glycosylation in mammalian cell culture. *Glycobiology* **2009**, *19*, 936-949.

59. Schiestl, M.; Stangler, T.; Torella, C.; Cepeljnik, T.; Toll, H.; Grau, R., Acceptable changes in quality attributes of glycosylated biopharmaceuticals. *Nat. Biotechnol.* **2011**, *29*, 310-312.
60. Lau, K.; Thon, V.; Yu, H.; Ding, L.; Chen, Y.; Muthana, M. M.; Wong, D.; Huang, R.; Chen, X., Highly efficient chemoenzymatic synthesis of beta1-4-linked galactosides with promiscuous bacterial beta1-4-galactosyltransferases. *Chem. Commun. (Camb)* **2010**, *46*, 6066-6068.
61. Wakarchuk, W.; Martin, A.; Jennings, M. P.; Moxon, E. R.; Richards, J. C., Functional relationships of the genetic locus encoding the glycosyltransferase enzymes involved in expression of the lacto-N-neotetraose terminal lipopolysaccharide structure in *Neisseria meningitidis*. *J. Biol. Chem.* **1996**, *271*, 19166-19173.
62. Tong, Y.; Reinhold, V.; Reinhold, B.; Brandt, B.; Stein, D. C., Structural and immunochemical characterization of the lipooligosaccharides expressed by *Neisseria subflava* 44. *J. Bacteriol.* **2001**, *183*, 942-950.
63. Song, W.; Ma, L.; Chen, R.; Stein, D. C., Role of lipooligosaccharide in Opa-independent invasion of *Neisseria gonorrhoeae* into human epithelial cells. *J. Exp. Med.* **2000**, *191*, 949-960.
64. White, L. A.; Kellogg, D. S., *Neisseria gonorrhoeae* identification in direct smears by a fluorescent antibody-counterstain method. *Appl. Microbiol.* **1965**, *13*, 171-174.

65. Sambrook, J.; Fritsch, E. F.; Maniatis, T., *Molecular Cloning: a laboratory manual*. 2nd ed.; Cold Spring Harbor Laboratory Press: Cold Spring Harbor, N.Y., 1989.
66. Laemmli, U. K., Cleavage of structural proteins during the assembly of the head of bacteriophage T4. *Nature* **1970**, *227*, 680-685.
67. Tsai, C. M.; Frasch, C. E., A sensitive silver stain for detecting lipopolysaccharides in polyacrylamide gels. *Anal. Biochem.* **1982**, *119*, 115-119.
68. Sambrook, J.; Russell, D. W., *Molecular cloning : a laboratory manual*. 3rd ed.; Cold Spring Harbor Laboratory Press: Cold Spring Harbor, N.Y., 2001.
69. Hirabayashi, J.; Yamada, M.; Kuno, A.; Tateno, H., Lectin microarrays: concept, principle and applications. *Chem. Soc. Rev.* **2013**, *42*, 4443-4458.
70. Lundquist, J. J.; Debenham, S. D.; Toone, E. J., Multivalency effects in protein-carbohydrate interaction: the binding of the Shiga-like toxin 1 binding subunit to multivalent C-linked glycopeptides. *J. Org. Chem.* **2000**, *65*, 8245-8250.
71. Aas, F. E.; Vik, A.; Vedde, J.; Koomey, M.; Egge-Jacobsen, W., *Neisseria gonorrhoeae* O-linked pilin glycosylation: functional analyses define both the biosynthetic pathway and glycan structure. *Mol. Microbiol.* **2007**, *65*, 607-624.
72. Børud, B.; Aas, F. E.; Vik, A.; Winther-Larsen, H. C.; Egge-Jacobsen, W.; Koomey, M., Genetic, structural, and antigenic analyses of glycan diversity in the O-linked protein glycosylation systems of human *Neisseria* species. *J. Bacteriol.* **2010**, *192*, 2816-2829.

73. Westphal, O.; Jann, K., Bacterial Lipopolysaccharides: extraction with phenol-water and further applications of the procedure. *Methods Carbohydr. Chem.* **1972**, *5*, 83-91.
74. Hitchcock, P. J.; Brown, T. M., Morphological heterogeneity among *Salmonella* lipopolysaccharide chemotypes in silver-stained polyacrylamide gels. *J. Bacteriol.* **1983**, *154*, 269-277.
75. Gildersleeve, J. C., Glycosyltransferases: carb loading strategy is spot on. *Nat. Chem. Biol.* **2012**, *8*, 741-742.
76. Ban, L.; Pettit, N.; Li, L.; Stuparu, A. D.; Cai, L.; Chen, W.; Guan, W.; Han, W.; Wang, P. G.; Mrksich, M., Discovery of glycosyltransferases using carbohydrate arrays and mass spectrometry. *Nat. Chem. Biol.* **2012**, *8*, 769-773.
77. Lairson, L. L.; Watts, A. G.; Wakarchuk, W. W.; Withers, S. G., Using substrate engineering to harness enzymatic promiscuity and expand biological catalysis. *Nat. Chem. Biol.* **2006**, *2*, 724-728.
78. Chandrasekaran, A.; Deng, K.; Koh, C. Y.; Takasuka, T.; Bergeman, L. F.; Fox, B. G.; Adams, P. D.; Singh, A. K., A universal flow cytometry assay for screening carbohydrate-active enzymes using glycan microspheres. *Chem. Commun. (Camb)* **2013**, *49*, 5441-5443.
79. Dowling, M. B.; Javvaji, V.; Payne, G. F.; Raghavan, S. R., Vesicle capture on patterned surfaces coated with amphiphilic biopolymers. *Soft Matter* **2011**, *7*, 1219-1226.
80. Musumeci, M. A.; Hug, I.; Scott, N. E.; Ielmini, M. V.; Foster, L. J.; Wang, P. G.; Feldman, M. F., In vitro activity of *Neisseria meningitidis* PglL O-

- oligosaccharyltransferase with diverse synthetic lipid donors and a UDP-activated sugar. *J. Biol. Chem.* **2013**, *288*, 10578-10587.
81. Berg, O. G.; Yu, B. Z.; Rogers, J.; Jain, M. K., Interfacial catalysis by phospholipase A2: determination of the interfacial kinetic rate constants. *Biochemistry* **1991**, *30*, 7283-7297.
82. Berg, O. G.; Rogers, J.; Yu, B. Z.; Yao, J.; Romsted, L. S.; Jain, M. K., Thermodynamic and kinetic basis of interfacial activation: resolution of binding and allosteric effects on pancreatic phospholipase A2 at zwitterionic interfaces. *Biochemistry* **1997**, *36*, 14512-14530.
83. Zhou, F.; Schulten, K., Molecular dynamics study of phospholipase A2 on a membrane surface. *Proteins* **1996**, *25*, 12-27.
84. Danoff, E. J.; Wang, X.; Tung, S. H.; Sinkov, N. A.; Kemme, A. M.; Raghavan, S. R.; English, D. S., Surfactant vesicles for high-efficiency capture and separation of charged organic solutes. *Langmuir* **2007**, *23*, 8965-8971.
85. Israelachvili, J. N., Intermolecular and surface forces : with applications to colloidal and biological systems. Academic Press: London, **1985**.
86. Brown, G. M.; Levy, H. A., Alpha-D-glucose: precise determination of crystal structure by neutron-diffraction analysis. *Science* **1965**, *147*, 1038-1039.
87. Lehninger, A. L.; Nelson, D. L.; Cox, M. M., Lehninger principles of biochemistry. 3rd ed.; Worth Publishers: New York, **2000**.
88. Richard, K.; Mann, B. J.; Stocker, L.; Barry, E. M.; Qin, A.; Cole, L. E.; Hurley, M. T.; Ernst, R. K.; Michalek, S. M.; Stein, D. C.; Deshong, P.; Vogel, S. N.,

- Novel Catanionic Surfactant Vesicle Vaccines Protect against *Francisella tularensis* LVS and Confer Significant Partial Protection against *F. tularensis* Schu S4 Strain. *Clin. Vaccine Immunol.* **2014**, *21*, 212-226.
89. Bingham, D.; John, C. M.; Levin, J.; Panter, S. S.; Jarvis, G. A., Post-injury conditioning with lipopolysaccharide or lipooligosaccharide reduces inflammation in the brain. *J. Neuroimmunol.* **2013**, *256*, 28-37.
90. Wang, H.; Huang, W.; Orwenyo, J.; Banerjee, A.; Vasta, G. R.; Wang, L. X., Design and synthesis of glycoprotein-based multivalent glyco-ligands for influenza hemagglutinin and human galectin-3. *Bioorg. Med. Chem.* **2013**, *21*, 2037-2044.
91. Blixt, O.; Cló, E.; Nudelman, A. S.; Sørensen, K. K.; Clausen, T.; Wandall, H. H.; Livingston, P. O.; Clausen, H.; Jensen, K. J., A high-throughput O-glycopeptide discovery platform for seromic profiling. *J. Proteome Res.* **2010**, *9* (10), 5250-5261.
92. Fry, S. A.; Afrough, B.; Lomax-Browne, H. J.; Timms, J. F.; Velentzis, L. S.; Leatham, A. J., Lectin microarray profiling of metastatic breast cancers. *Glycobiology* **2011**, *21*, 1060-1070.
93. Apicella, M. A.; Shero, M.; Jarvis, G. A.; Griffiss, J. M.; Mandrell, R. E.; Schneider, H., Phenotypic variation in epitope expression of the *Neisseria gonorrhoeae* lipooligosaccharide. *Infect. Immun.* **1987**, *55*, 1755-1761.